SCHOOL OF CIVIL ENGINEERING

JOINT HIGHWAY RESEARCH PROJECT

FHWA/IN/JHRP-79/25

STUDY OF THE SEGMENTAL BOX GIRDER BRIDGE AT TURKEY RUN: CONSTRUCTION, INSTRUMENTATION, AND DATA COLLECTION

S. P. Wanders
D. A. Winslow
C. Douglas Sutton

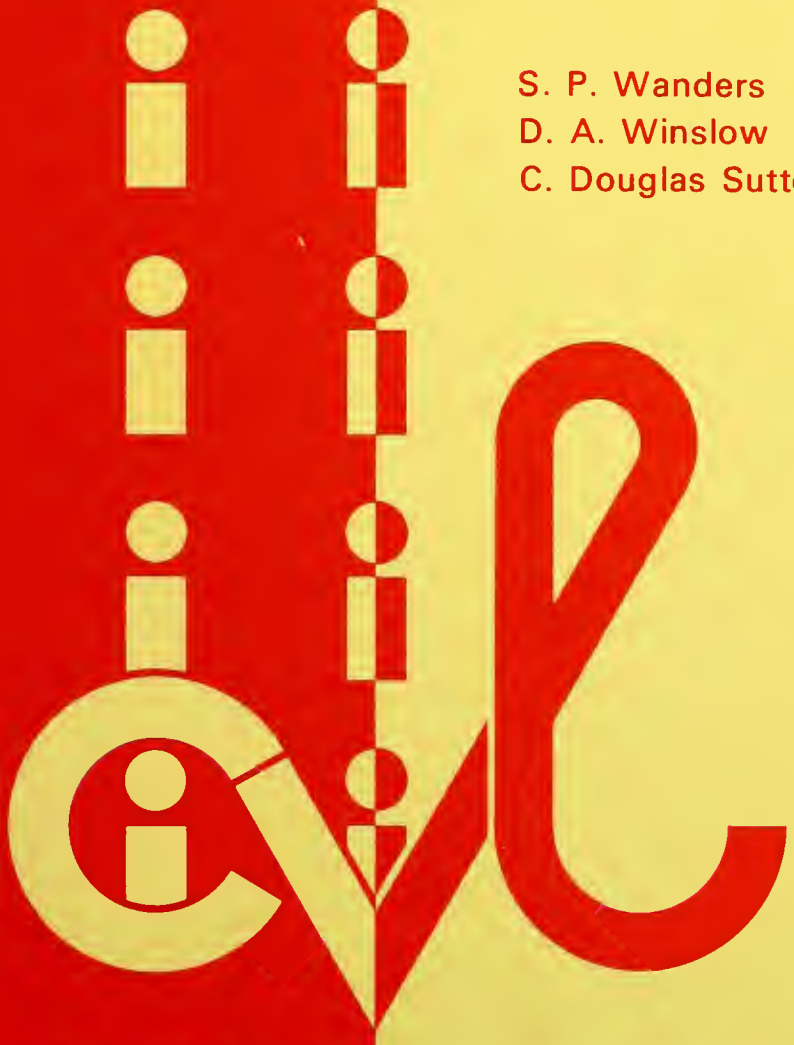

PURDUE UNIVERSITY
INDIANA STATE HIGHWAY COMMISSION

Interim Report

STUDY OF THE SEGMENTAL BOX GIRDER BRIDGE AT TURKEY RUN: CONSTRUCTION, INSTRUMENTATION AND DATA COLLECTION

TO: H. L. Michael, Director
Joint Highway Research Project

December 17, 1979

Project: C-36-56T

FROM: C. Douglas Sutton, Research Engineer
Joint Highway Research Project

File: 7-4-20

Attached is an Interim Report titled "Study of the Segmental Box Girder Bridge at Turkey Run: Construction, Instrumentation, and Data Collection". This is the first Interim Report for this HPR Part II study. It is authored by Stephen P. Wanders, David A. Winslow, and C. Douglas Sutton, all of, or formerly of, our staff.

The Report contains a review of the construction process for the Turkey Run Bridge and a complete description of the instrumentation system and its implementation. Detailed descriptions of the data collection methods for each of the investigative topics are also presented. Those data which have been collected, reduced, and analyzed during this initial phase of the project are summarized and noted as available.

The Report is submitted as partial fulfillment of the objectives of the study. Copies will also be submitted to ISHC and FHWA for their review and comment.

Respectfully submitted,

C. Douglas Sutton

C. Douglas Sutton
Research Engineer

CDS:ms

cc: A. G. Altschaeffl
W. L. Dolch
R. L. Eskew
G. D. Gibson
W. H. Goetz
M. J. Gutzwiller
G. K. Hallock
D. E. Hancher
K. R. Hoover
J. F. McLaughlin
R. D. Miles
P. L. Owens
G. T. Satterly
C. F. Scholer
K. C. Sinha
C. A. Venable
H. P. Wehrenberg
L. E. Wood
E. J. Yoder
S. R. Yoder

Interim Report

STUDY OF THE SEGMENTAL BOX GIRDER BRIDGE AT TURKEY RUN: CONSTRUCTION, INSTRUMENTATION AND DATA COLLECTION

by

Stephen P. Wanders
David A. Winslow
Graduate Instructors in Research

C. Douglas Sutton
Research Associate

Joint Highway Research Project

Project No.: C-36-56T

File No.: 7-4-20

Prepared as Part of an Investigation

Conducted by

Joint Highway Research Project
Engineering Experiment Station
Purdue University

in cooperation with the

Indiana State Highway Commission

and the

U.S. Department of Transportation
Federal Highway Administration

Purdue University
West Lafayette, Indiana
December 17, 1979

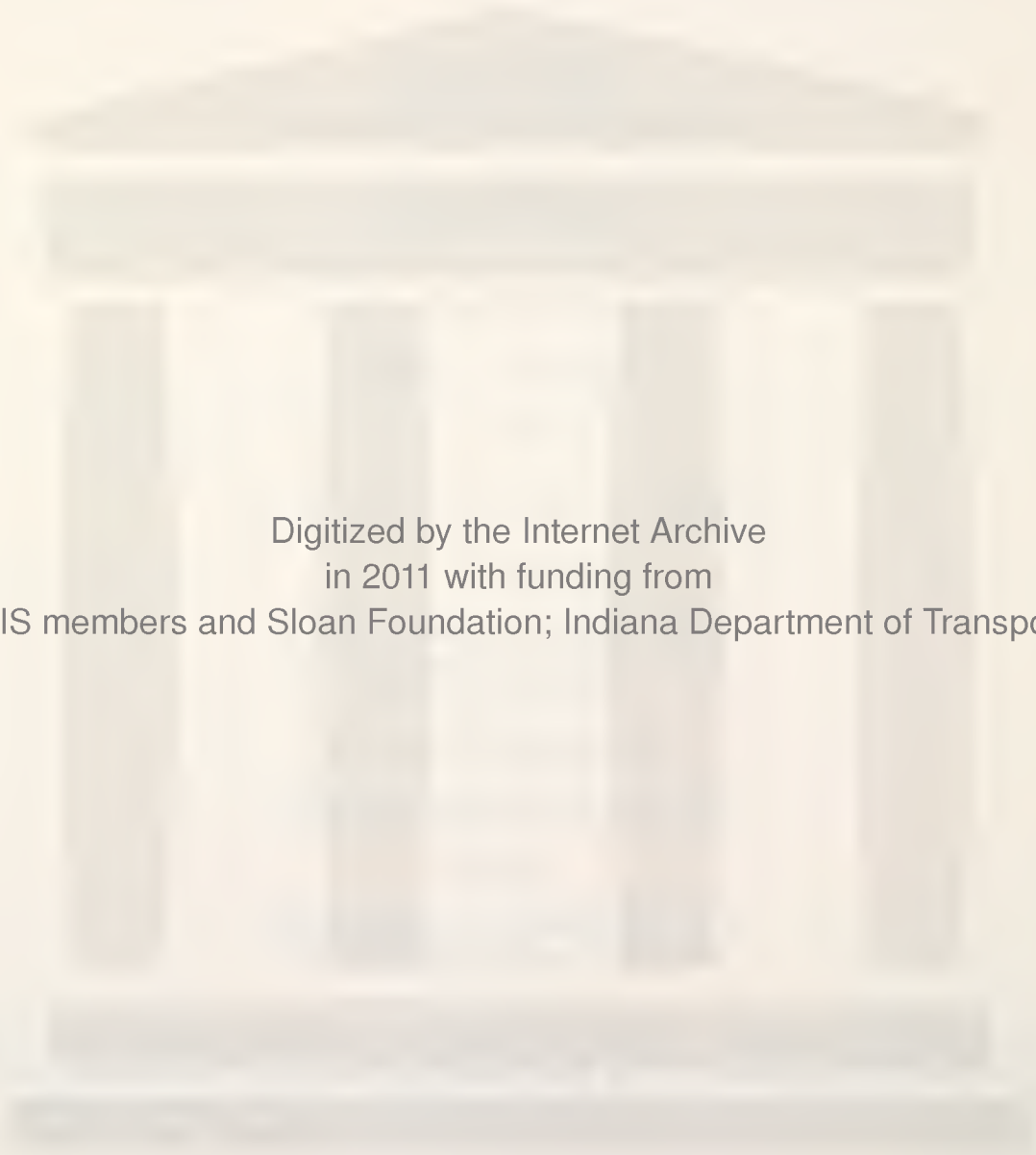

TECHNICAL REPORT STANDARD TITLE PAGE

1. Report No.	2. Government Accession No.	3. Recipient's Catalog No.
FHWA/IN/JHRP-79/25		

4. Title and Subtitle	5. Report Date
STUDY OF THE SEGMENTAL BOX GIRDER BRIDGE AT TURKEY RUN: CONSTRUCTION, INSTRUMENTATION, AND DATA COLLECTION	December 17, 1979
	6. Performing Organization Code

7. Author(s)	8. Performing Organization Report No.
Stephen P. Wanders, David A. Winslow, and C. Douglas Sutton	JHRP-79-25

9. Performing Organization Name and Address	10. Work Unit No.
Joint Highway Research Project Civil Engineering Building Purdue University West Lafayette, Indiana 47907	11. Contract or Grant No. HPR-1(17) Part II
	13. Type of Report and Period Covered
12. Sponsoring Agency Name and Address Indiana State Highway Commission State Office Building 100 North Senate Avenue Indianapolis, Indiana 46204	Interim Report I
	14. Sponsoring Agency Code

15. Supplementary Notes Prepared in cooperation with the U.S. Department of Transportation, Federal Highway Administration. Part of the study titled "Study of the Segmental Box Girder Bridge at Turkey Run".

16. Abstract

A review is made of the literature pertaining to segmental concrete box girder bridges. A relatively complete description of the construction of the segmental bridge at Turkey Run is presented.

The Turkey Run bridge has been instrumented to monitor certain aspects of its short-term and long-term behavior. Details of the instrumentation system design and installation procedure are given.

A study has been conducted to determine the transverse flexural response of selected sections due to prescribed truck loadings. Experimental measurements have also been made to determine long-term longitudinal strains and midspan deflections and the daily and seasonal variations in bridge temperatures. The data collected from these tests have been reduced and are presented in a form suitable for evaluation.

17. Key Words	18. Distribution Statement
Bridges (Concrete), Box Girder, Post-tensioning, Segmental Construction, Cantilever Erection, Field Measurements, Strains, Deflection, Temperature, Transverse Bending, Long-term Behavior.	No restrictions. This document is available to the public through the National Technical Information Service, Springfield, VA 22161.

19. Security Classif. (of this report)	20. Security Classif. (of this page)	21. No. of Pages	22. Price
Unclassified	Unclassified	175	

Form DOT F 1700.7 (8-69)

ACKNOWLEDGEMENTS

The authors wish to express their appreciation to Professors R. H. Lee and M. J. Gutzwiller for their assistance throughout the course of this project.

Financial assistance which made this study possible was provided by the Joint Highway Research Project of Purdue University in cooperation with the Indiana State Highway Commission (ISHC) and the U.S. Department of Transportation, Federal Highway Administration (FHWA).

Special thanks are extended to Steven J. Hull, ISHC, and Paul A. Hoffman, FHWA, for their technical assistance and consultation.

TABLE OF CONTENTS

LIST OF TABLES

LIST OF FIGURES

HIGHLIGHT SUMMARY

A review is made of the literature pertaining to segmental concrete box girder bridges. A relatively complete description of the construction of the segmental bridge at Turkey Run is presented.

The Turkey Run bridge has been instrumented to monitor certain aspects of its short-term and long-term behavior. Details of the instrumentation system design and installation procedure are given.

A study has been conducted to determine the transverse flexural response of selected sections due to prescribed truck loadings. Experimental measurements have also been made to determine long-term longitudinal strains and midspan deflections and the daily and seasonal variations in bridge temperatures. The data collected from these tests have been reduced and are presented in a form suitable for evaluation.

CHAPTER I
INTRODUCTION

General

The increasing popularity of precast prestressed segmental box girder bridges in the United States has brought about the need for more comprehensive research on their structural behavior. Current design practice in this country regarding segmental bridges is based largely on European experience and research. There has been only limited American research, especially concerning the experimental evaluation of performance of prototype structures. The fact that important design criteria are untested and unverified justifies performance measurements on full-scale structures.

In 1973, the first American precast prestressed concrete box girder bridge was built in Corpus Christi, Texas. In order to check the applicability and accuracy of the design criteria, analytical methods, and construction techniques, a one-sixth scale model of the three-span continuous bridge was built at the Civil Engineering Structures Research Laboratory of the University of Texas Balcones Research Center. The final report[1] from the project documents the construction and load testing of the bridge. Experimental results are compared with analytical values for the various stages of construction, service loadings, ultimate proof loadings, and final failure tests.

A similar study is now being conducted by The Pennsylvania Transportation

Institute at The Pennsylvania State University[2]. The research is concerned with the segmental concrete box girder test track bridge designed under a previous project. The objectives of this program are to make field measurements on the full-scale bridge, to study overload behavior, to observe torsional stresses and effects at several locations on the bridge, and to make a crack survey of the bridge. A theoretical analysis will also be performed.

At Purdue University, Batla[3] developed two methods for the elastic analysis of prestressed concrete box girder bridge superstructures with constant depth, subjected to a variety of surface or concentrated loads, prestressing forces and arbitrary boundary conditions. The development of these methods, which are based on the finite element technique of structural analysis, is directed towards the analysis of the box girder to determine vertical deflections of the superstructure and longitudinal membrane stresses and transverse bending moments in various plates of the box girder. The accuracy of the methods is checked by analyzing a box girder bridge superstructure for which solutions based on elasticity theory are also available.

Relatively more extensive research has been performed concerning thermal effects in concrete bridges. Priestly's[4,5,6] work deals mainly with the behavior of prestressed and reinforced concrete bridges under vertical temperature gradients induced by solar radiation input to the deck surface. Methods for predicting design temperature gradients from local meteorological conditions are discussed and a general analytical method for predicting the vertical distribution of thermally induced stress is developed. Results from laboratory and in situ experiments confirm the validity of the analytical approach.

Extensive research involving bridge temperatures has also been done at the Transport and Road Research Laboratory in Great Britain through a combination of theoretical studies and site experiments. Studies conducted by Emerson[7,8,9,10,11] have been concerned mainly with the measurement of extreme values of bridge temperatures as well as the distribution of temperatures in bridges. The results from these and similar investigations are presented in the proceedings of a Symposium on Bridge Temperatures held at the TRRL on October 5, 1977[12].

In a paper published by the Cement and Concrete Association, White[13] reviews the literature pertaining to temperature effects in concrete bridge structures. It is intended to provide insight into the research behind the non-linear differential temperature distributions included in codes of practice, together with some indication of how the effects of temperature could be included in the design procedure.

A paper by Reynolds and Emanuel[14] presents the state-of-the-art of the thermal behavior of bridges and of the consideration to be given to the resulting thermal effects. Results of studies related to bridge thermal effects are reviewed and grouped for continuity and clarity. The relationship of ambient temperature to bridge temperature and the relationship of both ambient and bridge temperatures to thermal stresses and movements are considered. Current code requirements of both the United States and Germany in regard to thermal effects on bridges are also presented.

Some of the European research dealing with segmental bridges has been concerned with the redistribution of moments in continuous structures caused by the combined effects of creep, shrinkage and loss of prestress. Instrumentation used to measure support reactions of the Champigny-Sur-Yonne

bridge in France has shown that the final stresses in the completed structure are significantly different from the initial stresses immediately following construction[15].

At the University of Illinois, Dannon and Gamble[16] developed a method for the analysis of time-dependent deformations of post-tensioned concrete bridge superstructures which are erected by cantilever methods. A step-by-step procedure is presented which takes into account the creep and shrinkage of concrete under variable stress, variation in Young's modulus of concrete, relaxation of the steel stress, friction between strand and ducts, and all elastic changes in stress accompanying the constructuion of additional segments. This analytical method was used to study the effects of variations of the parameters on the long-term behavior of two bridges which were built and designed in accordance with quite different criteria. Excellent agreement between measured and computed curvatures and strains were found in the two cases for which experimental data were available.

A long-term study of this phenomenon is presently being conducted by the Portland Cement Association[17]. The purpose of this research program is to verify procedures for the calculation of time-dependent deformations in segmental post-tensioned cantilever concrete box girder bridges. In particular the effects of creep and shrinkage on camber changes and prestress losses will be identified. The program consists of field measurements on the Kishawaukee River Bridge, a laboratory study of the concrete properties, and a comparison between measured and calculated values. The project, when completed, should provide information that can be used to improve the design and performance of future long span bridges constructed by the cantilever method.

As a contribution to the continuing evolution of prestressed concrete bridge construction, the Prestressed Concrete Institute and the Post-Tensioning Institute have published a manual[18] on precast segmental box girder bridges. This publication describes the development, design, analysis and construction of precast segmental box grider bridges in general.

In recognition of the importance of precast prestressed segmental box girder bridges and the relative lack of experimental research information pertaining to their behavior, the Joint Highway Research Project at Purdue University has conducted a project entitled "Instrumentation of the Turkey Run Segmental Bridge". During this project, which was carried out over the period between January 1976 and June 1977, an initial instrumentation scheme was designed by R. J. Holman for the Turkey Run bridge. This report represents a continuation of the work begun under the auspices of that original project.

The Turkey Run bridge, located at an aesthetically pleasing site on State Road 47 in Parke County, Indiana, carries two lanes of traffic over the Turkey Run Creek (see Figures 1.1 through 1.4). It is made up of a twin box cross-section and has two equal spans of 158'-6". Erected by the so-called cantilever method, the Turkey Run bridge is the first two-span bridge of its type in the nation. The Indiana State Highway Commission received, in October 1978, a national award for design excellence from the Prestressed Concrete Institute for this bridge.

Overall Scope of the Project

The goal of this study is to collect and analyze information regarding certain aspects of the short-term and long-term behavior of a

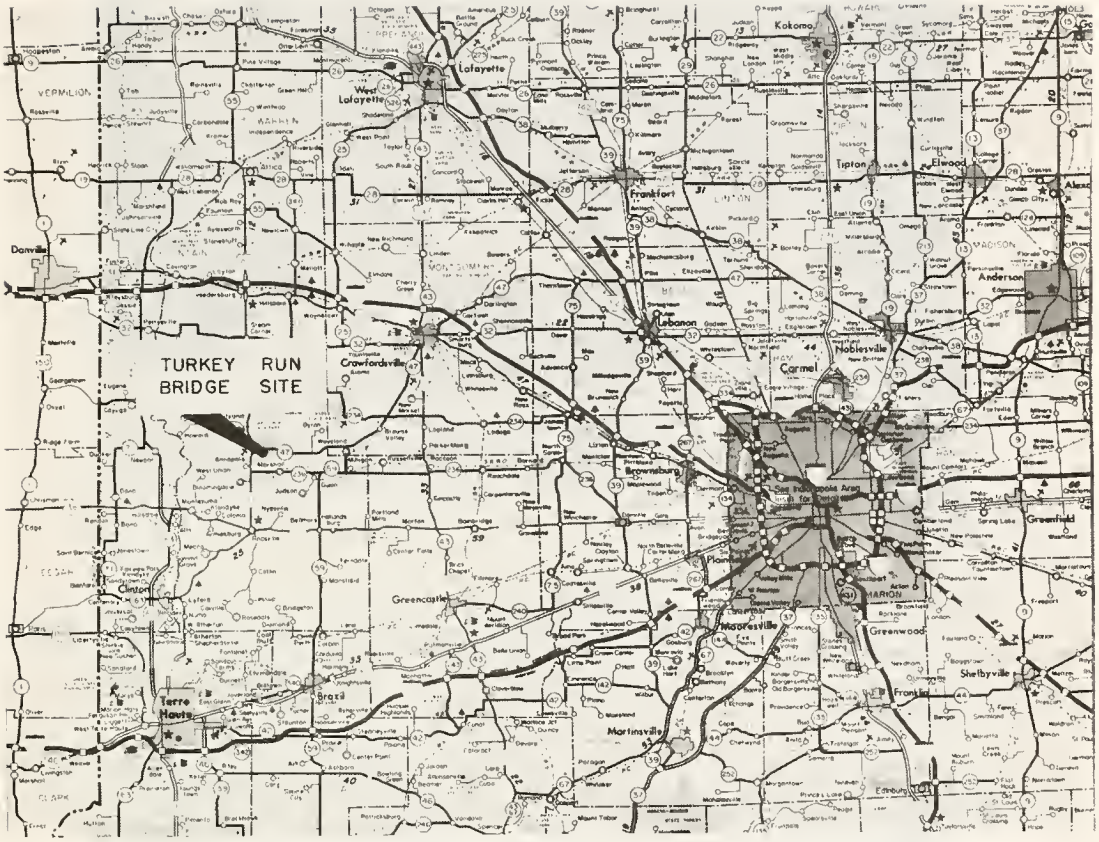

Figure 1.1 Turkey Run Bridge Site

Figure 1.2 State Road 47, Parke County, Indiana

Figure 1.3 Two Spans at 158' - 6"

Figure 1.4 Twin Box Cross-Section

prototype bridge, both during construction and under service conditions. As previously mentioned, it builds upon the work begun on a previous project carried out by Holman[19]. Work on the project will continue through June, 1981.

The specific objectives of this research are as follows:

1. To complete the development and installation of a suitable instrumentation scheme.
2. To determine, through experimental measurements and analysis, the transverse flexural response of representative cross-sections due to pre-specified truck loadings.
3. To determine, through experimental measurements, the daily and seasonal variations in temperature gradients through the bridge.
4. To measure thermally induced deflections and strains both during construction and in the completed structure.
5. To measure over a three year period the long-term deformations at key locations on the structure.
6. To compare the results obtained from the experimental analysis to the response predicted by currently recommended analytical methodology and design criteria.
7. To evaluate present design methodology and parameters in light of the experimental evidence and to either verify existing criteria or suggest changes.

Scope of the Work Covered by this Report

This report is concerned with reviewing the bridge construction process and the instrumentation system design and installation procedure. Detailed descriptions of the data collection procedures for each of the

investigative topics are presented herein. The data have been reduced and analyzed and are presented in a form suitable for evaluation.

Evaluation of present design methodology and parameters, in light of the experimental evidence, will be the main emphasis of the work to be undertaken during the next phase of the segmental bridge project. This information and any complementary data will be presented in a subsequent report.

Notes

1 Kashima, S. and Breen, J. E., "Construction and Load Tests of a Segmental Precast Box Girder Bridge Model", University of Texas at Austin, February, 1975.

2 Haight, F. A., "An Experimental Segmental Bridge - A Research Continuation Proposal to the Pennsylvania Department of Transportation", The Pennsylvania Transportation Institute, PTI 1777, The Pennsylvania State University, May, 1977.

3 Batla, F. A., "Finite Element Analysis of Prestressed Concrete Box Girders", Ph.D. Dissertation, Purdue University, December, 1976.

4 Priestly, M. J. N., "Thermal Gradients in Bridges - Some Design Considerations", New Zealand Engineering (Wellington), V. 27, No. 7, July, 1972, pp. 228-233.

5 Priestly, M. J. N., "Design Thermal Gradients for Concrete Bridges", New Zealand Engineering (Wellington), V. 31, N. 9, September, 1976, pp. 213-219.

6 Priestly, M. J. N., "Design of Concrete Bridges for Temperature", Journal of the American Concrete Institute, Vol. 75, No. 5, May, 1978, pp. 209-217.

7 Emerson, M., "The Calculation of the Distribution of Temperature in Bridges", Transport and Road Research Laboraotry Report LR 561, Crowthorne, Department of Environment, 1973.

8 Emerson, M., "Bridge Temperatures Estimated from Shade Temperature", TRRL Report LR 696, Crowthorne, Department of the Environment, 1976.

9 Emerson, M., "Extreme Values of Bridge Temperatures for Design Purposes", TRRL Report LR 744, Crowthorne, Department of the Environment, 1976.

10 Emerson, M., "Temperature Differences in Bridges: Basis of Design Requirements", TRRL Report LR 765, Crowthorne, Department of the Environment, 1977.

11 Emerson, M., "Temperatures in Bridges During the Hot Summer of 1976", TRRL Report LR 783, Crowthorne, Department of the Transport, 1977.

12 Transport and Road Research Laboratory, Department of the Environment/ Department of Transport, Bridge Temperatures, Supplementary Report 442, Crowthorne, 1978

13 White, I. G., "Non-Linear Differential Temperature Distributions in Concrete Bridge Structures: A Review of the Current Literature", Technical Report 525 of the Cement and Concrete Association, 1979.

14 Reynolds, J. C. and Emanuel, J. H., "Thermal Stresses and Movements in Bridges", Proceedings of the American Society of Civil Engineers, V. 100, St. 1, January, 1974, pp. 63-78.

15 Technical Bulletin of Association Francaise des Ponts et Charpentes, "Long-Term Experiments on a Prestressed Concrete Bridge: The Bridge of Champigny-Sur-Yonne", March, 1972, pp. 19-37.

16 Danon, J. R. and Gamble, W. L., "Time-Dependent Deformations and Losses in Concrete Bridges Built by the Cantilever Method", Department of Civil Engineering, University of Illinois, Urbana, IL/Illinois Department of Transportation, Springfield, IL, Report No. UILU-ENG-77-2002, January, 1977.

17 Portland Cement Association, Research and Development, Construction Technology Laboratories, "Time-Dependent Behavior of Segmental Cantilever Concrete Bridges", June, 1977.

18 Post-Tensioning Institute/Prestressed Concrete Institute, Precast Segmental Box Girder Bridge Manual, Glenview, IL/Chicago, IL, 1978

19 Holman, R. J., "Development of an Instrumentation Program for Studying Behavior of a Segmental Concrete Box Girder Bridge", Joint Highway Research Project 77-4, Purdue University, March 2, 1977.

CHAPTER II

CONSTRUCTION

Construction of the segmental bridge at Turkey Run was begun during the fall of 1976. Because the bridge was built during the period of time covered by this initial phase of the project, some attention will be given to the details of the construction procedure. The narrative contained herein, together with the accompanying photographs, constitute a relatively complete description of the construction process.

The segments for the Turkey Run bridge were precast using the short-line method by Construction Products Corporation at their plant in Lafayette, Indiana. This method involved sequential casting of the segments in a single set of adjustable metal forms in the same order in which they were to be placed in the structure. Each segment was match-cast against the immediately preceding segment to insure a near-perfect joint. After allowing sufficient time for curing, the preceding segment was taken away and the new segment was shifted to the place of the preceding segment. This casting operation is illustrated in Figures 2.1 through 2.3[1].

Reinforcement cages, made from conventional deformed steel reinforcing bars and welded wire fabric (see Figure 2.4), were assembled prior to placement in the form (see Figure 2.5). Post-tensioning ducts were positioned during cage assembly. Once the cage was secured in the form, the inside formwork was moved forward on rollers into its casting position (see Figure 2.6). The preceding segment was then placed next to the form

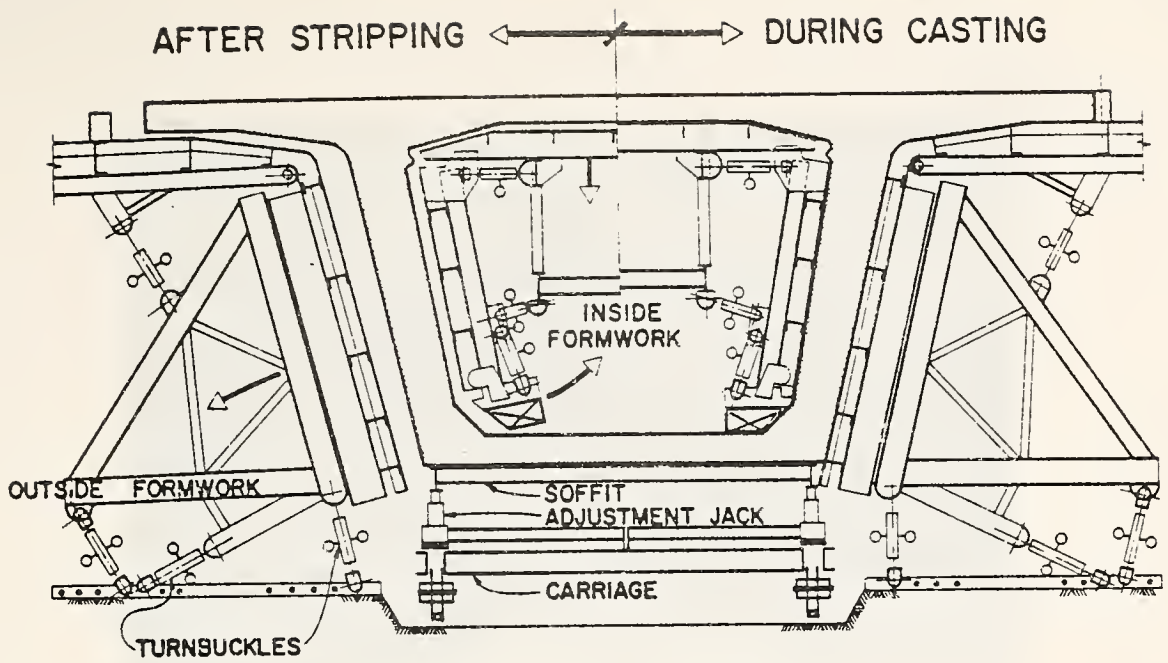

Figure 2.1. Formwork

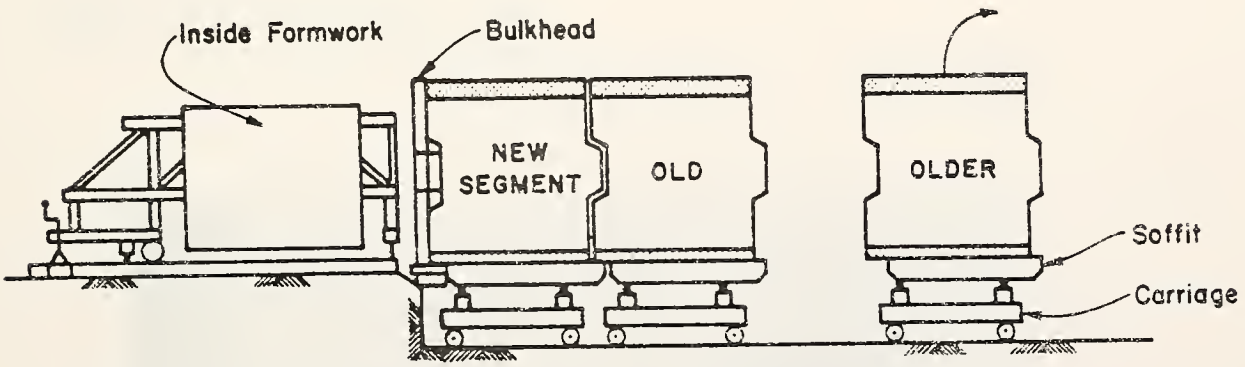

Figure 2.2. Just Before Separation of Segments

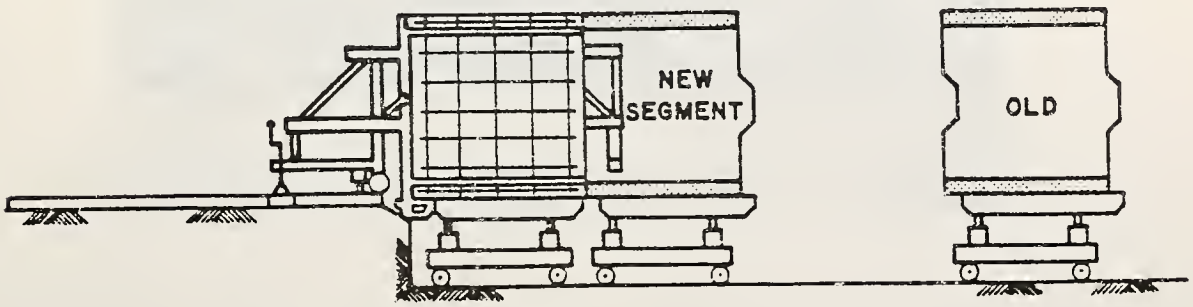

Figure 2.3. Just Before Casting Next Segment

Figure 2.4. Reinforcement Cage

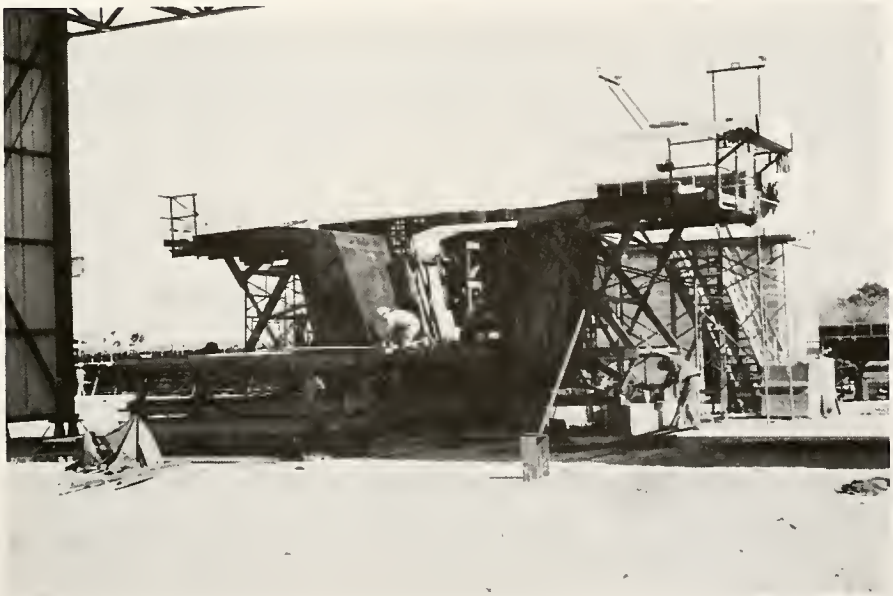

Figure 2.5. Segment Formwork

as shown in Figure 2.7. A bulkhead was used to close the opposite end of the form. Final adjustments of the formwork were then made and the concrete was placed. Since the relative position of the succeeding segments was dependent upon correct dimensioning of the preceding segments, proper adjustment of the formwork was an essential step in the casting process.

As the casting operation was repeated, segments no longer needed for match-casting were stockpiled until all segments for an entire girder were completed (see Figure 2.8). These segments were then trucked to the construction site for erection (see Figure 2.9). At the time of erection, the average age of the segments was approximately six months. For this reason creep and shrinkage effects were minimized, which is one advantage of precast segmental construction. The casting sequence is shown in Figure 2.10.

While the segments were being cast the general contractor, J. L. Wilson Company of Bloomfield, Indiana, had begun work at the bridge site on State Road 47 in Parke County. Demolition of the existing spandrel arch bridge (see Figure 2.11) was under way by late February of 1977. Deterioration of the concrete supporting arches was the reason for its removal.

After the site was cleared, work on the substructure was begun. By early June the abutments and central piers were completed. Because the segments were cast while the substructure work was being completed, a net savings in on-site construction time was achieved. This is a significant advantage of precast segmental construction over cast-in-place construction.

The Turkey Run bridge superstructure was erected by the balanced cantilever method. As its name implies, this method involves simply

Figure 2.6. Inside Formwork

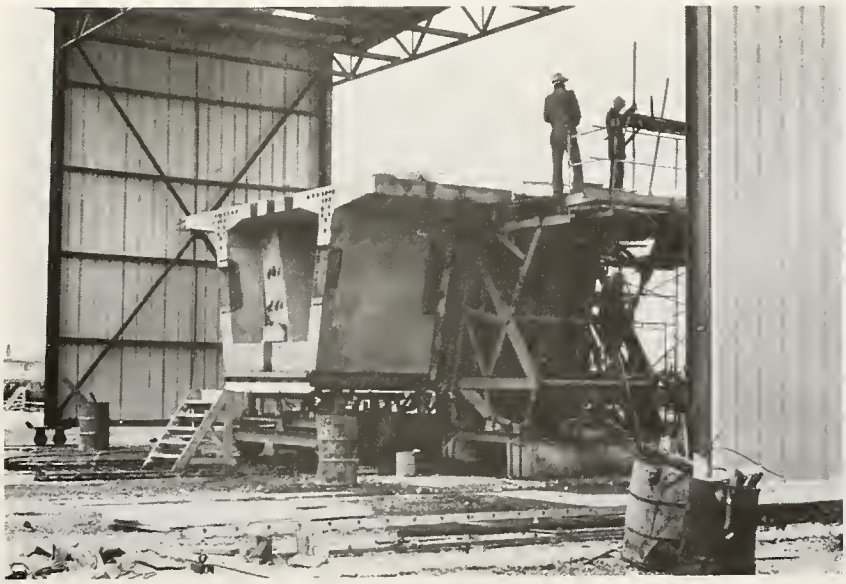

Figure 2.7. Match-Casting

Figure 2.8. Stockpiled Segments

Figure 2.9. Segments Trucked to Construction Site

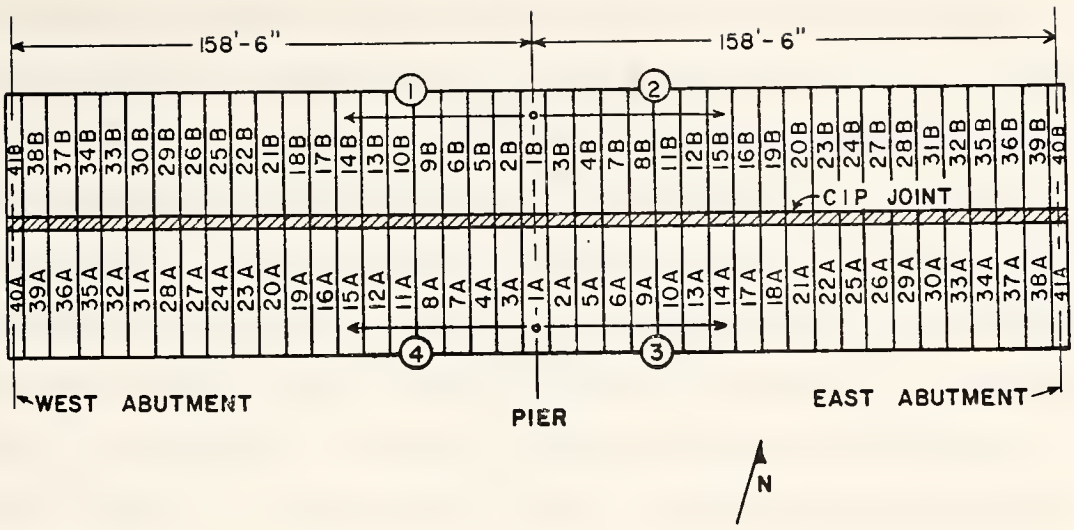

Figure 2.10. Casting Sequence

Figure 2.11. Existing Spandrel Arch Bridge

cantilevering segments from the central piers in a balanced fashion. The first segment was lifted into place and anchored to the pier (see Figure 2.12). The second segment was then temporarily post-tensioned to the pier segment with high-strength steel post-tensioning bars. Segment 3 was then placed in the same manner. Once the segments were in place in this balanced condition, permanent post-tensioning tendons were threaded through all three segments, jacked to achieve the specified prestressing force, and anchored. The temporary post-tensioning was then removed. This procedure was repeated until the last segments were placed on the abutments.

At the construction site, a working platform was mounted on top of the segment to be placed to facilitate lifting and alignment as well as to provide a safe working area (see Figure 2.13). A crane based on the ground below was utilized to hoist the next segment to within a foot of the segment to which it was to be attached. Once in this position, the temporary post-tensioning bars were threaded through the appropriate ducts (see Figure 2.14). Two bars were placed in the top slab and one in the bottom slab. A thin layer of epoxy was then applied by hand to the entire joint surface as shown in Figure 2.15.

To verify that the strength of the epoxy was adequate, a simple series of tests were conducted. For each joint a test block was bonded to the interior segment wall using the epoxy mix from that joint. After the epoxy had cured, the block was knocked off with a hammer (see Figure 2.16). In all cases failure occured in the concrete and not the epoxy.

Grouting tubes for the permanent post-tensioning ducts were placed into notches which were cast in the joint (see Figure 2.17). With the epoxy applied and the grouting tubes in place, the segment was then eased

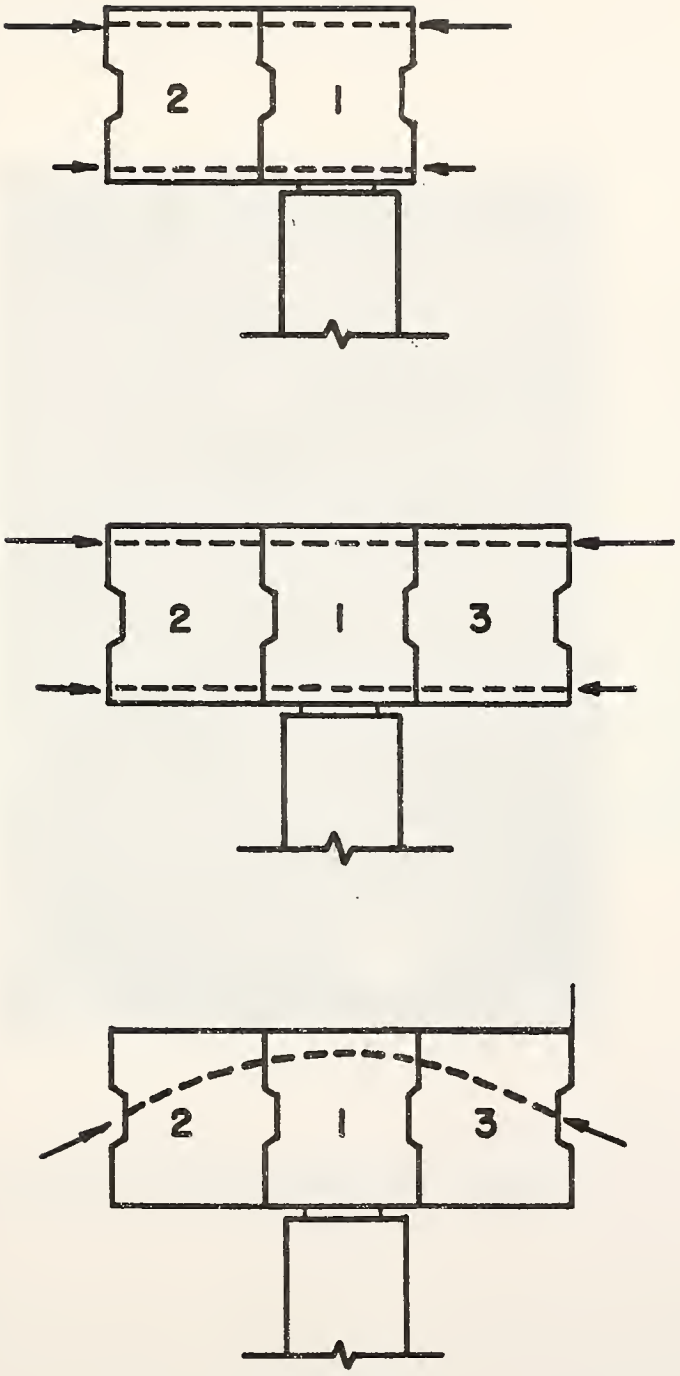

Figure 2.12. Balanced Cantilever Method

Figure 2.13. Working Platform Mounted on Segment

Figure 2.14. Temporary Post-Tensioning Bars

Figure 2.15. Epoxy Applied to Joint Surface

Figure 2.16. Test Block Verifying Strength of Epoxy

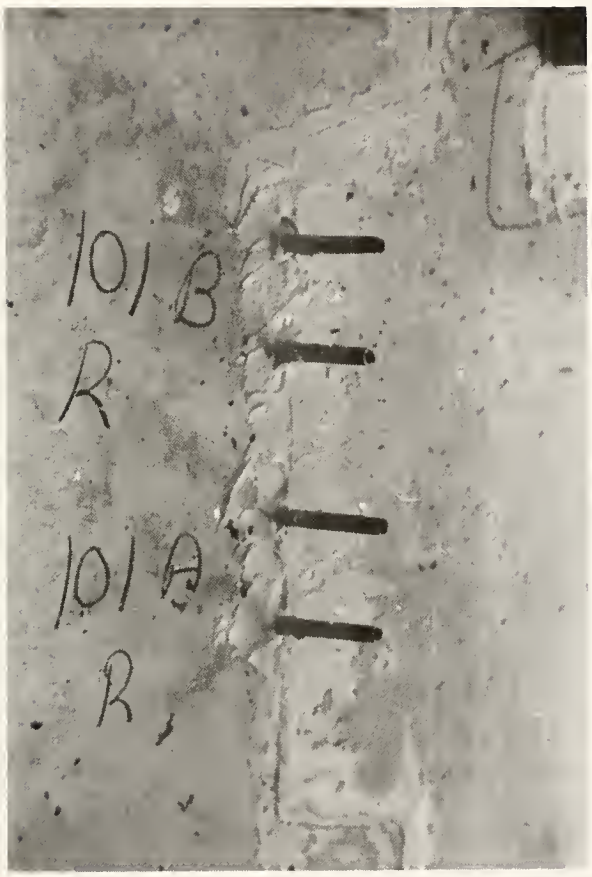

Figure 2.17. Grouting Tubes in Place

into position, as shown in Figure 2.18, and temporarily post-tensioned. In order to seat the segment properly and produce an adequate joint, the jacks were tightened systematically. The force in the two top jacks (see Figure 2.19) was initially increased to 50 percent of the specified value. The crane was then lowered and the bottom post-tensioning bar (see Figure 2.20) was jacked to develop its full specified force. Finally, the top bars were tensioned fully. The counter-balancing segment was then erected on the other end of the cantilever using the same procedure.

Permanent post-tensioning tendons, consisting of 12, 1/2 in. diameter, Grade 270 strands were then pulled through the appropriate ducts using a wire mesh grip (see Figure 2.21). A cable attached to the grip was placed in a pulley mounted on the working platform as shown in Figure 2.22. The cable was then pulled by a bulldozer until the tendons were in the desired position.

A 450 kip capacity hydraulic jack was then used on either end of the tendon to permanently post-tension the segments (see Figure 2.23). The force in the tendons was monitored by means of a hydraulic pressure gage. In order to provide a check on the gage reading, the elongation of the strands was also measured. When the desired force was attained, the strands were anchored in the webs of the segment, the jack was removed, and the excess strands were cut off (see Figure 2.24).

The temporary post-tensioning bars were then removed. The working platform was lifted from the segment just completed and mounted on the segment to be erected next. This procedure was repeated, alternately erecting segments on the north and south girders, until both spans were completed.

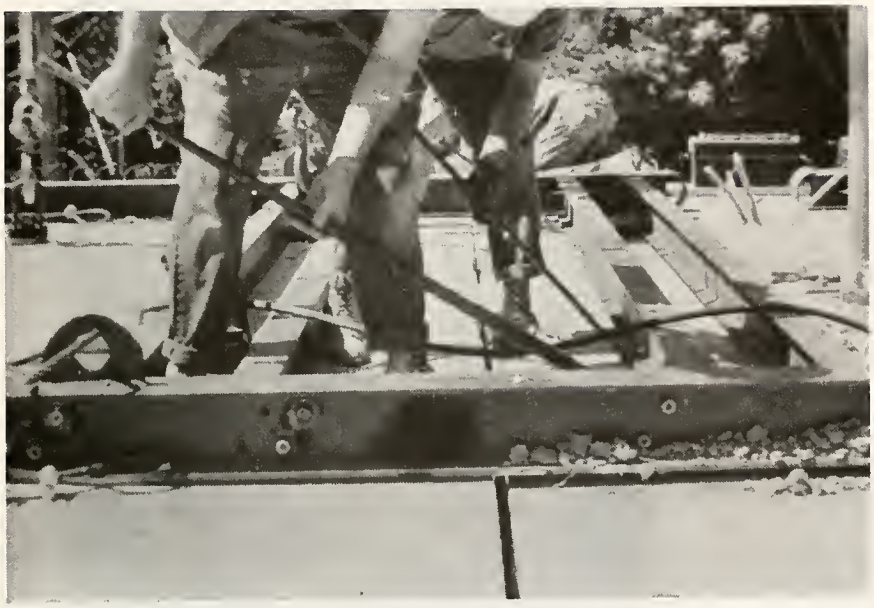

Figure 2.18. Segment Eased into Position

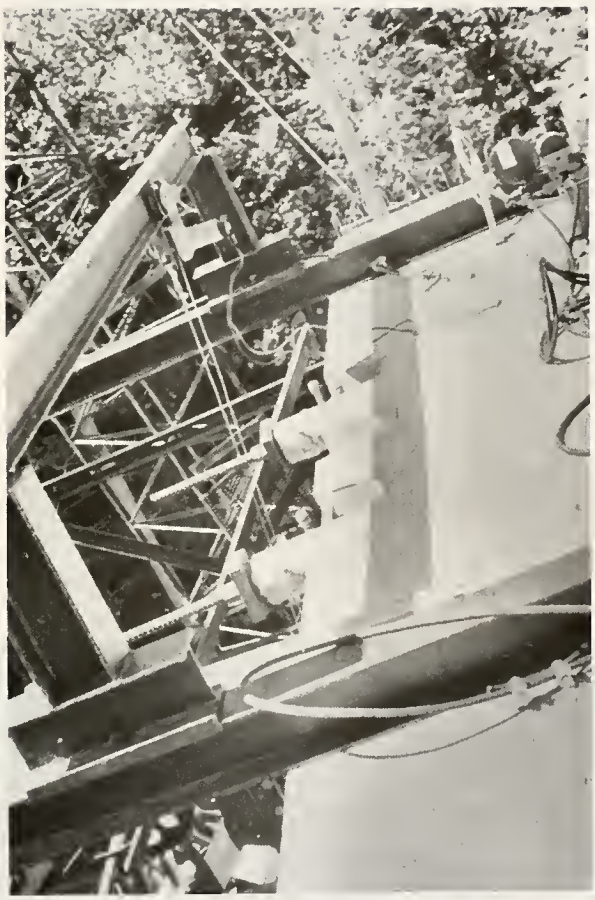

Figure 2.19. Top Temporary Post-Tensioning Jacks

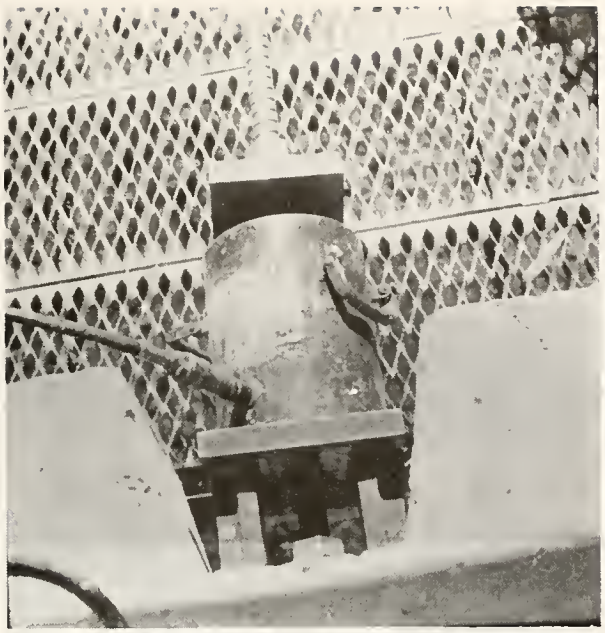

Figure 2.20. Bottom Temporary Post-Tensioning Jack

Figure 2.21. Wire Mesh Grip

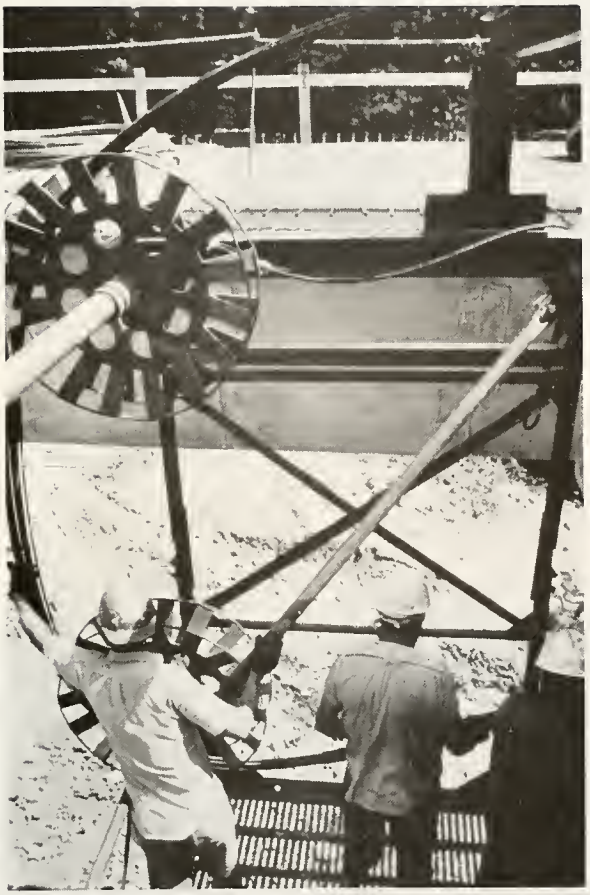

Figure 2.22. Cable Placed in Pulley on Working Platform

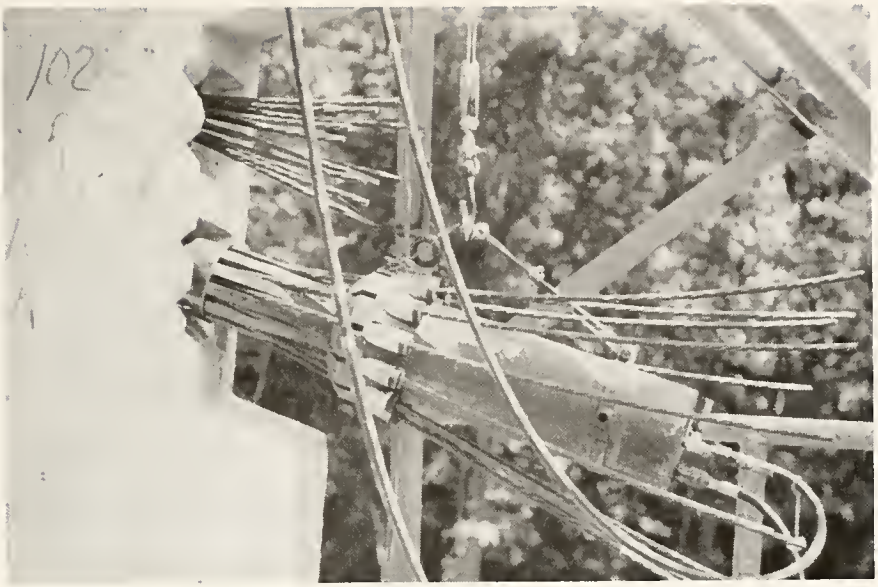

Figure 2.23. Jacking Post-Tensioning Tendons

Figure 2.24. Cutting Off Excess Strands

Figure 2.25 shows several segments in place in both spans. At the time this photograph was taken, work on the south girder was slightly ahead of that on the north girder. The temporary struts used to provide additional moment resistance at the pier during the construction process can also be seen in this figure. Temporary supports were also used once the girders extended a distance of about two thirds of the span length from the pier (see Figure 2.26). These supports made it possible to dimension the segments more economically because of the reduction in required moment capacity.

By early September 1977, the last segments were erected (see Figure 2.27). In order to provide moment continuity between the box girders, transverse reinforcement, consisting of conventional deformed steel bars, was lap spliced and a four foot joint was cast between the top flanges (see Figure 2.28). The tendons were then grouted.

Supported by the travelling scaffold assembly shown in Figure 2.29, workmen brushed a mortar mix on the exterior surface of the bridge, thus covering the joints and giving it a pleasing appearance. A two inch concrete overlay was poured on the top slab to provide a durable riding surface. Curbs were cast and guard rails were bolted in place to complete the structure.

The Turkey Run bridge was opened to traffic on November 15, 1977 (see Figure 2.30). Further details concerning the construction process are given in Appendix A of this report.

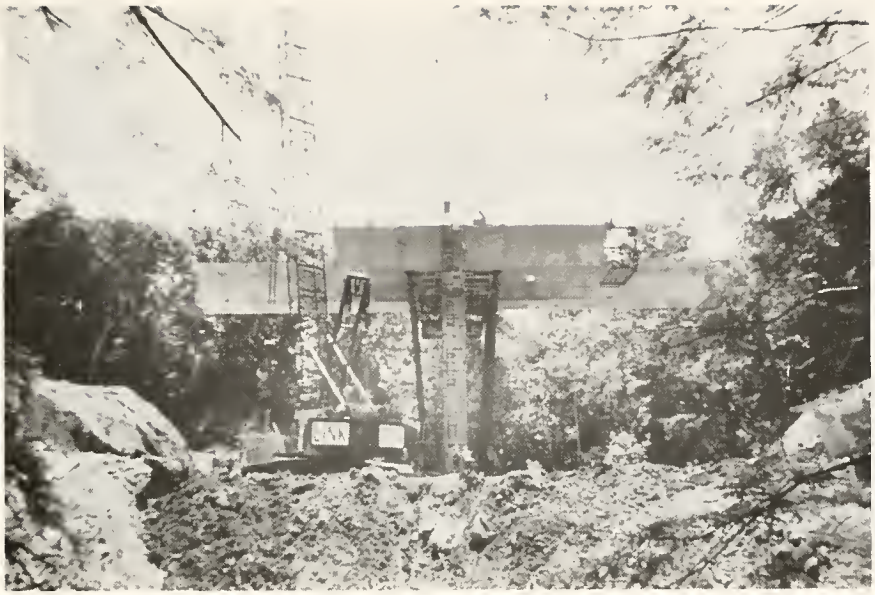

Figure 2.25. Initial Construction

Figure 2.26. Temporary Support Assembly

Figure 2.27. Last Segments in Place

Figure 2.28. Cast-In-Place Joint

Figure 2.29. Travelling Scaffold Assembly

Figure 2.30. Completed Structure

NOTES

1 Permission granted for reproduction on November 9, 1979 by the Prestressed Concrete Institute and on November 21, 1979 by the Post-Tensioning Institute.

CHAPTER III

INSTRUMENTATION

General

Development and implementation of a suitable instrumentation system was a primary objective of this phase of the research. Accordingly, a slightly modified version of the instrumentation scheme originally designed and reported by Holman[1] has been installed on the Turkey Run bridge. This permanent system of transducers and implants is utilized together with appropriate external equipment to obtain the desired data on transverse flexural response, temperature distributions and long-term deformations.

In this chapter the various components of the instrumentation system are described and details of the procedures employed in installing the system are presented.

Transverse Bending Instrumentation

The instrumentation for transverse bending is located at the sections where strain levels, resulting from distortional effects, are maximized for the prescribed loading situations. According to Holman[2], maximum distortional effects occur near the point of maximum vertical deflection; therefore, instrumented sections are located near the centerlines of segments 24 and 25, as illustrated in Figure 3.1. The greater stiffness supplied by the thickened bottom slab and the interior diaphragms near the pier results in more pronounced transverse moments in the vicinity of the pier. Instrumented sections are located near the pier at the centerline

of segments 2 and 3 as shown in Figure 3.1. The instrumented sections are referred to herein as sections A through D.

Figures 3.2 through 3.5 illustrate the relative positions of strain gage installations at each instrumented section. No gages are located in the bottom slab of segments 2 and 3 because the tapered slab thickness would cause difficulties in traction interpretation. The various types of strain gage installations utilized and the means by which they were installed is described subsequently. Additional details are presented in Appendix C.

Interior Reinforcing Bar Gages

Each group of gage installations includes two electrical resistance strain gages, one each affixed to the interior and exterior reinforcing bars of the slab or web supplemented by ERS gage(s) cemented to the interior surface of the segment. The gages supply strain distribution data at each section. With the strain distribution known, transverse moment tractions can be inferred.

Installation of the gages on the reinforcing bars was done in the structural laboratory at Purdue University prior to segment fabrication. Gage installations on the reinforcing bars are labeled as Type III installations herein (see Figure 3.6). Weldable ERS gages from Micro-Measurements, Inc. (Romulus, Michigan) were used because of their moisture resistance and durability. A three-wire lead configuration was used to minimize desensitization errors, as explained by Holman[3]. Details of the gage installation are shown in Figure 3.7.

After the gages were tack welded to the machined surfaces of the bars, they were wired and then coated with three different types of protective

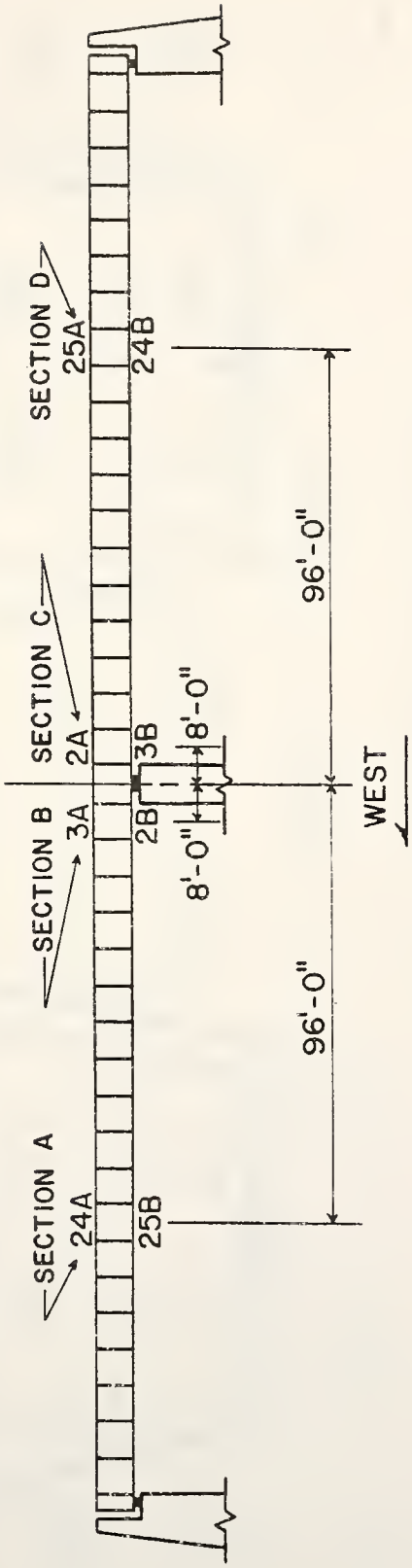

Figure 3.1. Instrumented Segments for Transverse Bending

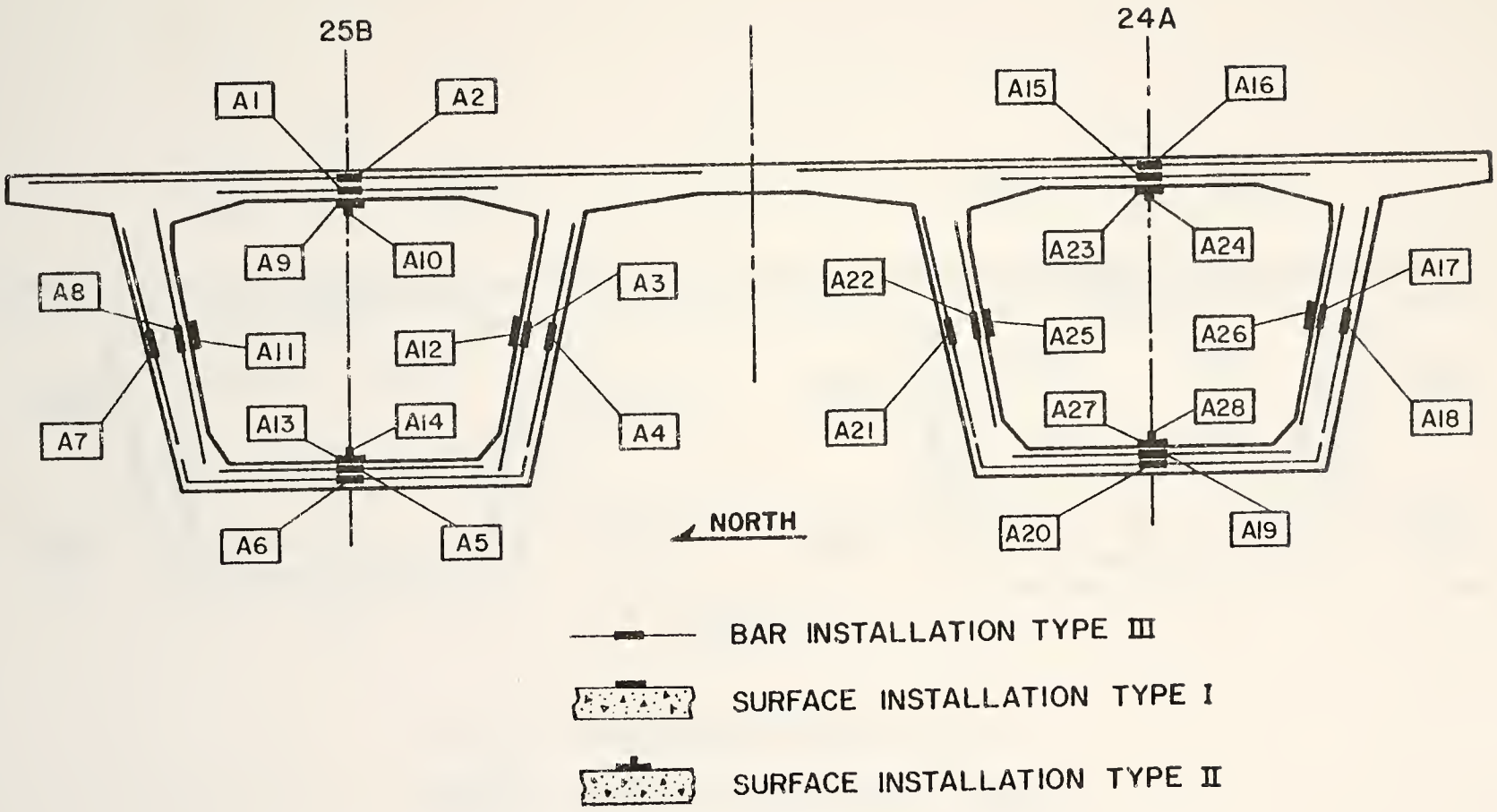

Figure 3.2. Section A Instrumentation

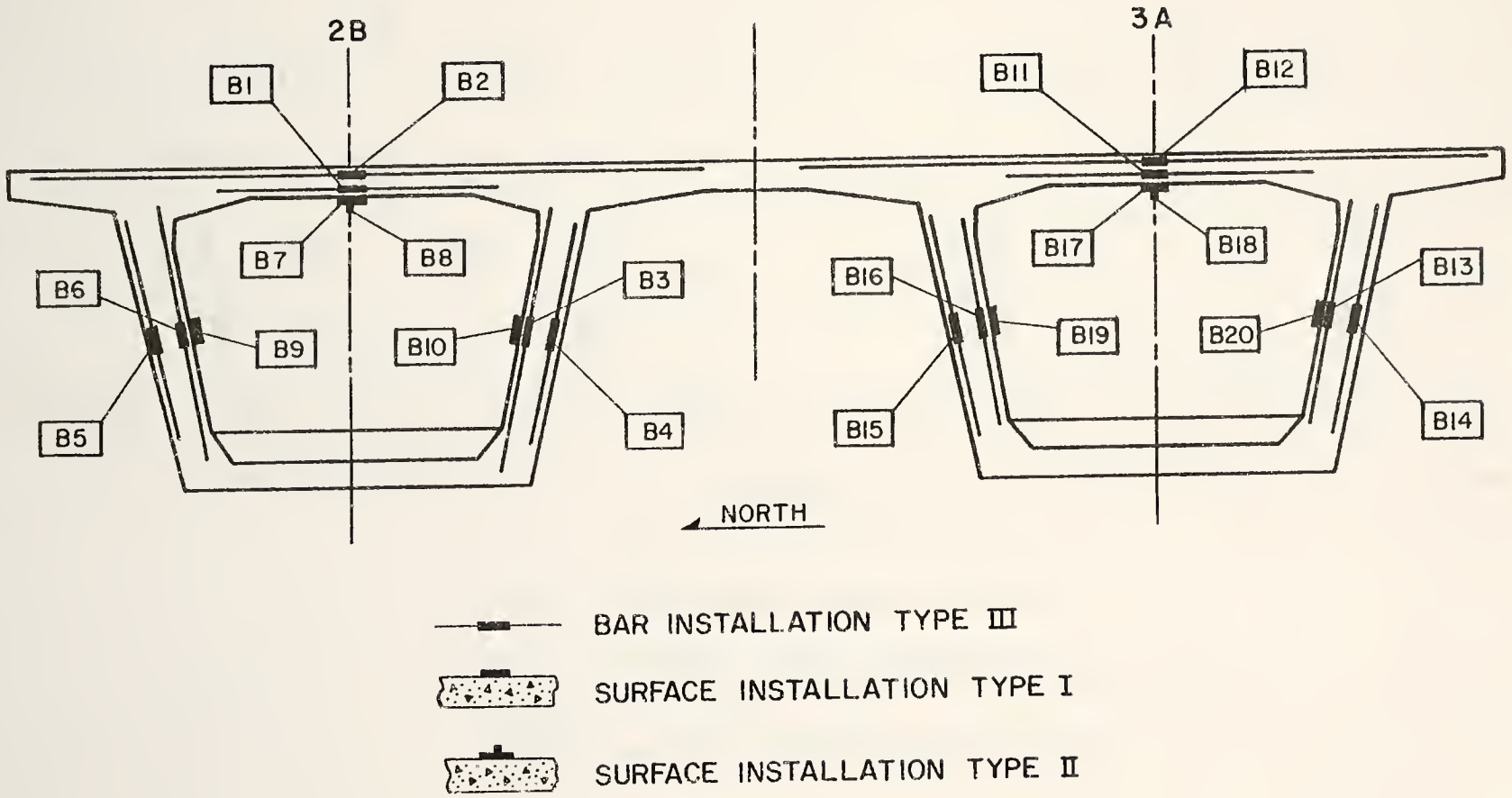

Figure 3.3. Section B Instrumentation

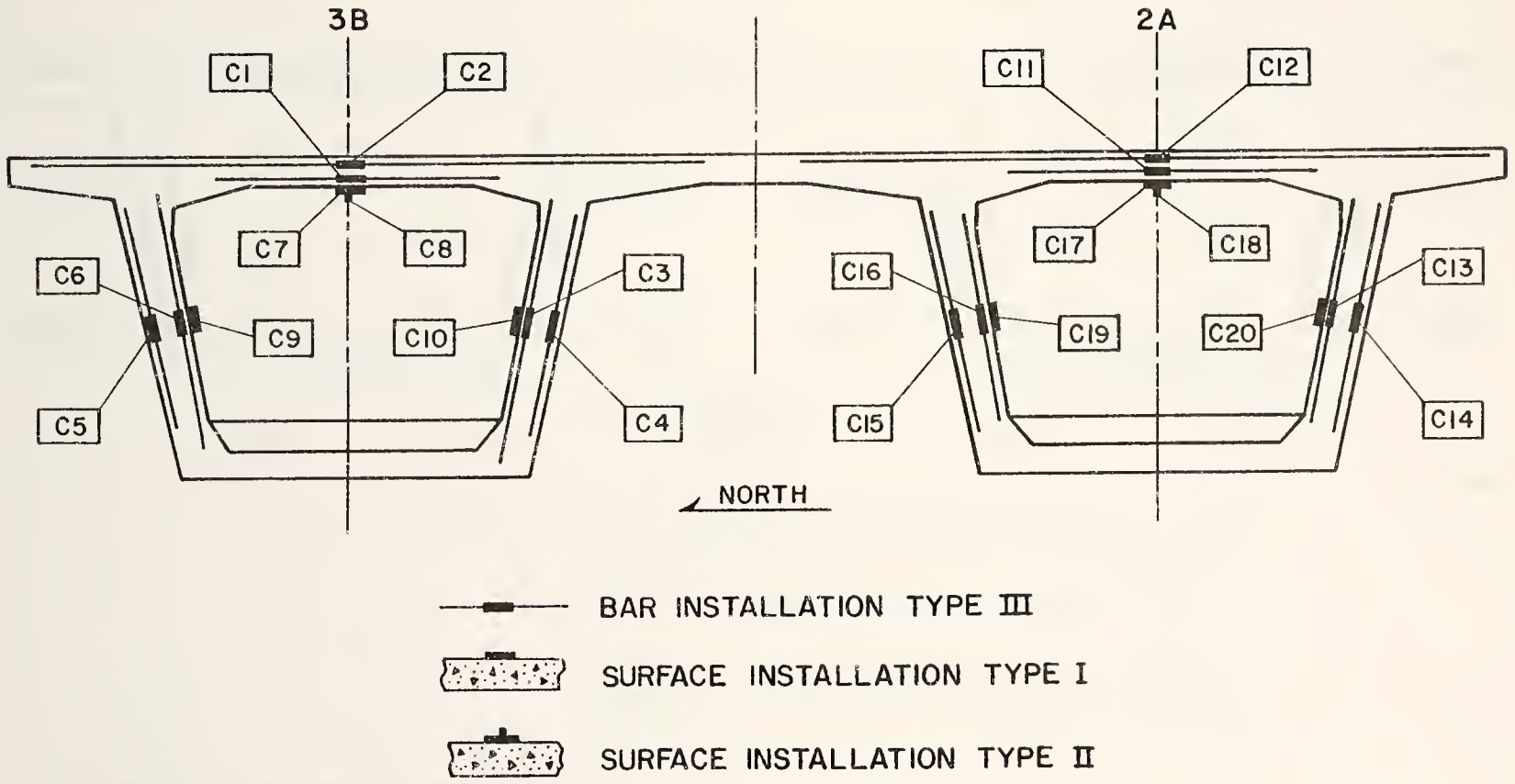

Figure 3.4. Section C Instrumentation

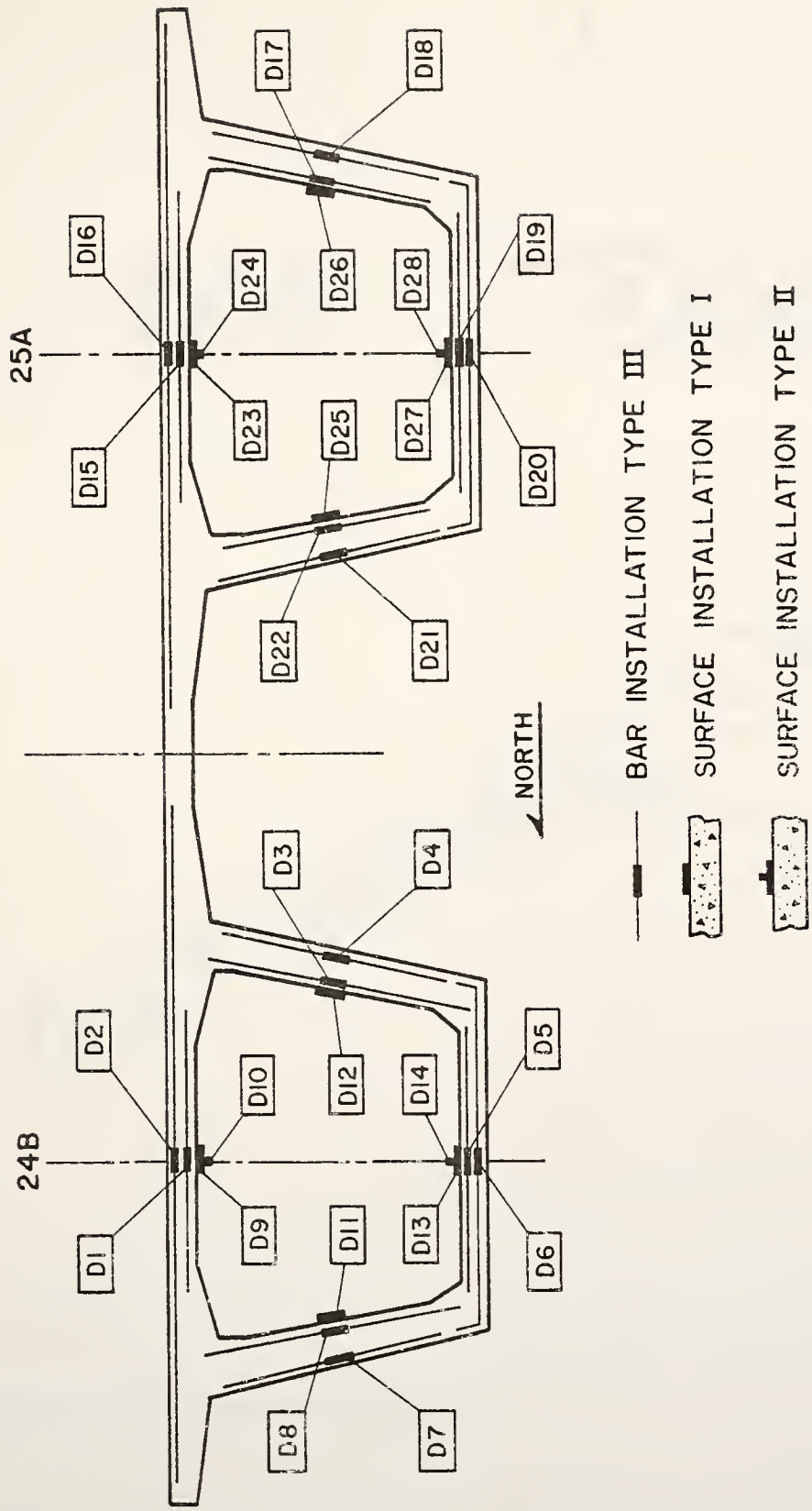

Figure 3.5. Section D Instrumentation

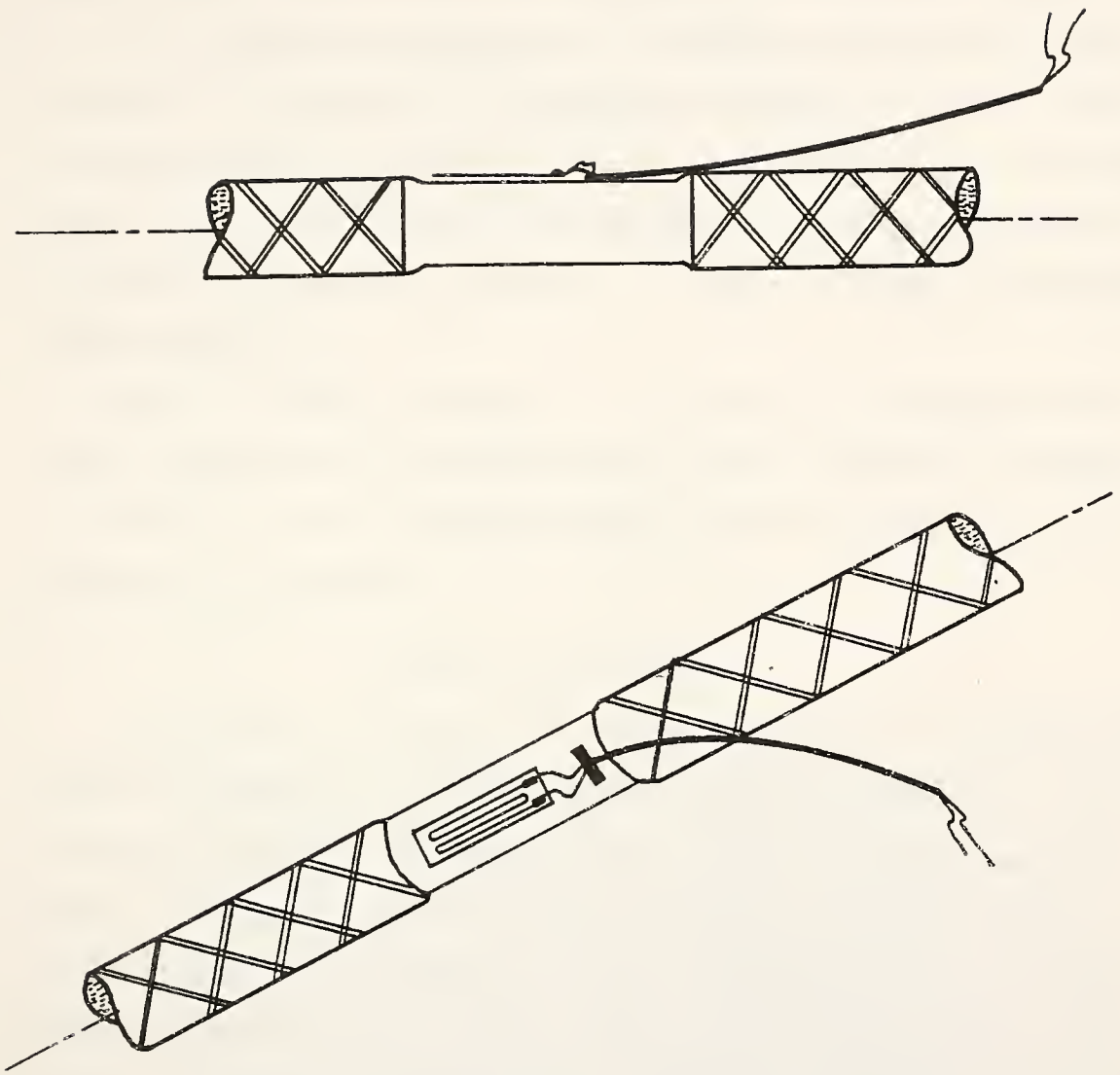

Figure 3.6. Bar Installation Type III

coatings. A latex enamel was applied, followed by a rubber compound coating and a metal foil coating. Finally, the gages were sealed with a joint sealer. Steps of the application procedure are illustrated in Figure 3.8

The instrumented reinforcing bars were taken to Construction Products Corporation and assembled into place during the cage fabrication. Examples of web and slab installations are shown in Figures 3.9 and 3.10, respectively. The lead wires were enclosed in a small length of conduit and protected by Styrofoam as illustrated in Figure 3.11. Figure 3.12 shows an instrumented segment being cast.

After the segments had cured, the lead wires were extracted and the voids created by the Styrofoam were patched with a mortar mix (see Figures 3.13 and 3.14). The instrumented segments were then stockpiled until they were needed for erection.

Concrete Surface Gages

The concrete surface gages are included in the system to provide more complete information on strain distribution through the thickness at the instrumented sections. On the web surfaces, gages are located near the neutral axis of the box girder and are therefore in a low longitudinal stress field. Thus, corrections for transverse sensitivity of the strain gages are unnecessary and a single transverse surface gage (Type I installation) is adequate (see Figure 3.15). Essentially, transverse sensitivity is the error in gage output caused by strain transverse to the longitudinal gage axis. The surface gages on the top and bottom slabs are located in relatively high longitudinal stress fields. Therefore, data collected from these gages must be adjusted, or corrected, to account for transverse sensitivity. In order to make this correction, a longitudinal gage is

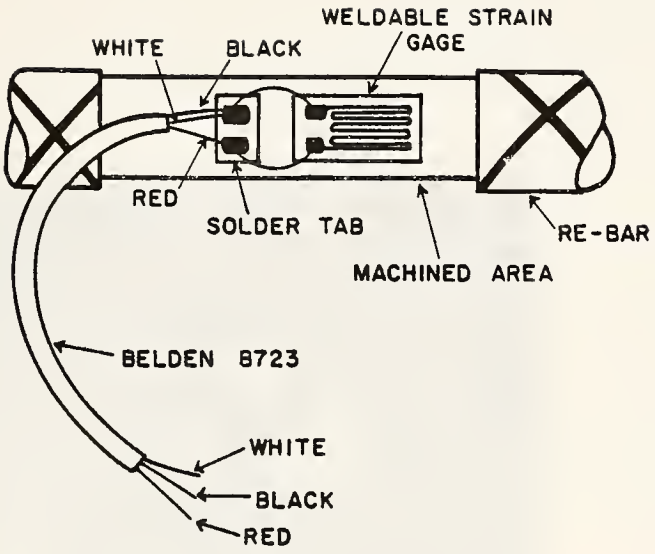

Figure 3.7. Details of Bar Gage Installation

Figure 3.8. Steps in Application of Bar Gages

Figue 3.9. Web Bar Gage Installation

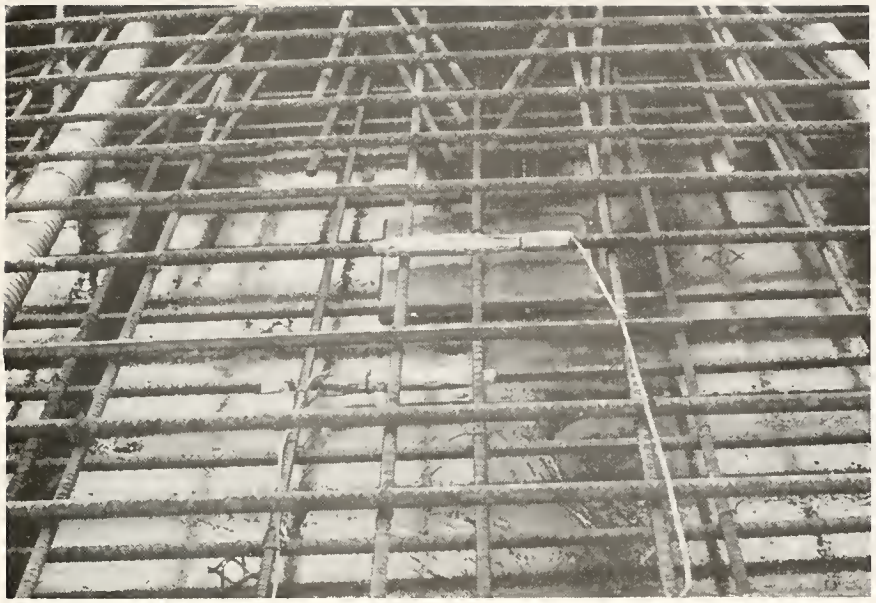

Figure 3.10. Slab Bar Gage Installation

Figure 3.11. Lead Wires Enclosed

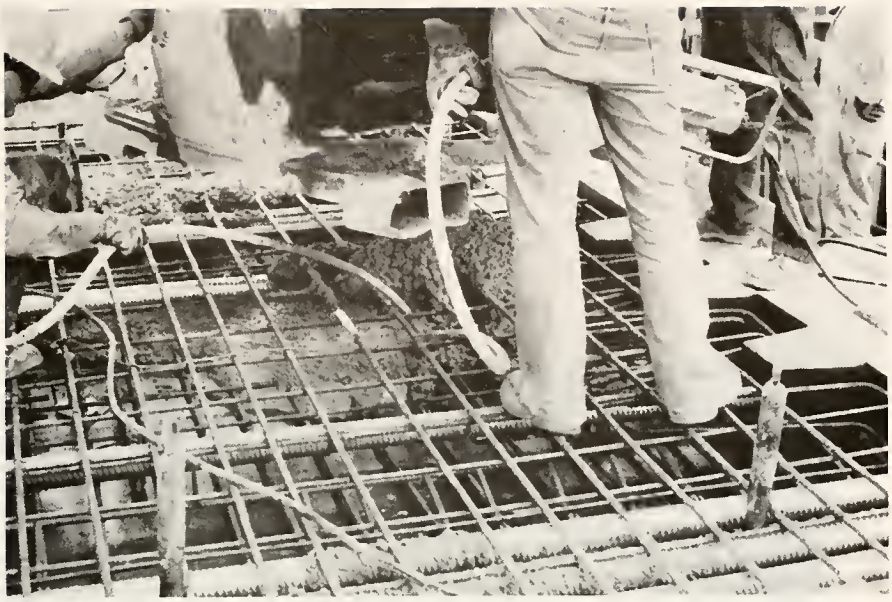

Figure 3.12. Casting Instrumented Segment

Figure 3.13. Lead Wires Extracted

Figure 3.14. Void Patched

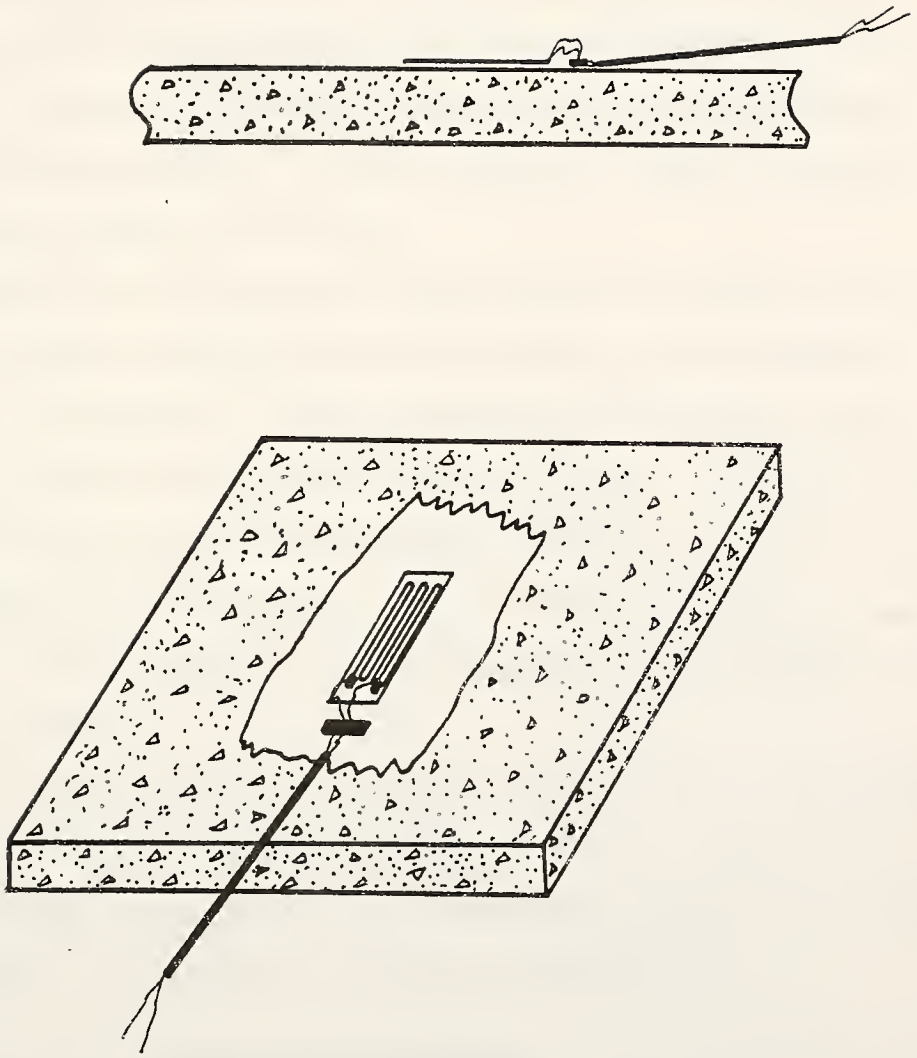

Figure 3.15. Surface Installation Type I

placed adjacent to the transverse gage to measure longitudinal strain intensity. This arrangement is called a Type II surface installation (see Figure 3.16). For further details on the transverse sensitivity correction, reference is made to Holman's report[4].

The surface gages were installed at Construction Products Corporation while the segments were stockpiled. Foil-back electrical resistance strain gages from Micro-Measurements were employed and wired with three-wire leads. These particular gages, which have a two inch gage length pattern, are made especially for use on concrete. Details of the gage installation are shown in Figure 3.17.

The surface of the concrete, in the areas where the gages were to be applied, was sanded, cleaned and then sealed with an epoxy coating as illustrated in Figure 3.18. When the sealant had cured, another epoxy coating was applied to the bottom surface of the gage. The gage was then aligned and placed on the concrete surface. Pressure was applied to the gage by means of the clamp assembly shown in Figure 3.19 until the epoxy had cured. A teflon sheet and a neoprene pad were used to protect the gage during clamping.

After the gages were wired (see Figure 3.20), a series of waterproofing agents were used for protective purposes. A clear acrylic spray was applied, followed by coatings of a silicone rubber and an acrylic lacquer. This procedure is illustrated in Figures 3.21 through 3.23.

Thermal Instrumentation

The instrumentation used for collection of temperature data is located in the sections corresponding to A and D of Figure 3.24. These transducers are to be used to determine, through experimental measurements

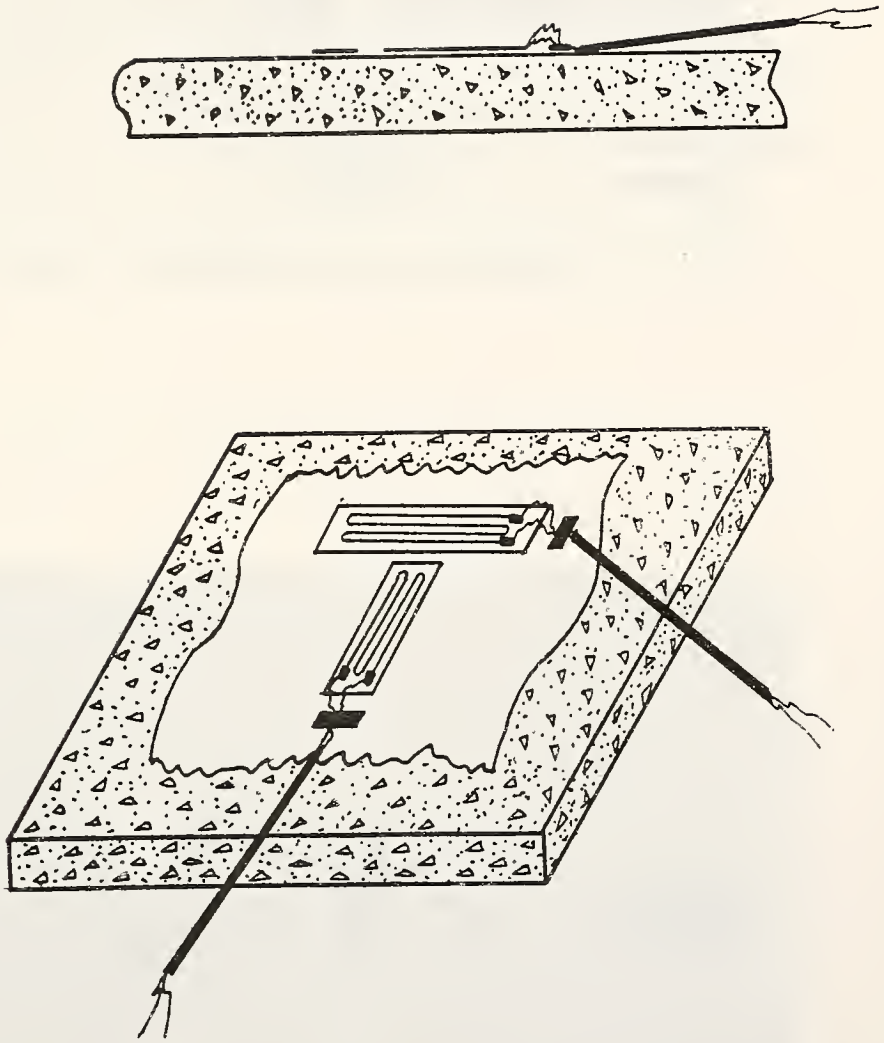

Figure 3.16. Surface Installation Type II

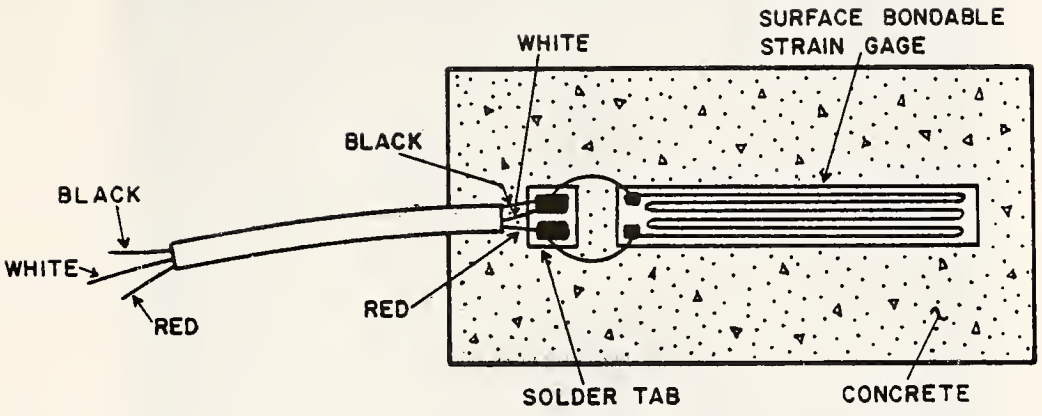

Figure 3.17. Details of Surface Gage Installation

Figure 3.18. Surface Sanded, Cleaned and Sealed

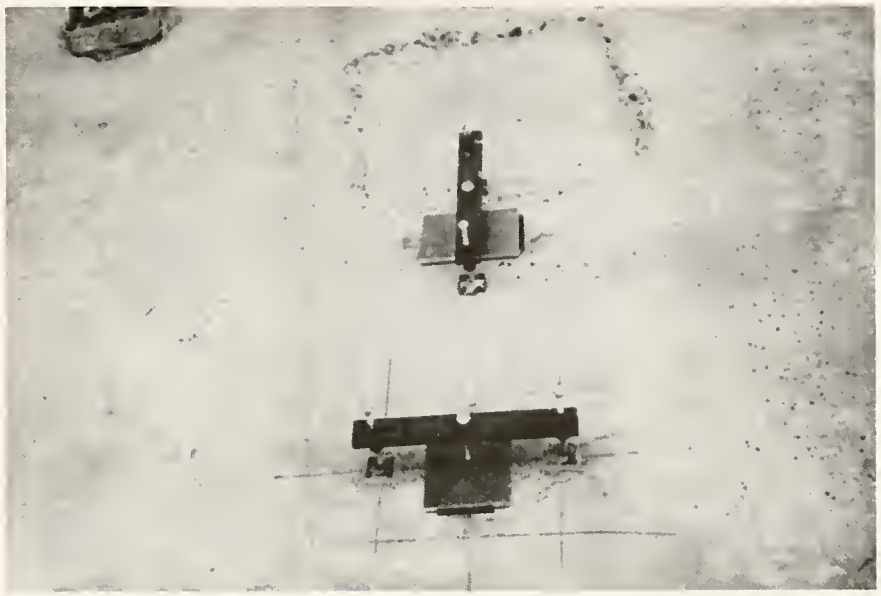

Figure 3.19. Clamping Assembly

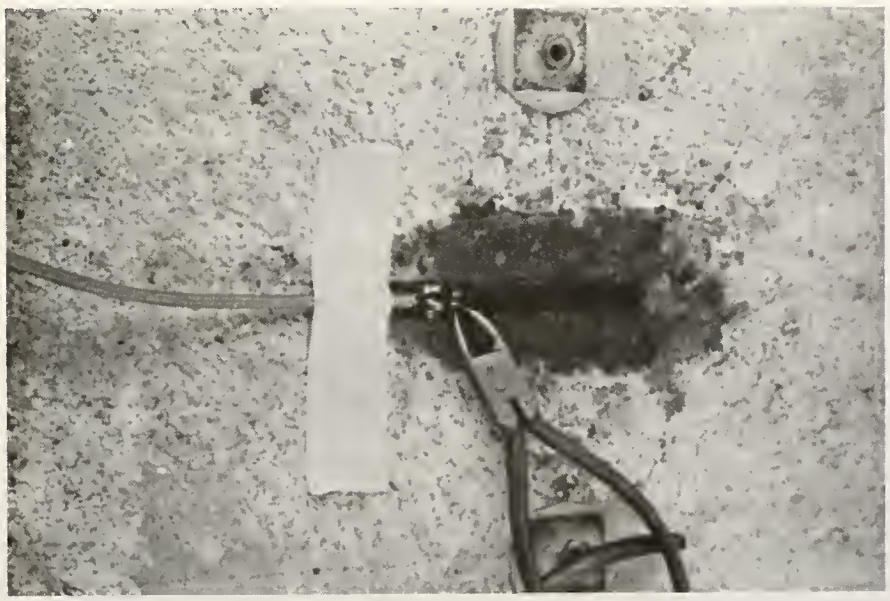

Figure 3.20. Surface Gage Wired

Figure 3.21. Clear Acrylic Spray Applied

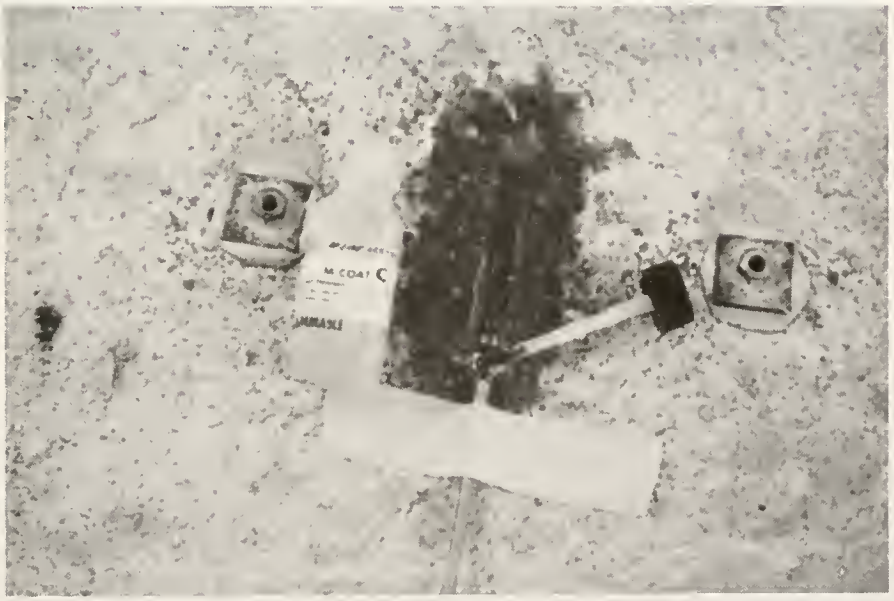

Figure 3.22. Silicone Rubber Applied

Figure 3.23. Acrylic Lacquer Applied

daily and seasonal variations in temperature distributions through the bridge depth at these sections. The longitudinal and transverse deformations and stresses due to these temperature distributions, both during construction and in the completed structure, are of considerable interest. The following sections describe the procedure used to install the temperature transducers. Engineering data pertaining to thermal instrumentation are presented in Appendix B.

Original Design Implementation

Installation of the original instrumentation scheme designed and reported by Holman[5] took place at Construction Products Corporation. While the reinforcement cages were being assembled, Thermilinear temperature probes, or thermistors, manufactured by Yellow Springs Instrument Co. (Yellow Springs, Ohio), were installed. Four YSI 701 general purpose thermistors were placed at each of the test sections (D and A) as illustrated in Figures 3.25 and 3.26.

The thermistors (see Figure 3.27) were wired in place at mid-depth of the segment slabs prior to casting as shown in Figure 3.28. The lead wires were encased in a section of conduit and capped with a Styrofoam plug for protection (see Figure 3.29). Figure 3.30 shows an instrumented segment being cast.

After the forms were stripped, the Styrofoam plugs were removed giving access to the thermistor lead wires from inside the box section. The voids were patched with a mortar mix and the instrumented segments were stockpiled until they were needed for erection.

Additional Instrumentation

The original instrumentation scheme admits the gathering of temperature

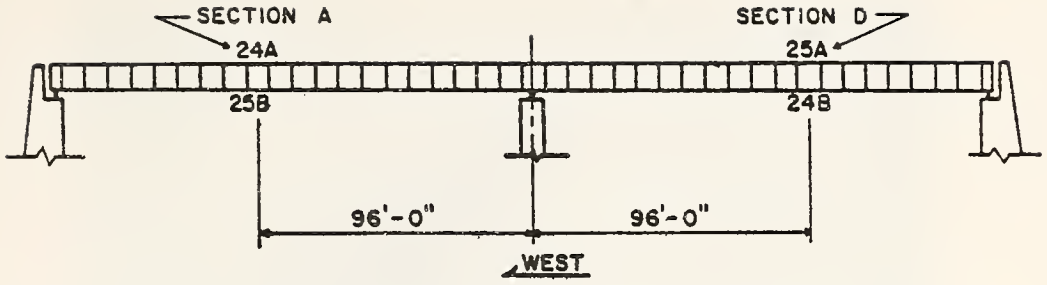

Figure 3.24. Instrumented Sections for Temperature Measurement

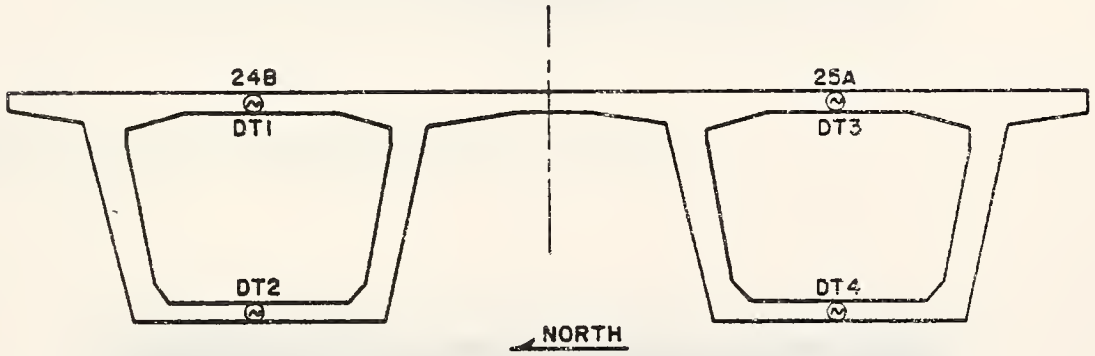

Figure 3.25. Section D

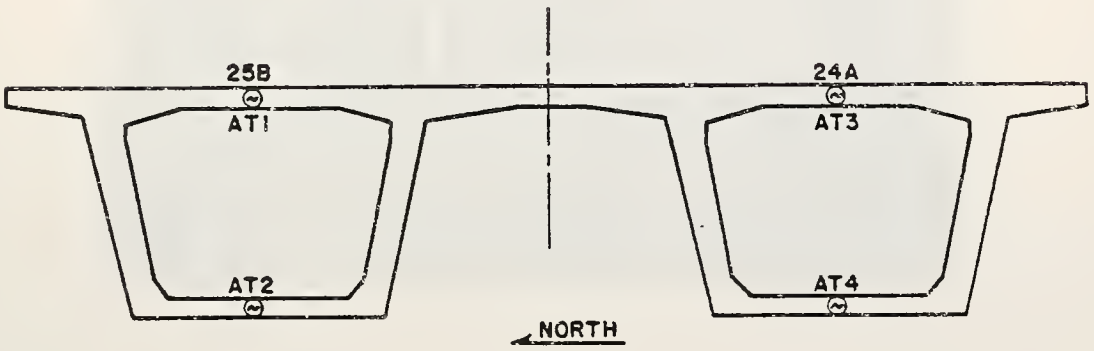

Figure 3.26. Section A

Figure 3.27. YSI 701 General Purpose Thermistor

Figure 3.28. Thermistor Installation

Figure 3.29. Lead Wire Encased

Figure 3.30. Instrumented Segment Being Cast

samples from the top and bottom slabs of the instrumented segments. In order that present design assumptions concerning non-linear temperature gradients through the box girders[6] might be checked, additional instrumentation has been installed. As illustrated in Figure 3.31, six thermistors were placed in the webs of one segment at each test section in order to permit collection of more complete information regarding the temperature distribution through the bridge depth.

Installation of the additional temperature instrumentation was carried out at the bridge site after the bridge was constructed. Holes were drilled in the webs of segments 24B and 25B to accomodate the thermistors. The thermistors were placed at approximately mid-thickness and the holes were grouted. Steps in the installation procedure are illustrated in Figures 3.32 through 3.34. Further detail concerning the location of the thermistors is presented in Appendix C.

Transducer Wiring

To facilitate the data collection procedure, all of the strain gage and thermistor leads were spliced and extension wires were routed to a central junction box in the pier segment of the north girder. From this location, data acquisition systems are used to monitor strain and temperature response of the instrumented segments during the testing operations.

The lead wires are protected by a system of electrical junction boxes and conduit. Junction boxes were glued with epoxy cement to the concrete at each transducer lead location (see Figure 3.35). In order to prevent localized stresses in the area around the concrete surface gages, the junction boxes were bolted to the surface at only two points as illustrated in Figure 3.36. Flexible conduit was then placed between the junction

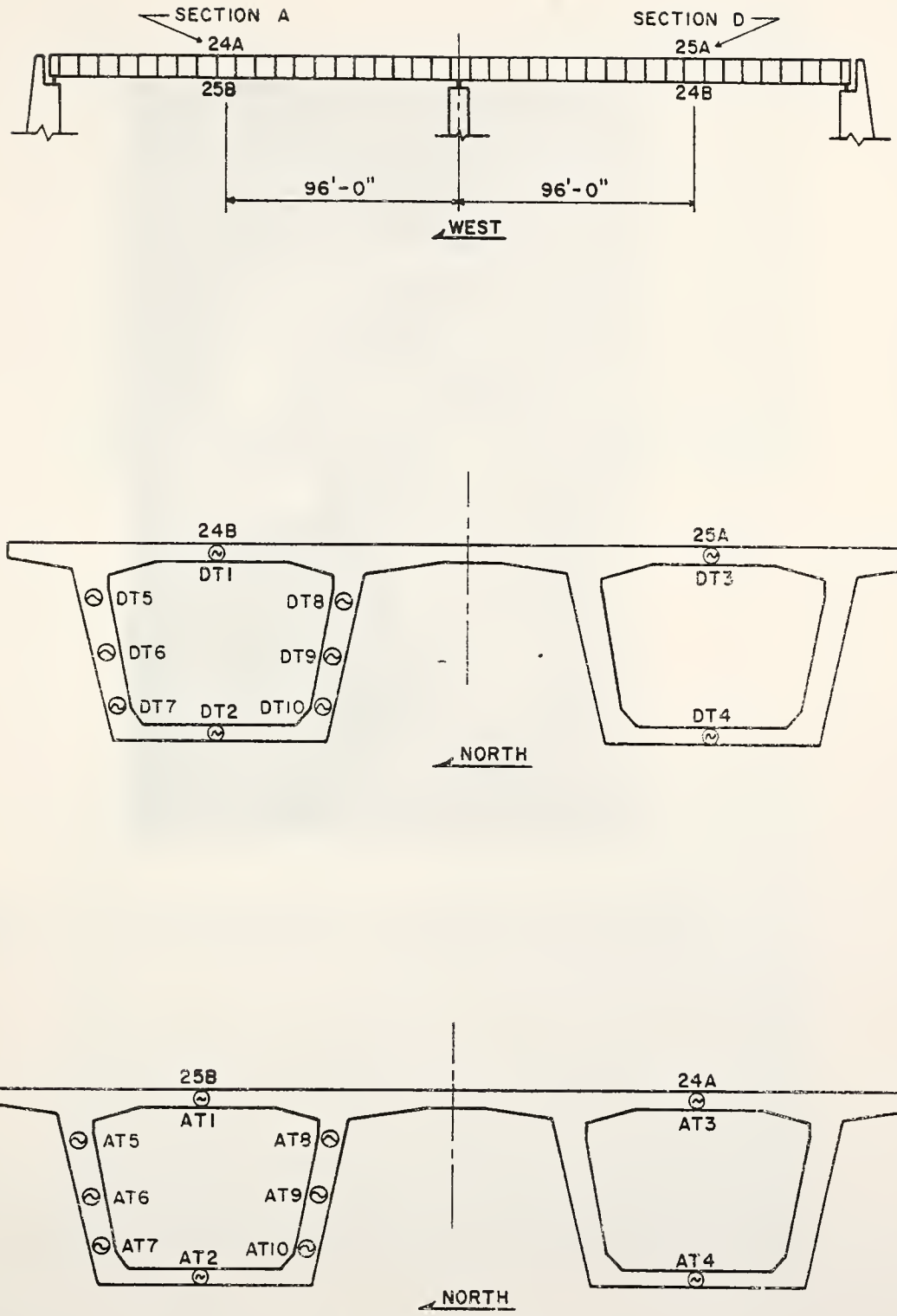

Figure 3.31. Additional Thermal Instrumentation

Figure 3.32. Drilling Holes for Additional Thermistors

Figure 3.33. Thermistor in Place

Figure 3.34. Grouting Hole

Figure 3.35. Instrumented Area Protected by Electrical Junction Boxes

Figure 3.36. Top Slab of Instrumented Segment

boxes, joining them to a common box as seen in Figures 3.37 and 3.38. From the common box at each instrumented segment, thinwall conduit was run to the central junction box (see Figure 3.39). Figure 3.40 shows the conduit extending between the girders so that the leads from the instrumentation in the south girder could be routed to the central junction box.

After the transducer leads were appropriately tagged (see Figure 3.41), they were spliced to extension lead wires. The soldered joints were protected with heat-shrink tubing as illustrated in Figures 3.42 and 3.43. The wires were then pulled through the conduit to the central junction box (see Figure 3.44). Strain gage leads were stripped and tinned, as seen in Figure 3.45, to permit easy attachment to the gage blocks of the data acquisition systems used during transverse bending tests. Jack plugs were soldered to the thermistor leads to make them compatible with the external instrumentation used for temperature measurement. Engineering data concerning gage and thermistor leads is presented in Appendix C.

Long-Term Deformation Instrumentation

Long-term deformations due to creep and shrinkage are important factors which must be considered when designing concrete structures. Measurement of these effects on the Turkey Run bridge is an objective of this phase of the research. Accordingly, the bridge has been instrumented so that strain and deflections can be monitored periodically at key locations.

Whittemore Instrumentation

The instrumentation used for determining long-term longitudinal strains is located at the sections indicated in Figure 3.46. Three sets of implants were epoxied to the inside surface of the top and bottom slabs of each instrumented segment. These implants consist of two square metal

Figure 3.37. Conduit Protecting Strain Gage Leads

Figure 3.38 Thermistor Leads in Conduit

Figure 3.39. Conduit Running to Pier Segment

Figure 3.40. Conduit Extending Between North and South Girders

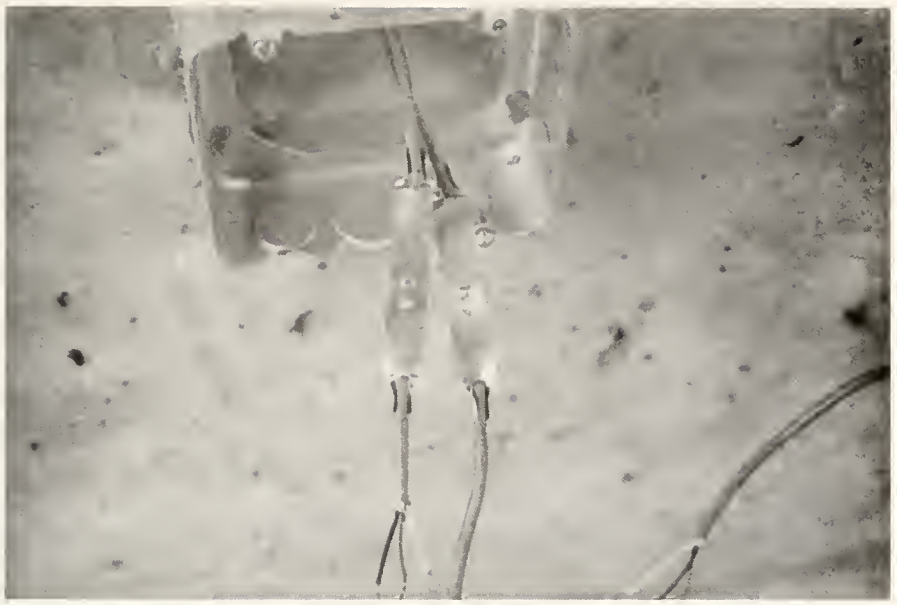

Figure 3.41. Transducer Leads Tagged

Figure 3.42. Soldered Wires Protected with Heat-Shrink Tubing

Figure 3.43. Splice Completed

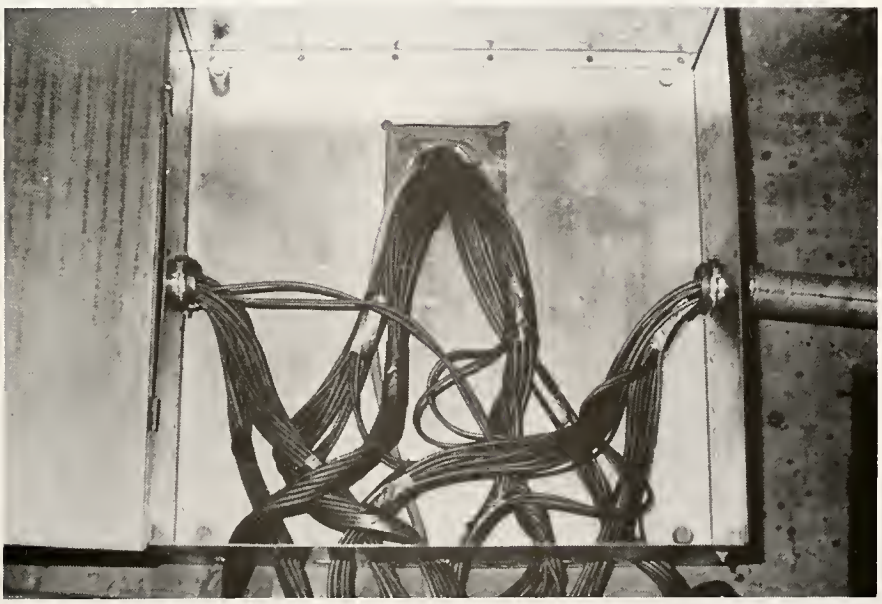

Figure 3.44. Lead Wires Running into Central Junction Box

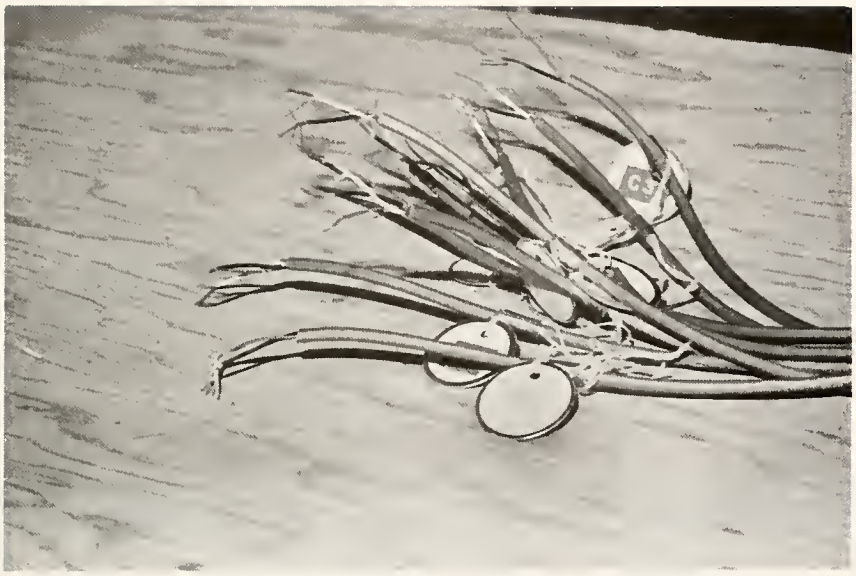

Figure 3.45. Strain Gage Leads Stripped and Tinned

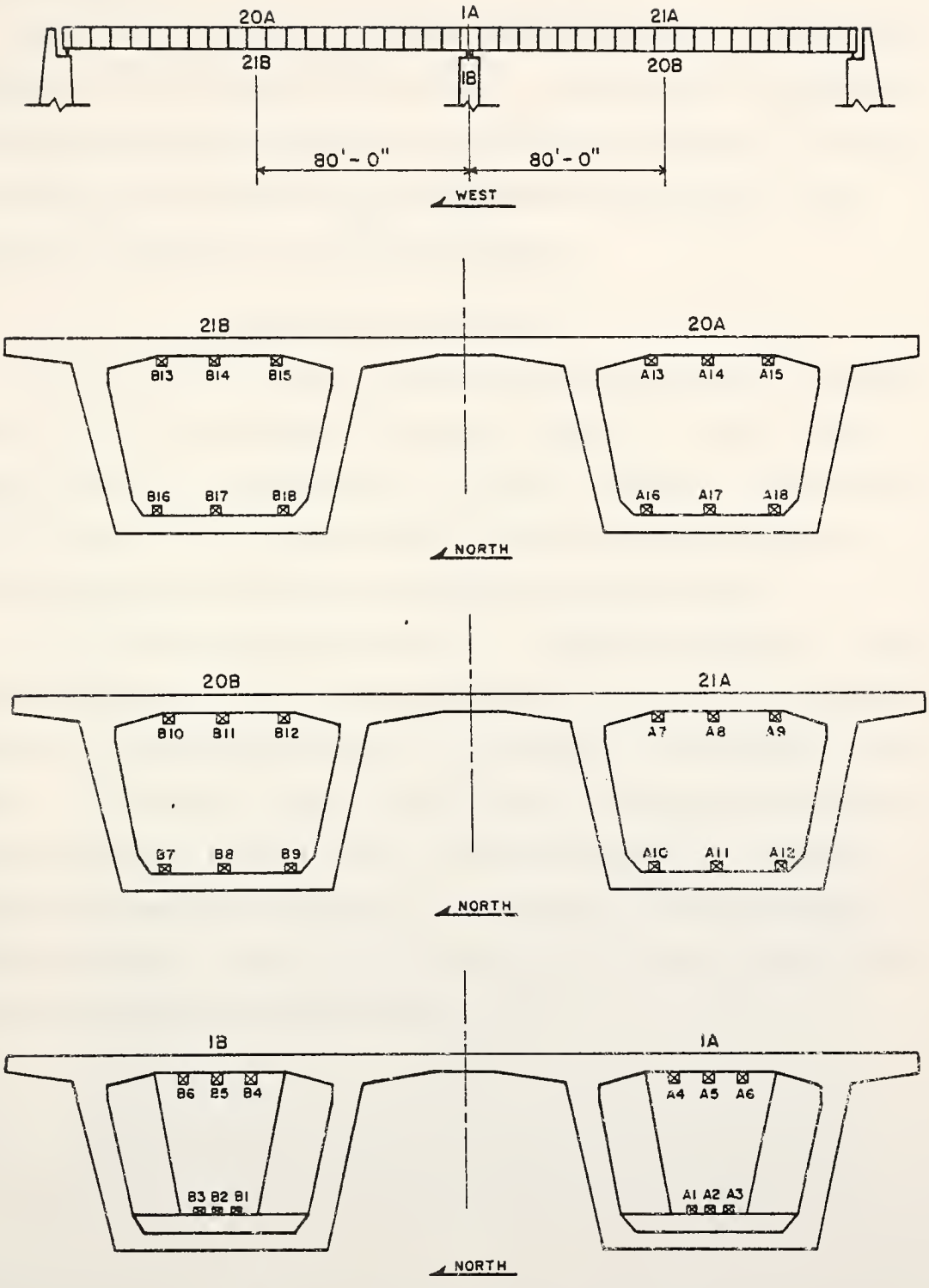

Figure 3.46. Instrumented Sections for Long-Term Strain

plates located approximately ten inches apart as illustrated in Figures 3.47 and 3.48.

Holes were drilled in the plates to permit the use of a Whittemore mechanical strain gage (see Figure 3.49). The Whittemore gage measures the distance between the holes to the nearest ten thousandth of an inch. The strain in the concrete is then determined as the quotient of the change in length and the original gage length.

Deflection Instrumentation

The instrumentation used to measure bridge deflections is located at the sections corresponding to those of Figure 3.50. Three implants were placed on the bridge deck at the center of each span. Implants are also located at the pier and abutment sections to provide a reference for determining relative deflections of the midspan sections.

Each deflection implant consists of a square metal plate with a nut welded to the top surface as shown in Figures 3.51 and 3.52. These implants are used as base plates for a Philadelphia rod when taking elevations. A Zeiss Ni-2 automatic level is used to measure the elevations of the deflection implants with a resolution of 0.005 ft. Elevation measurements are made with respect to a permanent benchmark embedded in the west abutment of the bridge (see Figure 3.53). Midspan deflections are then determined from the elevation data.

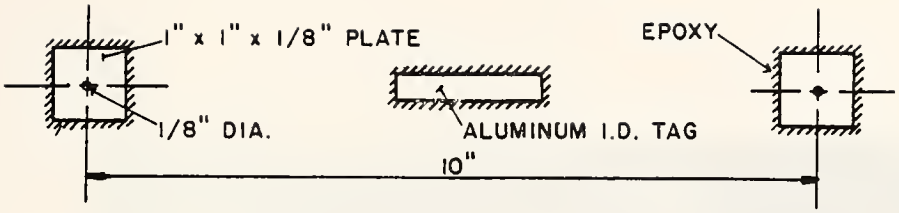

Figure 3.47. Whittemore Strain Gage Implant

Figure 3.48. Instrumented Segment

Figure 3.49. Measuring Strain with Whittemore Gage

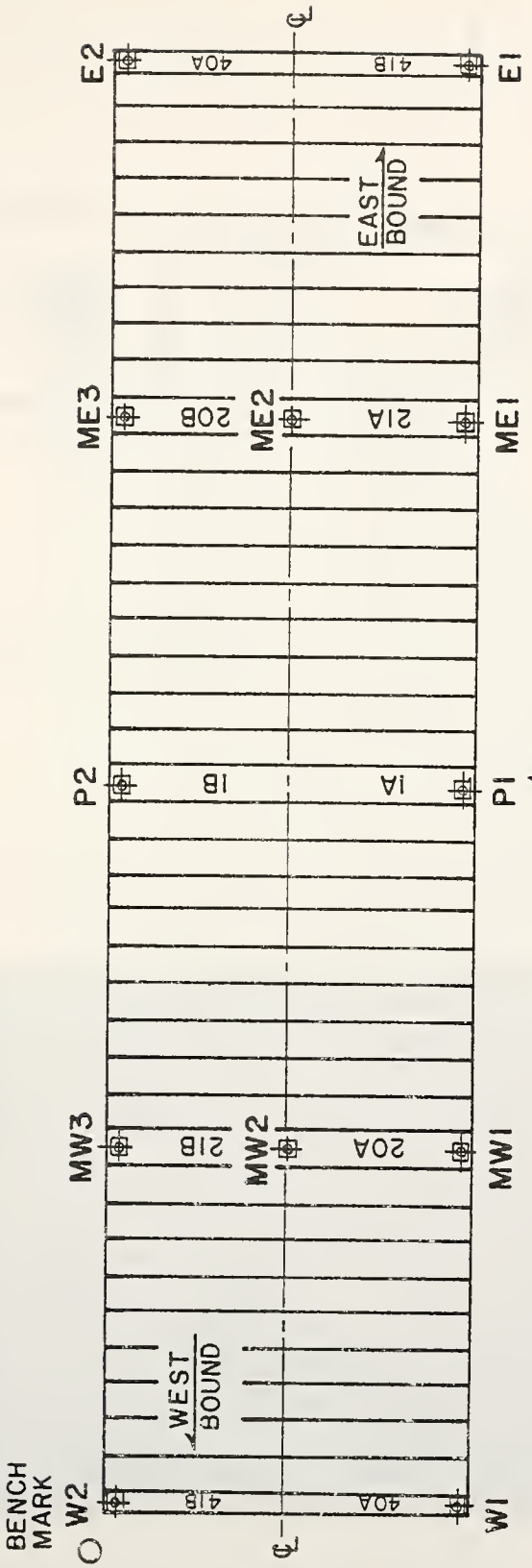

Figure 3.50. Instrumented Sections for Long-Term Deflections

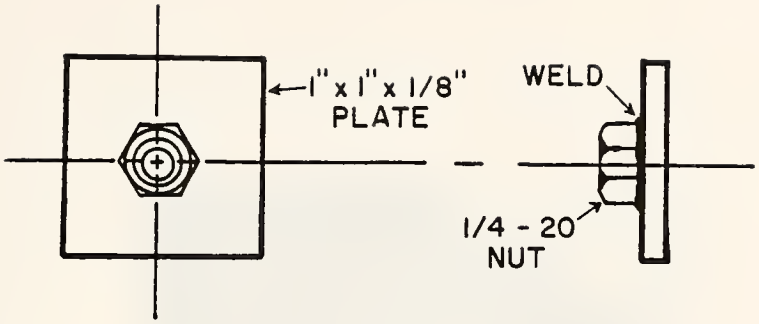

Figure 3.51 Deflection Implant

Figure 3.52. Base Plate on Bridge Deck

Figure 3.53. Permanent Benchmark on Bridge Abutment

NOTES

1 Holman, R. J., "Development of an Instrumentation Program for Studying Behavior of a Segmental Concrete Box Girder Bridge", Joint Highway Research Project 77-4, Purdue University, March 2, 1977.

2 Ibid., pp. 58-59.

3 Ibid., pp. 73-74.

4 Ibid., pp. 71-72.

5 Ibid., pp. 88-92.

6 Post-Tensioning Institute/Prestressed Concrete Institute, Precast Segmental Box Girder Bridge Manual, 1978, p. 41.

CHAPTER IV

TRANSVERSE BENDING

Introduction

In conventional concrete deck girder bridges, wheel loads are delivered to multiple girders directly and by slab action. Each girder behaves independently in the transverse direction with the only secondary distortions resulting from continuous slab action. Segmental box girder bridges differ considerably in that they require relatively high torsional and transverse stiffness for load transfer into the webs and supports. As a result, significant transverse stresses can occur in the webs as well as the top and bottom slabs of the segments[1]. To establish proper section and element proportions and design the transverse reinforcement system for a box section, it must be possible to predict transverse bending tractions with acceptable accuracy.

Analytical predictions of the transverse bending tractions produced by prescribed loadings have been obtained for the Turkey Run bridge using two independent elastic analysis methods. Details of the finite element analysis and a modified frame analysis used to approximate the transverse flexural response have been presented by Holman[2].

This chapter is concerned with determining, through experimental measurements, transverse bending responses of the actual structure for the same loadings that were used in obtaining the analytical solutions. A description of the field testing scheme is presented, as well as details

of the data collection and reduction procedures utilized. Bending tractions determined from strain measurements are tabulated so that they may be compared with the analytical predictions.

Material Properties

In order to compute tractions from the strain data collected during experimental testing, the constitutive relationships between stress and strain must be known for the materials involved. Accordingly, extensive testing of sample concrete cylinders and representative transverse steel reinforcing bars has been conducted in the structural laboratory at Purdue University. A regression analysis was performed on the data from each specimen tested. Mean values for strength and modulus of elasticity were determined for the concrete and steel. The following is a description of the testing and data reduction techniques utilized.

Reinforcing Steel Tests

Samples of the transverse reinforcing bars used in the bridge segments were provided by the steel fabricator. Nine, 24 in. specimens were instrumented with electrical resistance strain gages. The test specimens were loaded in tension, during which time the applied load and strain in the bar were monitored.

A linear regression analysis was performed for each specimen using the stress-strain data in order to determine the elastic modulus of elasticity of the steel. The results from the nine tension tests are presented in Table 4.1.

The mean value for the modulus of elasticity was found to be 29.63 x 10^6 psi; this value will be used in all subsequent calculations. The sample standard deviation and coefficient of variation were 315,000 psi and 1.1 percent, respectively.

Table 4.1 Modulus of Elasticity for Steel Test Specimens

SAMPLE NUMBER	MODULUS OF ELASTICITY, E_s (psi)
1	29,520,000
2	29,560,000
3	29,260,000
4	29,920,000
5	29,890,000
6	29,470,000
7	30,060,000
8	29,580,000
9	29,430,000

AVERAGE VALUE (psi)	29,630,000
STANDARD DEVIATION (psi)	315,000
COEF. OF VARIATION (%)	1.1

Concrete Cylinder Tests

During the casting operation at Construction Products Corporation, several test specimens were cast from the same concrete as that used in the instrumented segments. The six inch diameter, 12 in. long test cylinders were steam cured under the same conditions as the bridge segments. The cylinders were then stored with the segments while they were stockpiled in the prestressing yard. When the segments were transported to the bridge site for erection the test specimens were moved to the structural laboratory at Purdue University.

The concrete cylinders were tested in accordance with ASTM C-39 specifications. During the standard compression tests, the strain in the concrete was measured with a compressometer, as shown in Figure 4.1. Once extensive inelastic deformation was observed, the compressometer was removed and the specimen was loaded to failure (see Figure 4.2).

The modulus of elasticity and ultimate strength of each specimen were determined; these values are presented in Table 4.2. The table has been divided into two groups because different mix designs were used. The concrete for segments 2 and 3 was designed to have slightly higher ultimate strength than that of segments 24 and 25. Mean values were computed from this data. Those cylinders which yielded significantly lower strengths because the samples and/or tests were deficient were omitted from the statistical interpretation. The mean, sample standard deviation and coefficient of variation for the modulus of elasticity and ultimate strength are given in Table 4.3.

For purposes of comparison, a plot of ultimate strength versus modulus of elasticity has been constructed (see Figure 4.3). On the same graph, two curves which represent currently recommended equations have also been

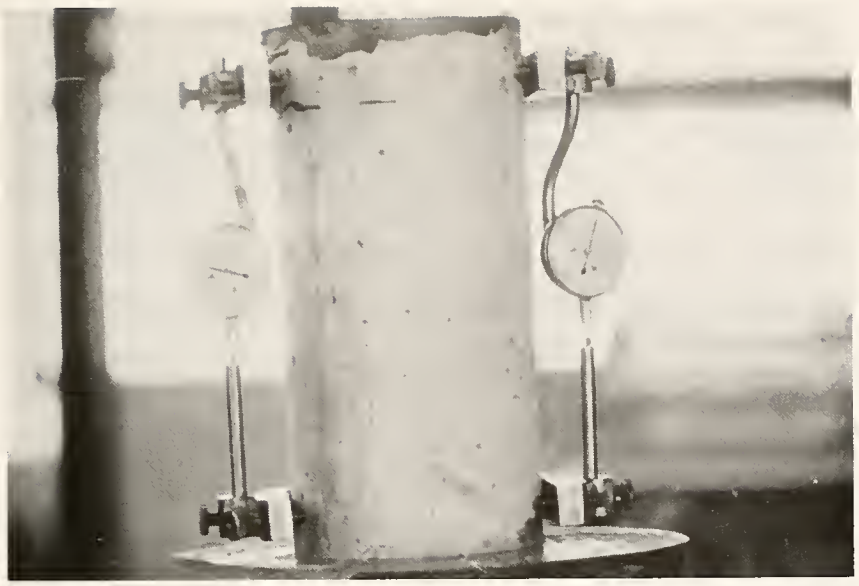

Figure 4.1. Concrete Cylinder with Compressometer Attached

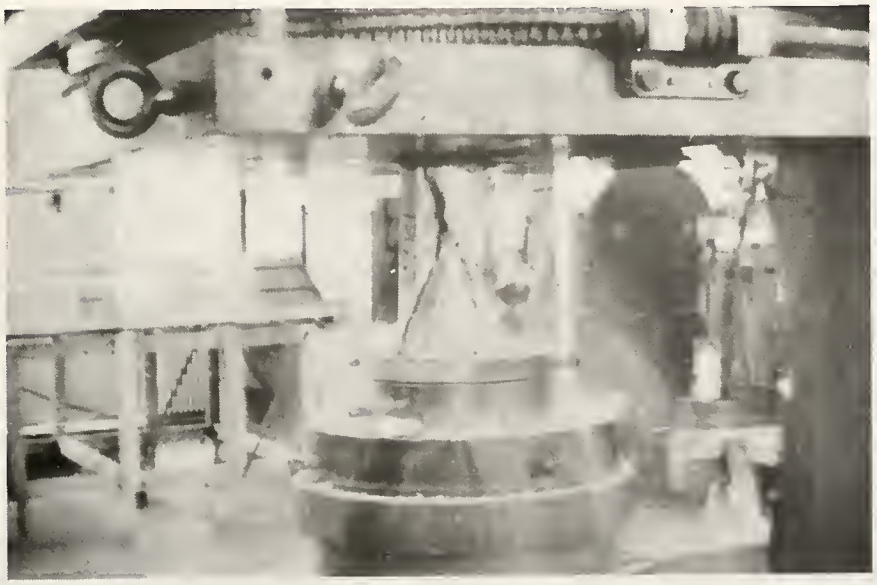

Figure 4.2. Failure of Concrete Cylinder

Table 4.2 Modulus and Ultimate Strength for Concrete Test Cylinders

SPECIMEN CAST FROM SEGMENT	AGE OF SPECIMEN (MONTHS)	MODULUS OF ELASTICITY, E (psi)	ULTIMATE STRENGTH, f'c (psi)
2B	16	4,294,000	7,500
2B	16	4,219,000	7,800
2B	16	4,064,000	7,090
3B	13	4,913,000	6,470
3B	13	3,877,000	6,100
2A	10	3,827,000	7,110
2A	12	4,559,000	6,470
3A	9	4,476,000	8,140
3A	10	3,298,000	5,700
3A	10	4,350,000	7,690
25B	15	3,581,000	6,460
25B	15	4,317,000	6,520
24B	12	4,260,000	7,320
24B	12	4,118,000	6,760
24B	13	3,875,000	7,120
25A	11	4,518,000	7,370
25A	11	3,816,000	7,680
25A	11	4,515,000	6,540
25A	11	4,004,000	6,280
24A	10	4,052,000	6,510
24A	10	3,480,000	6,670
24A	10	4,166,000	6,540
24A	9	4,749,000	7,750

Table 4.3 Concrete Properties

	MODULUS OF ELASTICITY		ULTIMATE STRENGTH	
	SEGMENTS 2 and 3	SEGMENTS 24 and 25	SEGMENTS 2 and 3	SEGMENTS 24 and 25
MEAN (psi)	4.188×10^6	4.112×10^6	7010	6890
STANDARD DEVIATION (psi)	0.450×10^6	0.370×10^6	800	500
COEF. OF VARIATION (%)	10.7	9.0	11.4	7.2

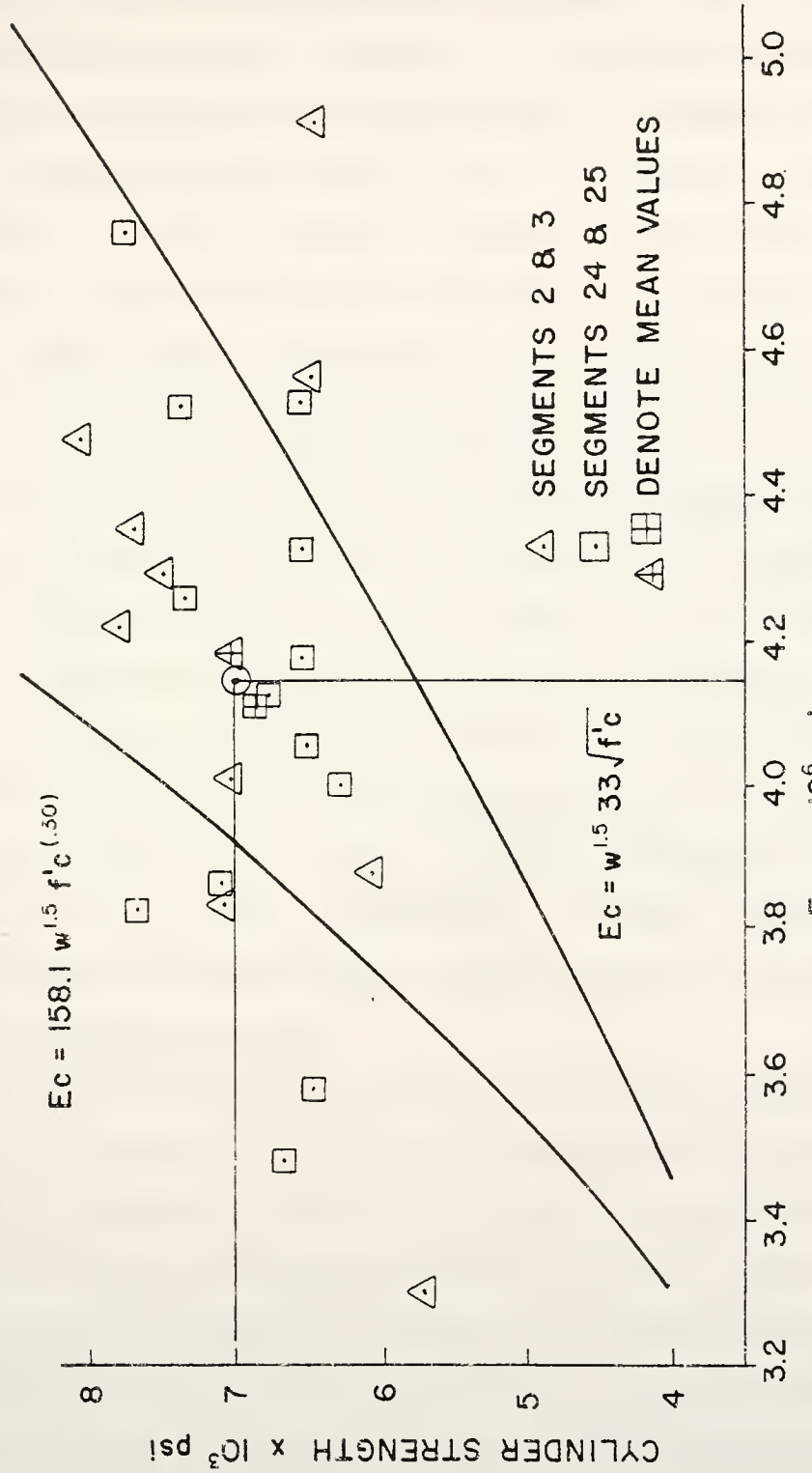

Figure 4.3 Concrete Cylinder Strength vs. Modulus of Elasticity

plotted. The lower curve is that which appears in the ACI Building Code. The upper curve represents an equation suggested by Pauw[3] for determining the modulus of elasticity of concrete. As can be seen from this figure, the mean values from both groups of cylinders lie between the two curves.

Since the mean values are so close to one another, a single average value will be used in subsequent calculations. This average value is denoted by a circle on the plot and corresponds to an ultimate strength of 7000 psi and a modulus of elasticity of 4.15×10^6 psi.

Field Testing Scheme

The static loadings used for the transverse bending tests were produced by a tandem axle sand truck (see Figure 4.4). A schematic drawing of a typical test truck used for this purpose is shown in Figure 4.5. The axle spacings and loads indicated hereon are identical to those which were used in the analysis. It is possible to scale the resulting internal tractions to provide a check on the analytical results if different loads are used, provided that a front to rear axle load ratio of 0.4 is maintained for the test truck. Nevertheless, in order to avoid problems with resolution of strain measurements, loadings which are less than those specified should not be used.

Figure 4.6 illustrates the test truck positions. There are eight transverse positions at each of the four longitudinal test sections. This loading arrangement is similar to that used in the finite element analysis with the exception of transverse positions 1 and 8. At these locations it is physically impossible to duplicate the loading used for the analytical solution because of the curb and railing on the bridge deck and the fixed axle dimensions of the test vehicle. The concentrated loads used

Figure 4.4 Tandem Axle Sand Truck

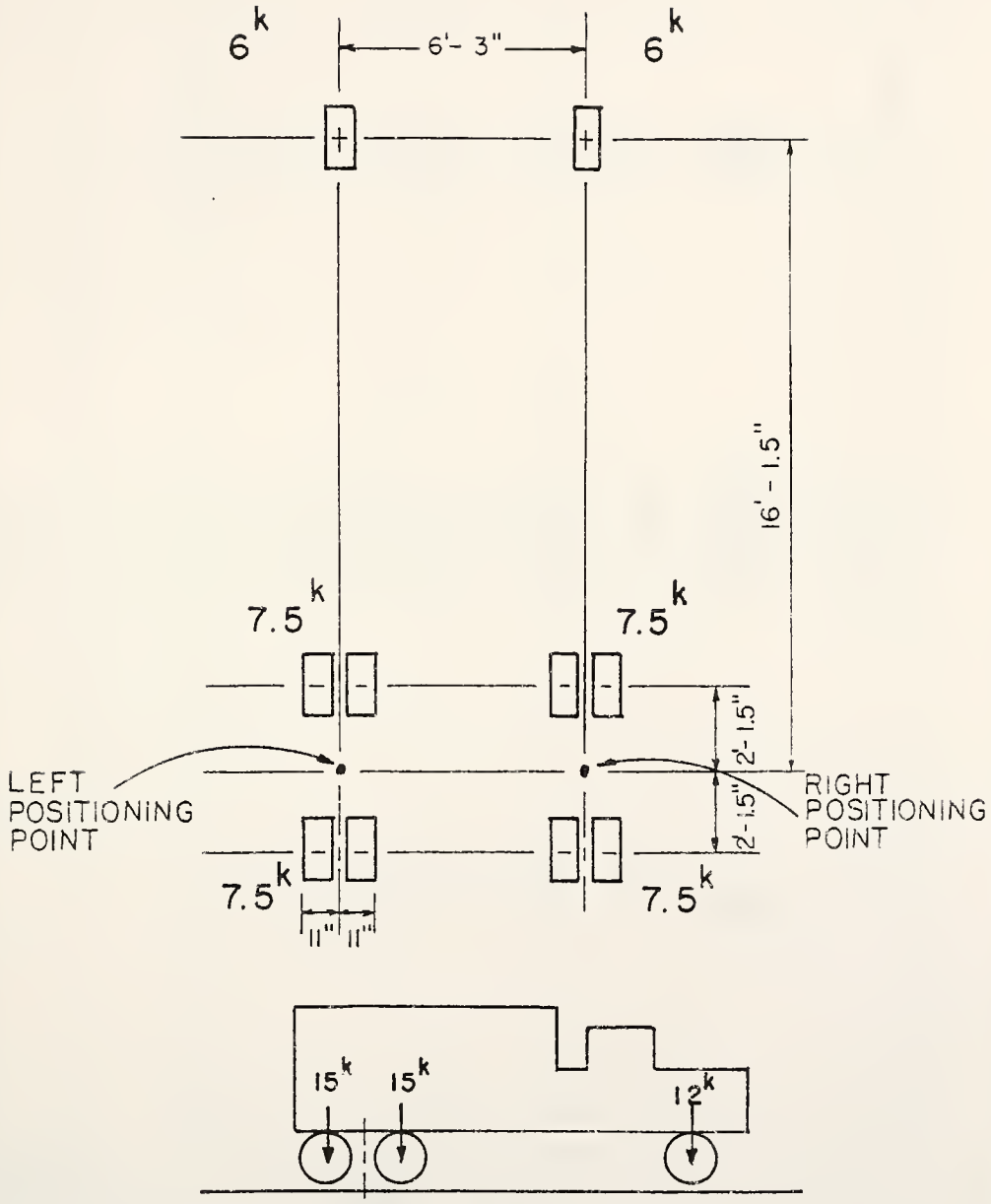

Figure 4.5 Test Truck Axle Loads and Spacings

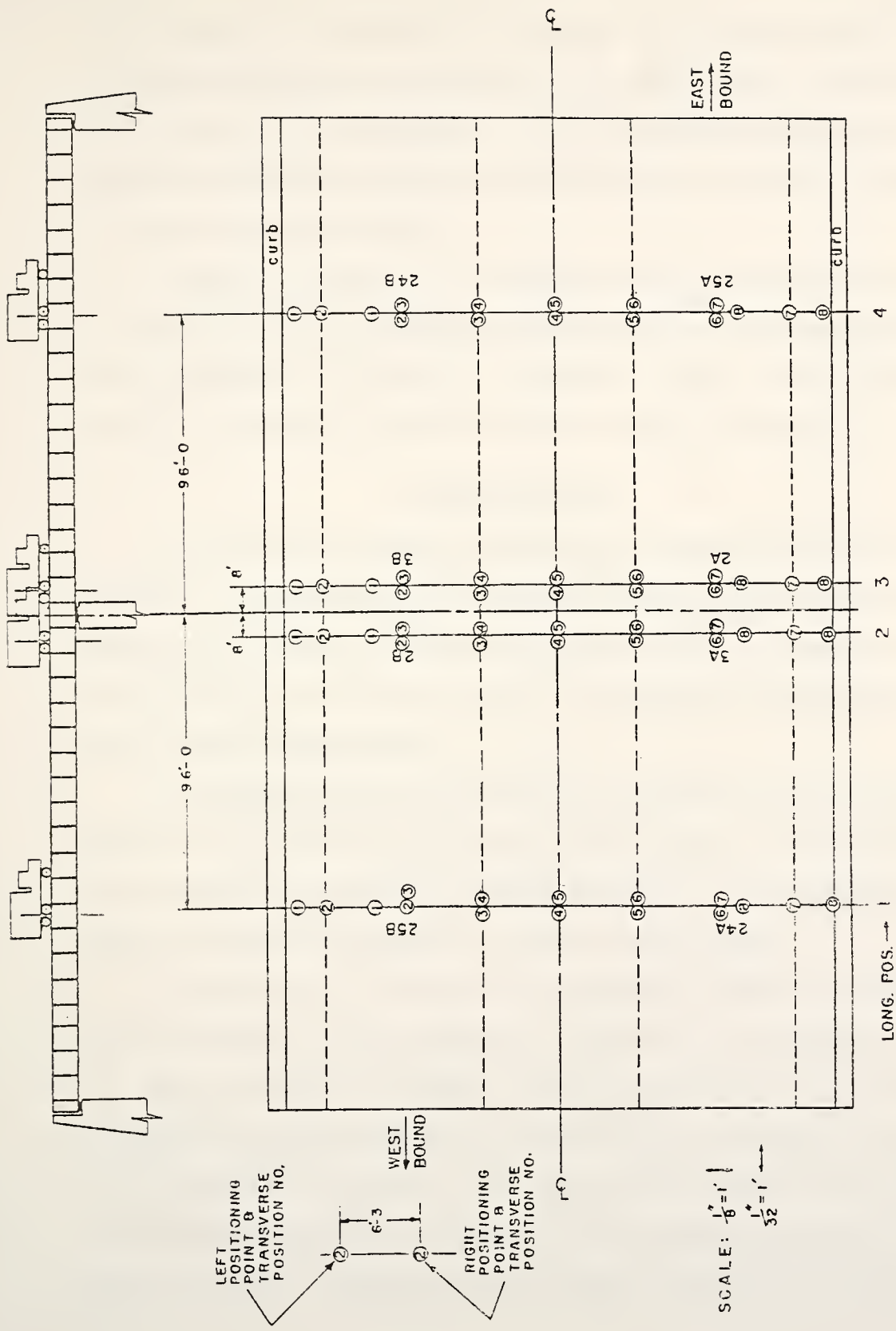

Figure 4.6 Longitudinal and Transverse Truck Positions

for the analytical solutions were located at the outside edge of the cantilevered top slab and over the outside web, corresponding to nodal coordinates of the finite element mesh. For this reason, meaningful direct comparisons cannot be made between test results and analytical solutions for these loading positions.

Figures 4.7 through 4.10 illustrate the exact transverse positions of the test truck. These test locations have been permanently marked on the bridge deck (see Figures 4.11 and 4.12). They are used to locate the center of each set of four rear wheels, as shown in Figure 4.13.

Preliminary Test

A preliminary transverse bending test was conducted during the summer of 1979. The purpose of this study was to verify that the strain gages were working properly, to measure the strain levels at several key locations on the structure and to identify and remedy any problems which might occur during future testing.

The tandem axle sand truck which was used had a gross weight of 47,900 pounds and a front to rear axle load ratio of 0.401. The truck was weighed at the gravel pit operated by Western Materials, Inc. in Montezuma, Indiana, where the sand was obtained (see Figures 4.14 and 4.15).

During the test, the truck was sequentially placed in all eight transverse positions at both longitudinal position 1 and longitudinal position 2. Because the plow is somewhat wider than the truck, it was impossible to locate the wheel loads properly for transverse positions 1 and 8 without the guardrail interfering with the plow (see Figure 4.16). However, as was stated previously, test results for transverse positions 1 and 8 are not subject to comparison with analytical predictions. Figures 4.17

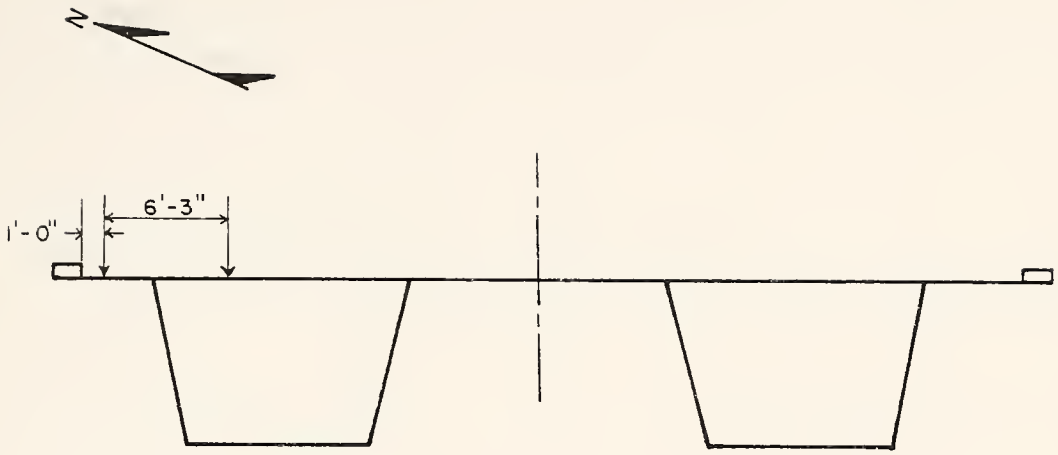

TRANSVERSE POSITION NO. 1

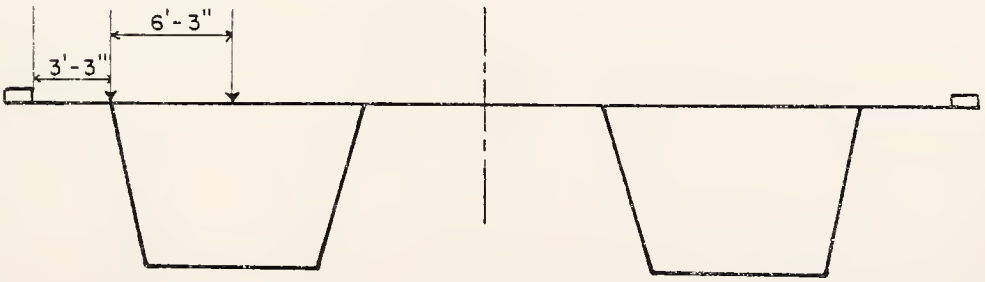

TRANSVERSE POSITION NO 2

Figure 4.7 Transverse Positions 1 and 2

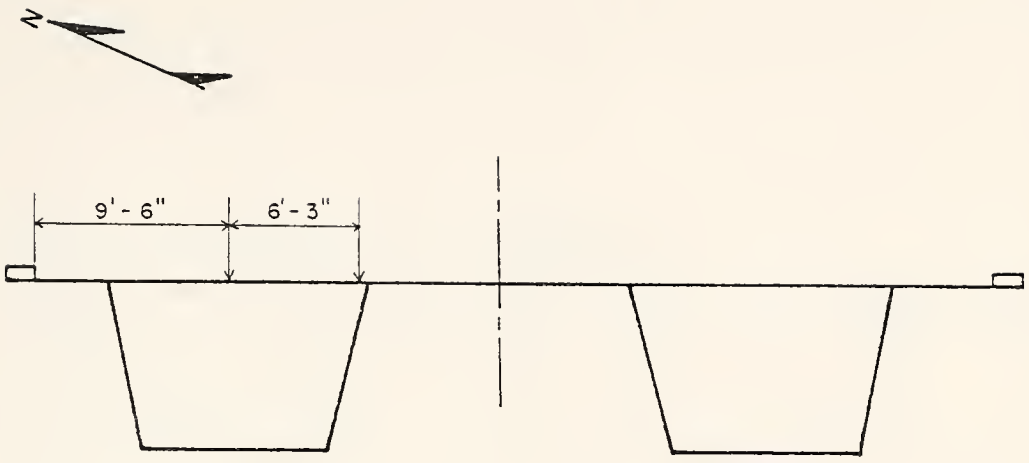

TRANSVERSE POSITION NO. 3

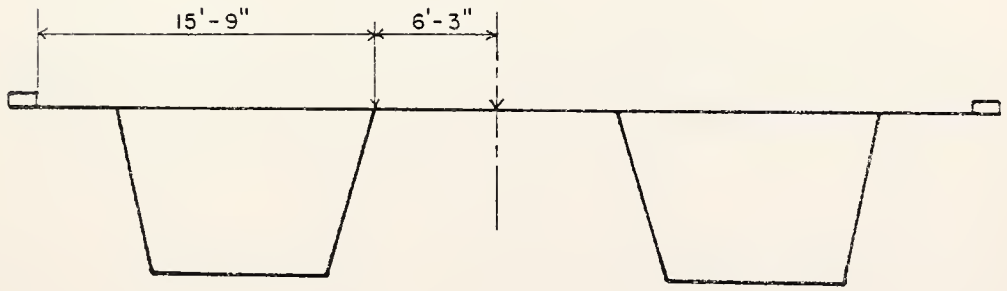

TRANSVERSE POSITION NO. 4

Figure 4.8 Transverse Positions 3 and 4

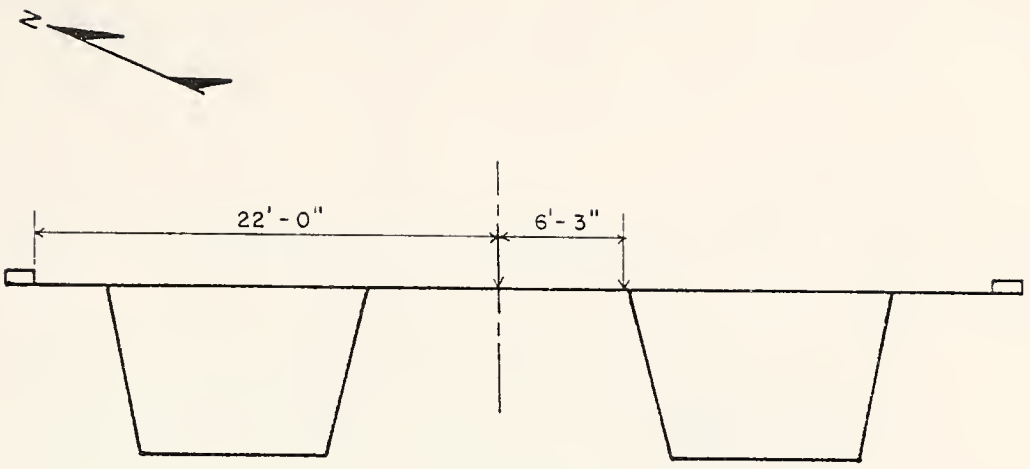

TRANSVERSE POSITION NO. 5

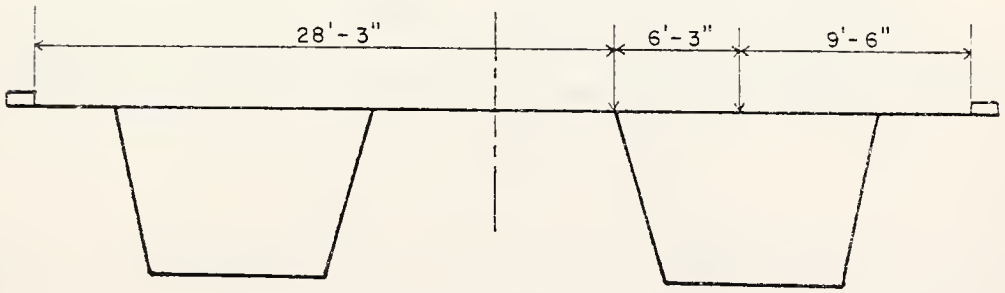

TRANSVERSE POSITION NO. 6

Figure 4.9 Transverse Positions 5 and 6

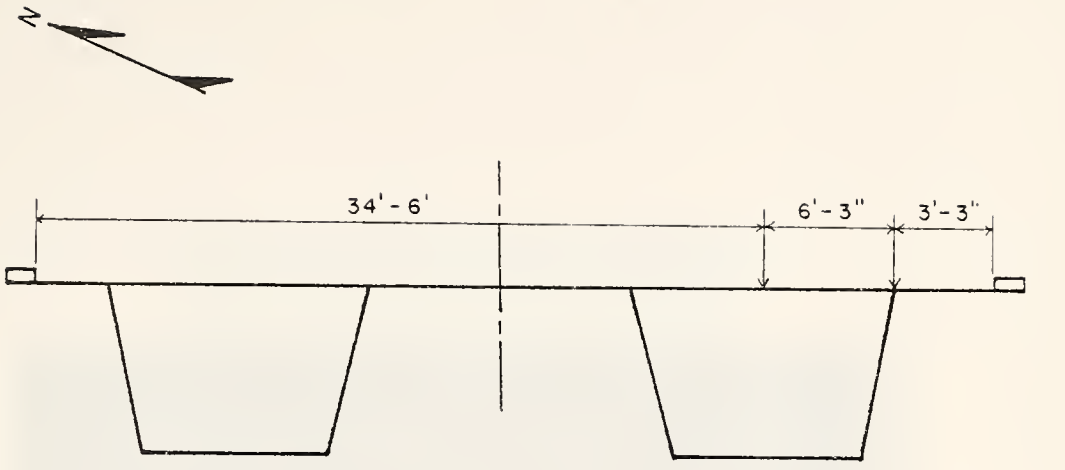

TRANSVERSE POSITION NO. 7

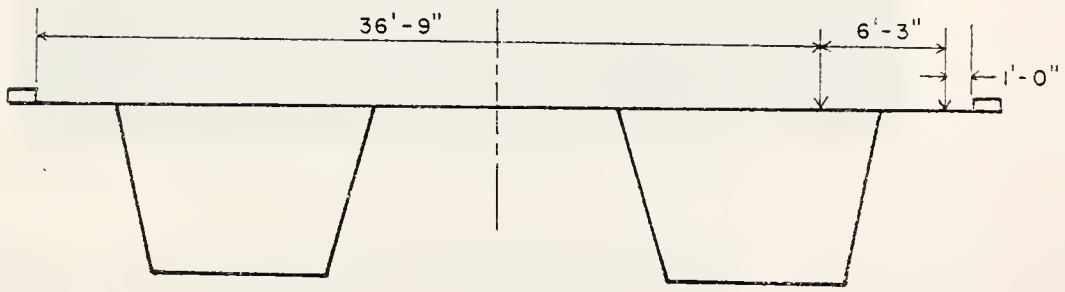

TRANSVERSE POSITION NO. 8

Figure 4.10 Transverse Positions 7 and 8

Figure 4.11. Test Locations Marked on Bridge Deck

Figure 4.12. Test Locations Marked on Bridge Deck

Figure 4.13. Positioning Wheel Loads

Figure 4.14. Loaded Sand Truck

Figure 4.15. Truck Scale - Western Materials, Inc.

through 4.19 show the test truck in various positions during the testing operation.

Strains were measured in the top slab and both webs of segments 24A and 3A, corresponding to stations 5, 6 and 8 of Tables 4.4 and 4.5. Readings were taken in segment 24A only when the truck was in longitudinal position 1 and in segment 3A only when the truck was in longitudinal position 2. A manual digital strain indicator (Vishay/Ellis 21A) was utilized in measuring the strain levels from the 20 gages being monitored (see Figures 4.20 and 4.21). Strain readings were taken for each of the 16 loading cases. Several times during the course of the test readings were taken with no load on the structure so that the strain data could be corrected for temperature effects and instrument drift during the data reduction process. Several of the positions which indicated relatively high strain levels were retested to provide a check on the first set of readings.

Because of symmetry, this particular loading arrangement and selection of gages provided data for most of the regions where relatively high bending tractions were expected.

Data Reduction

Prior to conducting the transverse bending test, each channel of the strain indicator was set up with the proper span, i.e. exciting voltage to the Wheatstone bridge circuit. This value was determined from the gage factor specified for each strain gage by the manufacturer and corrected for desensitization due to the long lead wire lengths. Consequently, strain levels were read directly from the digital strain indicator.

Because of instrument drift and temperature induced strains, it was necessary to correct the readings so they would represent the strains

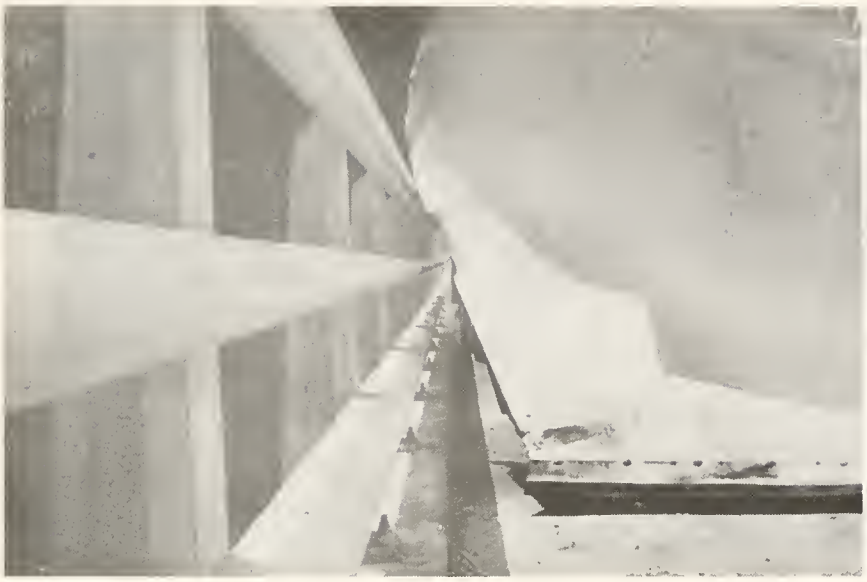

Figure 4.16. Transverse Position 8

Figure 4.17. Transverse Position 2

Figure 4.18. Transverse Position 4

Figure 4.19. Transverse Position 5

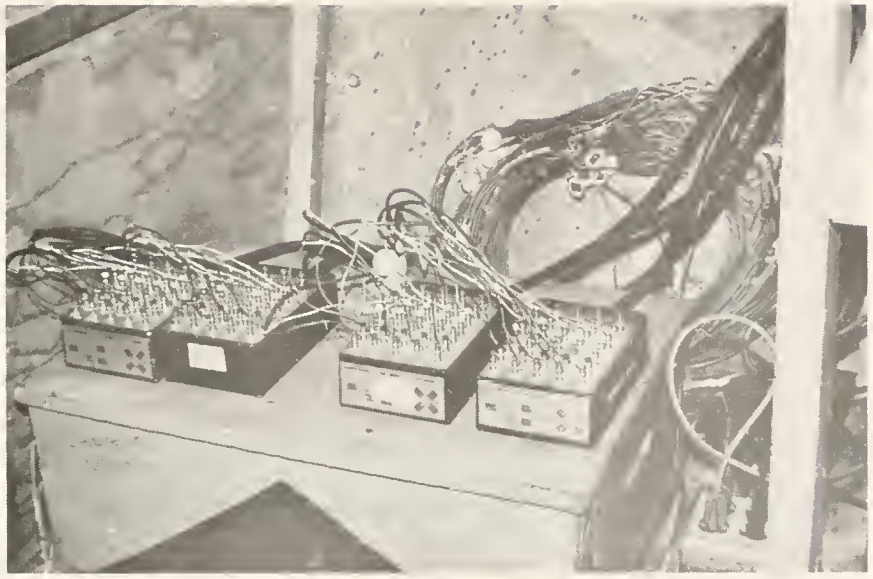

Figure 4.20. Gages Wired to Gage Blocks

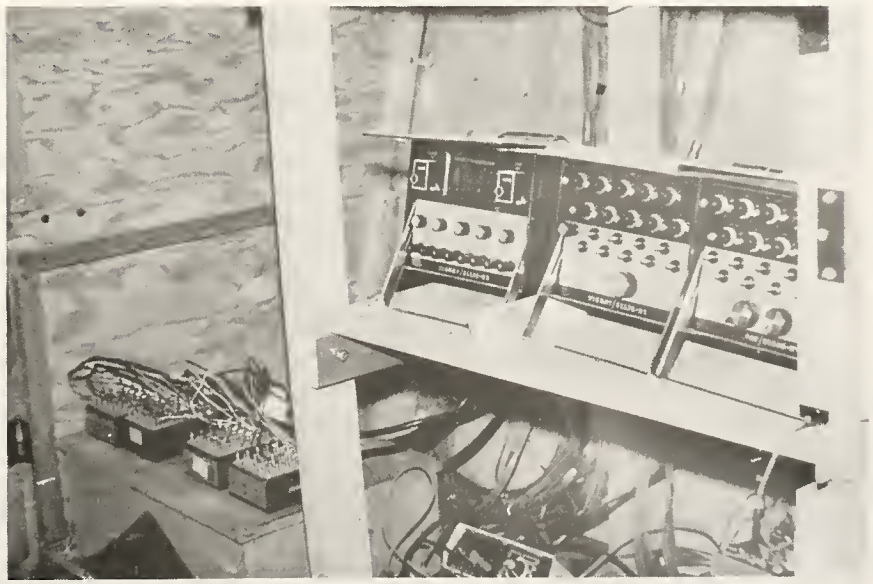

Figure 4.21. 20-Channel Digital Strain Indicator

resulting strictly from the applied truck loadings. Accordingly, the data were adjusted by subtracting apparent strain due to extraneous phenomena, as established from the no-load readings cited previously.

Before the strain linearity through a given section could be checked, it was necessary to correct those transverse strains measured with concrete surface gages located in high longitudinal stress fields for transverse sensitivity effects. This correction was described in detail by Holman[4] and is outlined in Chapter III of this report.

Once the necessary adjustments had been made, the three strain values at each instrumented section were plotted to scale to facilitate checking the strain linearity through the sections. The strain distributions were found to be quite linear, despite the fact that most of the strain levels were relatively low, and therefore more susceptible to inaccuracies.

Transverse bending tractions were calculated for each loading case based upon the strains measured in the transverse reinforcement. It was assumed that the sections were uncracked because of the relatively low bending moments and thus the following analysis was used (see Figure 4.22).

Utilizing the measured strains in the inside and outside layers of reinforcement and the actual dimensions and section properties, the neutral axis was located from strain geometry; thus,

$$d_1 = \frac{\varepsilon_{s_1}}{(\varepsilon_{s_2} - \varepsilon_{s_1})} [h - (d_1' + d_2')]$$

$$d_2 = d_1 + [h - (d_1' + d_2')]$$

Surface strains in the concrete were then computed as follows.

$$\varepsilon_{c_2} = \frac{d_2 + d_2'}{h - (d_1' + d_2')} [\varepsilon_{s_2} - \varepsilon_{s_1}]$$

$$\varepsilon_{c_1} = \frac{d_1 - d_1'}{h - (d_1' + d_2')} [\varepsilon_{s_2} - \varepsilon_{s_1}]$$

The forces in the steel and concrete were then calculated using the stress-strain relationships and cross-sectional areas of the materials.

$$F_{s_1} = \varepsilon_{s_1} E_s A_{s_1}$$

$$F_{s_2} = \varepsilon_{s_2} E_s A_{s_2}$$

$$F_c = 1/2(\varepsilon_{c_2} + \varepsilon_{c_1}) E_c [h(12) - (A_{s_1} + A_{s_2})]$$

The total axial force in each section was determined as the sum of the individual forces.

$$P = F_{s_1} + F_{s_2} + F_c$$

The bending moments were obtained by summing the moments of the internal forces about the centroid of the section. Since the reinforcement is essentially symmetric, the moments were taken about the mid-depth.

$$M = \{F_{s_2}(\frac{h}{2} - d_2') - F_{s_1}(\frac{h}{2} - d_1') + 1/2(\varepsilon_{c_2} - \varepsilon_{c_1}) E_c[h(12) - (A_{s_1} + A_{s_2})](\frac{h}{6})\} 1/12$$

The resulting transverse bending moments from the preliminary bending test are presented in Tables 4.4 and 4.5. They have been scaled by a factor of .877 so that direct comparisons can be made between the experimental data and the moments determined by the finite element analysis. This scaling factor was determined as the ratio of the nominal loading used for the initial analysis to the actual applied loading.

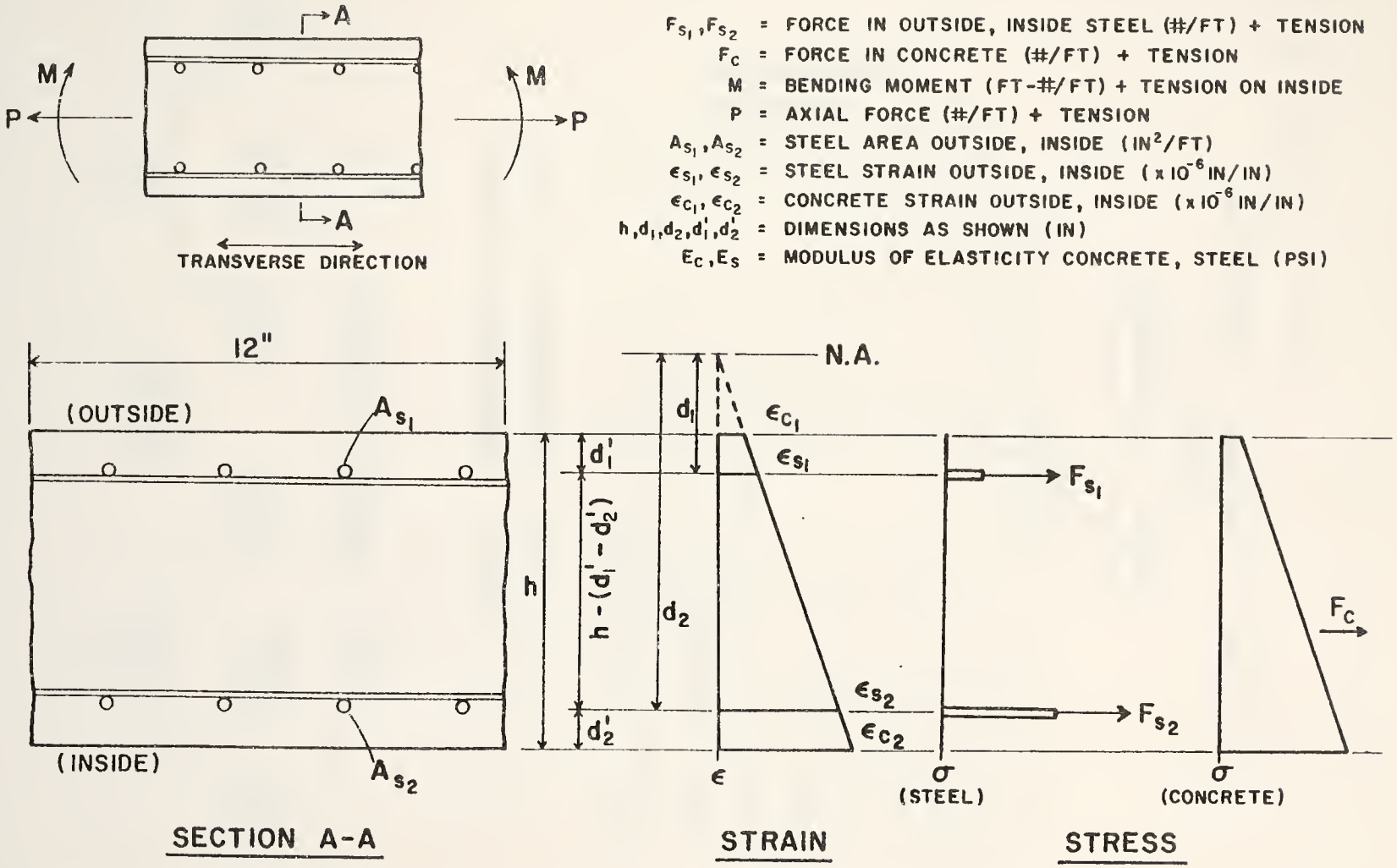

Figure 4.22 Strain and Stress Distribution

Table 4.4 Preliminary Test Results

TRANSVERSE BENDING MOMENTS
(ft—lbs/ft)
+TENSION ON INSIDE
—TENSION ON OUTSIDE

TRANSVERSE POSITION \ STATION	1	2	3	4	5	6	7	8
1					+ 60	0		- 80
2					- 20	0		+ 140
3					+ 21	0		+ 180
4					+ 20	0		+ 399
5					+ 61	0		+ 160
6					+ 978	- 439		- 759
7					+1008	- 479		- 679
8					+ 463	- 240		- 399

TRUCK LONGITUDINAL POSITION NO. 1

READING LONGITUDINAL POSITION NO. 1

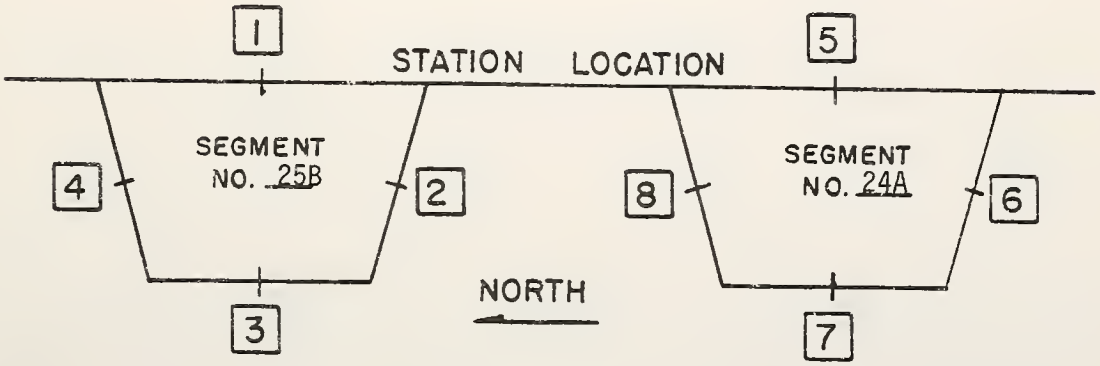

Table 4.5 Preliminary Test Results

TRANSVERSE BENDING MOMENTS
(ft—lbs/ft)

+TENSION ON INSIDE
—TENSION ON OUTSIDE

TRANSVERSE POSITION \ STATION	1	2	3	4	5	6	7	8
1					0	0		0
2					- 21	- 42		- 42
3					- 41	- 42		- 85
4					- 82	0		+ 253
5					- 61	0		+ 169
6					+ 698	- 21		- 63
7					+ 677	- 190		- 105
8					+ 185	0		- 84

TRUCK LONGITUDINAL POSITION NO. 2

READING LONGITUDINAL POSITION NO. 2

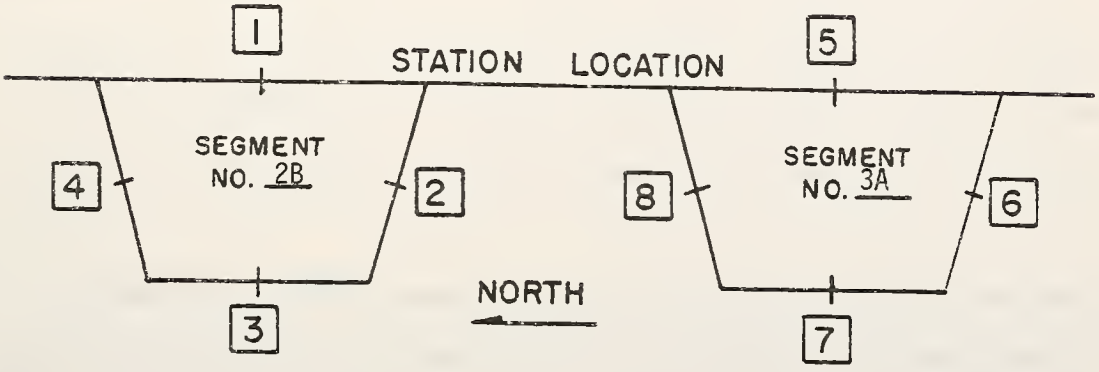

Comparison of Experimental and Analytical Results

The transverse bending moments predicted by the finite element analysis are presented in Tables 4.6 and 4.7. These tables include only those values needed for comparison with the preliminary test results. A more complete set is tabulated in Appendix E of this report.

It appears from these tables that at the locations where small bending moments were expected, the experimental values are quite erratic. However, it must be realized that the computed bending moments are very sensitive to changes in strain, and thus less reliable, because the strain levels are so low. For instance, a difference in strain between the inside and outside layers of steel of only 1×10^{-6} in/in produces an internal moment of approximately 40 ft-lbs per ft for the top slab and 80 ft-lbs per ft for the webs. It is for this reason that experimental results for situations where the bending moments are relatively small are considered to be quite inaccurate.

When the truck was located at transverse positions 6 and 7 for longitudinal positions 1 and 2, relatively large bending moments occured at station 5 (top slab). However, the measured tractions were only about 45 percent of the predicted values. The same trend was found at station 6 for loadings at transverse positions 6 and 7 and at station 8 for loadings at transverse positions 4, 5, 6 and 7. At these stations, located in the webs, the resulting moments were approximately 60 percent of the analytical values.

Although the results appear to reflect a general trend, further testing is necessary before any conclusions can be reached. It does appear that, since the instrumentation is working properly and the strains are linear through the sections, the experimentally determined tractions are generally reliable.

Table 4.6 Finite Element Bending Moments

TRANSVERSE BENDING MOMENTS
(ft—lbs/ft)

+TENSION ON INSIDE
—TENSION ON OUTSIDE

TRANSVERSE POSITION \ STATION	1	2	3	4	5	6	7	8
1					- 70	+ 51		+ 366
2					- 72	+ 47		+ 372
3					- 80	+ 56		+ 419
4					- 102	+ 73		+ 717
5					- 15	- 21		+ 253
6					+2220	- 682		- 989
7					+2202	- 615		- 950
8					- 134	+1398		- 193

TRUCK LONGITUDINAL POSITION NO. 1

READING LONGITUDINAL POSITION NO. 1

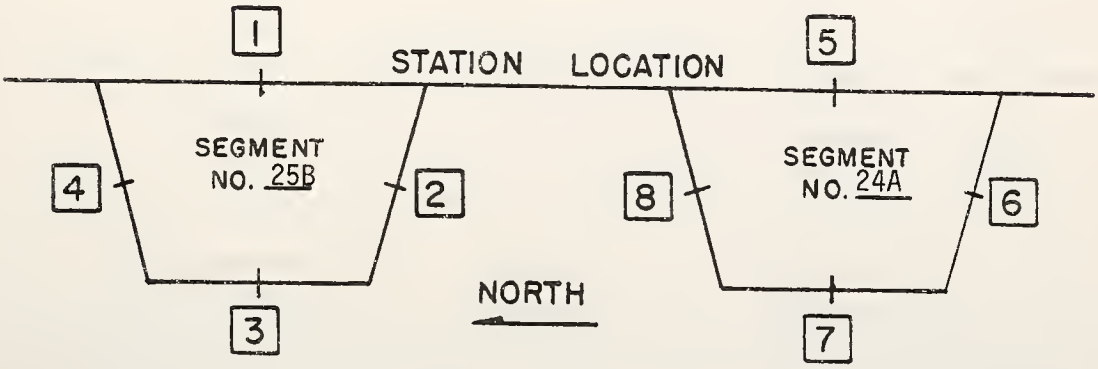

Table 4.7 Finite Element Bending Moments

TRANSVERSE BENDING MOMENTS
(ft—lbs/ft)
+TENSION ON INSIDE
—TENSION ON OUTSIDE

TRANSVERSE POSITION \ STATION	1	2	3	4	5	6	7	8
1					- 2	+ 1		+ 12
2					0	0		- 9
3					- 2	+ 3		+ 2
4					- 40	+ 60		+ 403
5					- 47	+ 84		+ 365
6					+2094	- 433		- 478
7					+2092	- 493		- 403
8					- 117	+1109		+ 160

TRUCK LONGITUDINAL POSITION NO. 2

READING LONGITUDINAL POSITION NO. 2

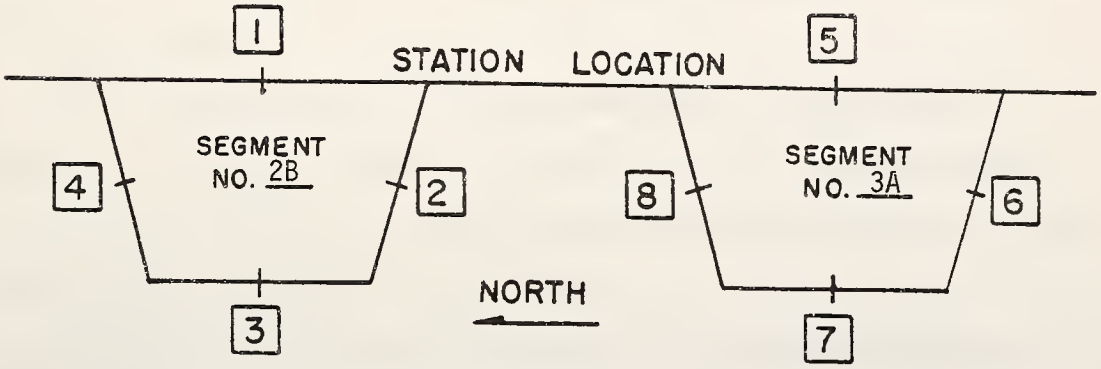

Comprehensive Test

A comprehensive transverse bending test will be conducted before the conclusion of the Turkey Run bridge project. Strains will be monitored at each of the instrumented sections for all 32 truck loadings. The same analysis will be used to determine the internal bending moments produced by the applied loadings. The results will be presented in a final report to be submitted during the summer of 1981.

Strains will be measured and recorded with a 100-channel automatic data acquisition system (see Figure 4.23). Readings will be taken frequently, under zero applied load, to monitor net apparent strain and instrument drift so that they may be accounted for in the data reduction process. The optimum time to conduct the test would be early in the morning to minimize these extraneous effects. Readings should be repeated at locations of high strain in order to check for consistency of results.

The data will be reduced using the following procedure: 1) adjust data for apparent strain and instrument drift, 2) correct necessary strains for transverse sensitivity, 3) check linearity of strains, 4) compute bending tractions.

Bending moments from the finite element analysis are presented in Appendix E for future reference. Although it will be impossible to detect strains in sections far removed from the loading, all of the loading cases have been included for completeness.

The results from the preliminary test will be used to augment the data from this test. The validity of the analytical technique will then be evaluated.

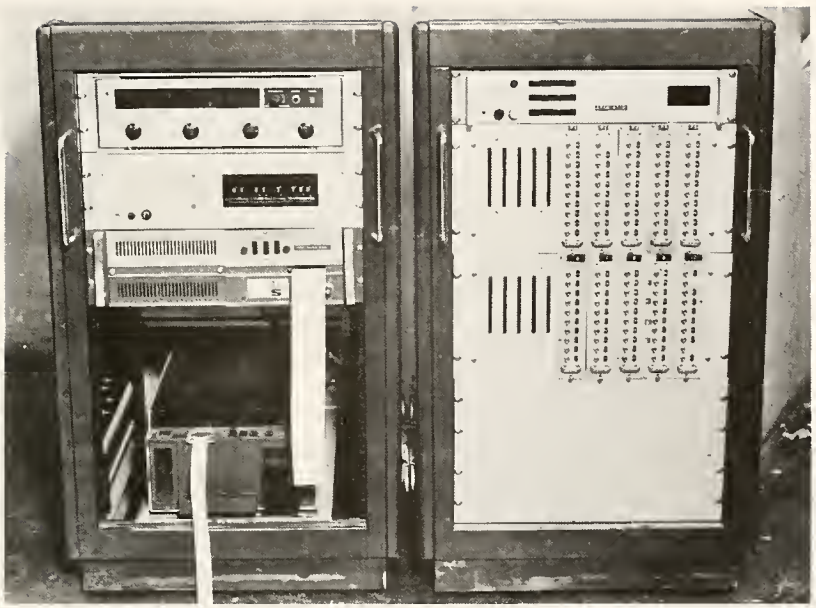

Figure 4.23. 100-Channel Data Acquisition System

Notes

1 Holman, R. J., "Development of an Instrumentation Program for Studying Behavior of a Segmental Concrete Box Girder Bridge", Joint Highway Research Project 77-4, Purdue University, March 2, 1977, p. 11.

2 Ibid., Chapter III.

3 Pauw, Adrain, "Static Modulus of Elasticity of Concrete as Affected by Density", Journal of the American Concrete Institute, V. 57, No. 6, December 1969, pp. 679-688.

4 Holman, pp. 71-72.

CHAPTER V

THERMAL RESPONSE

Introduction

Temperature effects in concrete box girder bridges are quite significant and must be considered in the design of such structures.

Changes in temperature cause the total length of a structure to increase or decrease. For the Turkey Run bridge this change in length is accomodated, however, by relatively flexible bearing details and/or flexure of the central piers, and thus has little effect on internal stresses in the superstructure.

The effects of temperature differentials between the top and bottom slabs do, however, cause the support reactions in statically indeterminate bridges to undergo significant variations. The internal stresses which are induced as a result of these effects must not be overlooked.

During the cantilevering phase of construction, the structure is statically determinate and temperature differentials cause curvature along the span. The resulting tip deflections, being dependent on ambient conditions, are relatively unpredictable. This causes problems in vertical alignment which must be dealt with during erection.

This chapter is concerned with the measurement of temperature gradients through the depth of the Turkey Run bridge superstructure. Daily and seasonal variations of thermal gradients have been determined and are presented. Temperature induced strains and deflections, which have

been measured both during construction and in the completed structure, are also presented in this chapter.

Tip Deflections During Construction

During erection of the superstructure, vertical alignment must be controlled as segments are cantilevered from the central pier. Accordingly, elevations are monitored during the construction process in order to check the vertical alignment against the design grades. Deflections produced by temperature differentials create difficulties in determining the corrections which must be made. Therefore, it is often stipulated in segmental construction that alignment corrections be made during times of minimum temperature differentials, thus causing costly loss of time.

The objective of this part of the research is to determine the nature of the relationship between cantilever tip deflections and existing temperature differentials in the structure. With this information, vertical alignment corrections can be made regardless of the existing environmental conditions, thus hastening the construction process. Test results are presented graphically for comparison with predictions from beam theory.

Tip deflections were monitored during construction after placement of segments 24 and 25. Elevations were measured using a Zeiss Ni-2 automatic level with a resolution of 0.005 ft. Readings were taken hourly over a 24 hour period at the locations shown in Figure 5.1. The temperature in the slabs at the same sections were monitored concurrently through the use of thermistors embedded in the concrete. Photographs taken during the data collection procedure are shown in Figures 5.2 and 5.3.

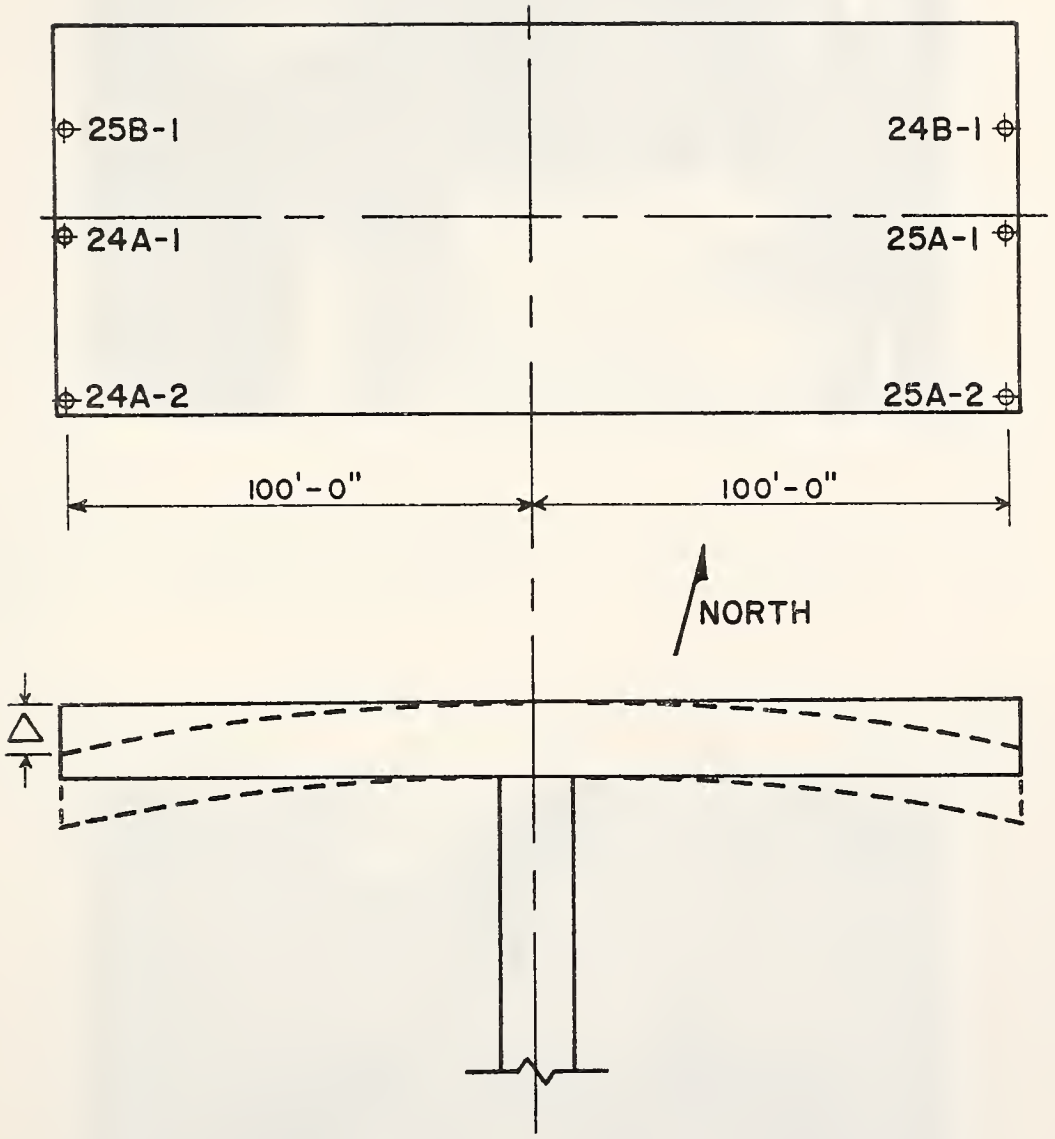

Figure 5.1 Instrumented Sections for Tip Deflections

Figure 5.2 Taking Elevation Reading

Figure 5.3 Taking Thermistor Reading

The test results are plotted on the graph of Figure 5.4. Negative temperature differentials were experienced as a result of the rain and overcast skies which occured during the field testing operation. A dashed line, which was determined using a linear regression analysis, has been drawn through the data. This set of observed values yielded a slope of -2.955×10^{-3} ft/°F with a point estimate of the correlation coefficient of -0.81.

An approximate method of analysis for the effect of temperature is suggested by the Post-Tensioning Institute and the Prestressed Concrete Institute in their publication entitled "Precast Segmental Box Girder Bridge Manual"[1]. For purposes of this study, the basic assumptions and procedures employed in this method have been used to develop a theoretical relationship between tip deflections and temperature differentials.

If the temperature of the top slab increases with respect to the bottom of the section, the slab will tend to expand. Expansion of the top slab is considered to be restrained by the relatively stiff webs. Thus, the primary effect of the increase in temperature of the top slab is a compressive force P acting at the centroid of the slab as illustrated in Figure 5.5. External equilibrium is restored by superposing an equal and opposite force P' at the same location. P' may then be considered as an axial force and a moment M applied at the centroid of the full cross-section. Once this equivalent static loading is known, deflections can be determined using beam theory.

If the temperature differential is assumed to be constant along the entire length of the bridge, this structure can be modeled with a fixed

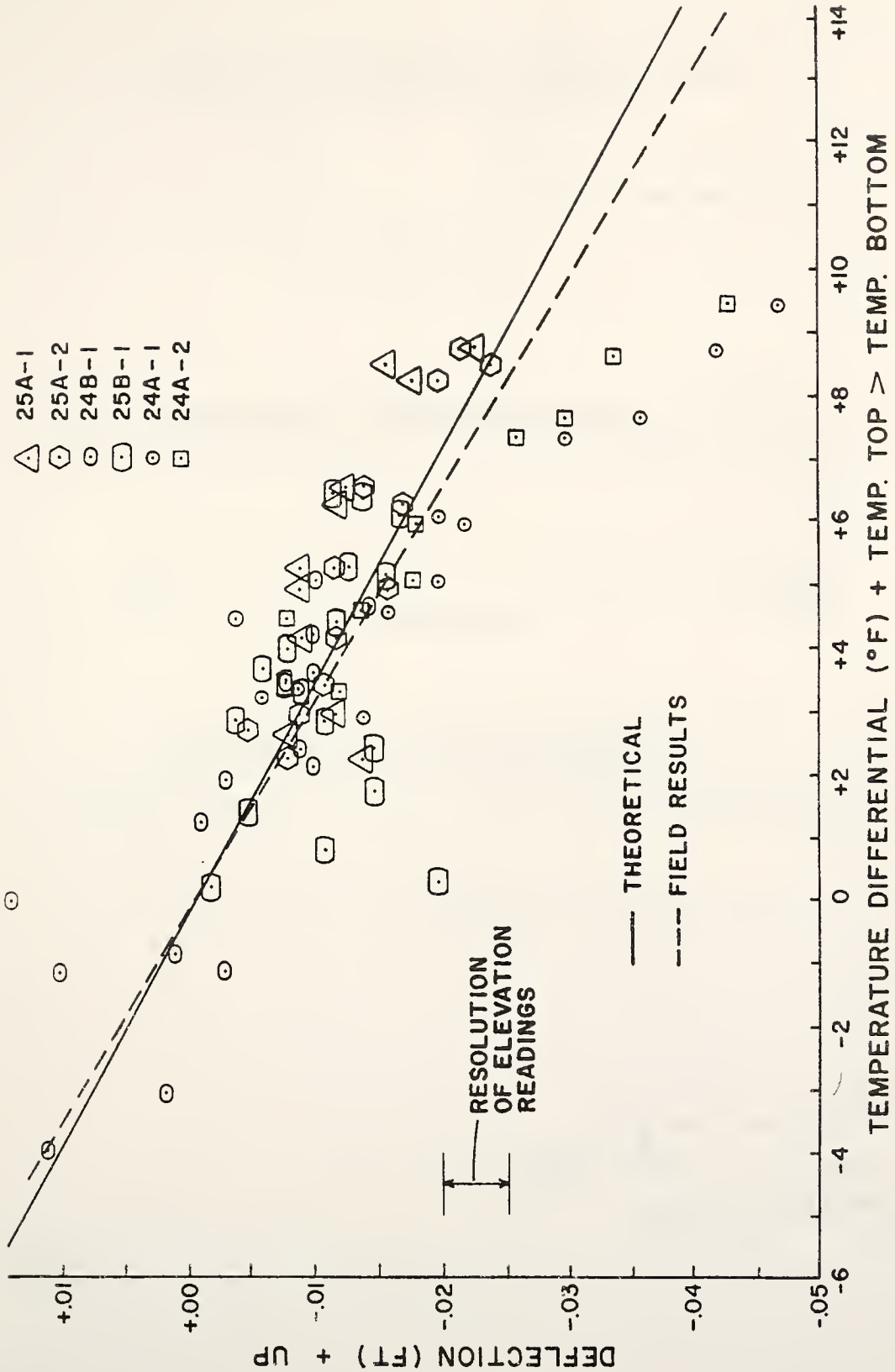

Figure 5.4 Tip Deflection vs. Temperature Differential

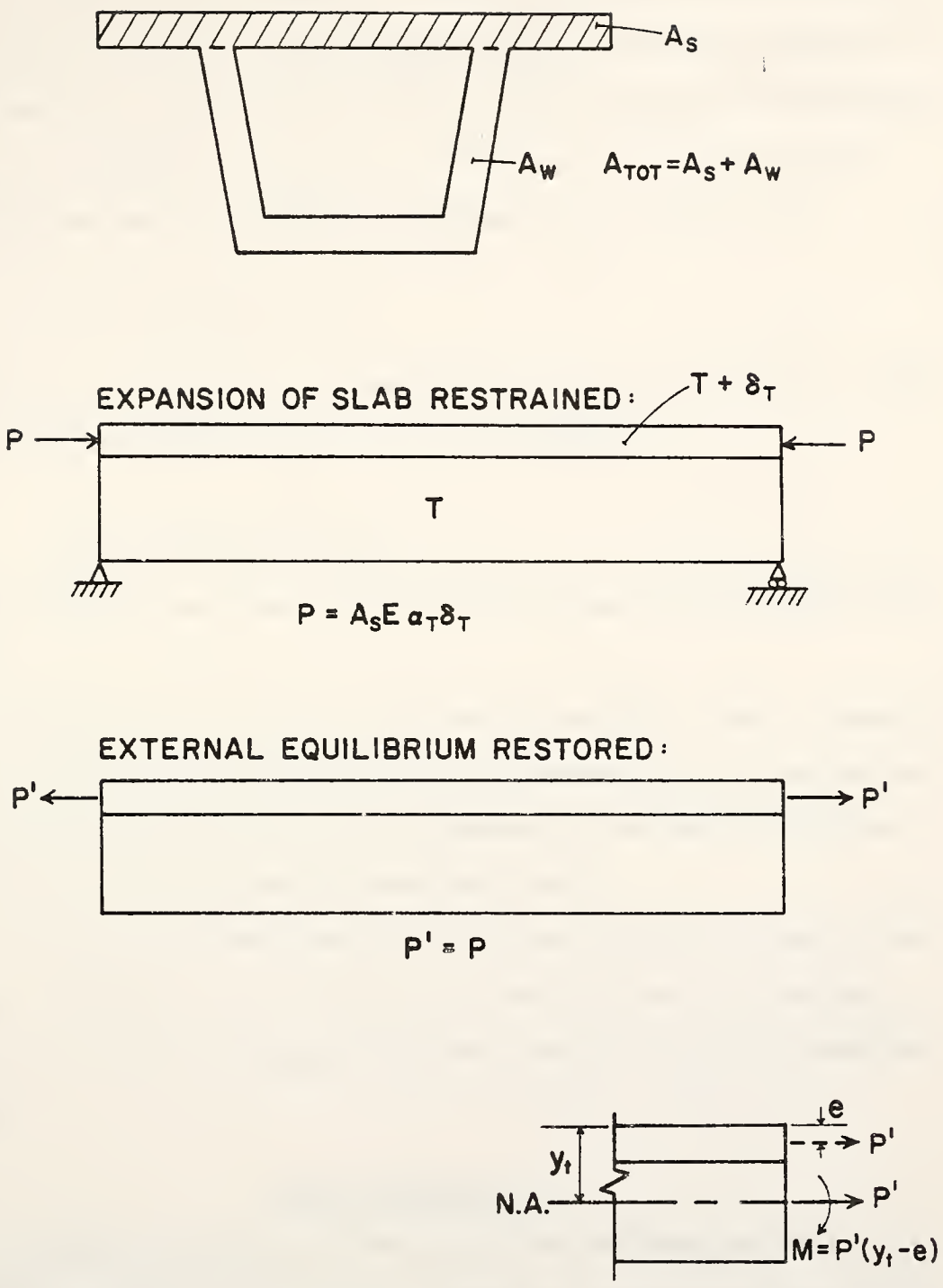

Figure 5.5 Equivalent Static Loading

end at the pier section because of symmetry (see Figure 5.6). The variable moment of inertia of the segments adjacent to the pier section has been modeled by a single average value. Using linear-elastic deflection theory, the relationship betwen the deflection Δ at a section 100 ft. from the pier and the temperature differential δ_T is found to be

$$\Delta = - 502.0 \ (\alpha_T) \ (\delta_T),$$

where α_T is the coefficient of thermal expansion of the concrete. Using a value of 5.5×10^{-6} ft/ft/°F for α_T, this reduces to

$$\Delta = - 2.761 \times 10^{-3} \ (\delta_T)$$

This relationship has been plotted as a solid line on the graph of Figure 5.4.

Although the resolution of the readings was quite large in comparison to the magnitude of the deflections being measured, causing some scatter in the observed values, the general agreement of the results with the analytical prediction equation seems quite good.

The results obtained from this study were utilized by agents of the general contractor, J. L. Wilson Co., in making elevation corrections when establishing superstructure-abutment connections for the Turkey Run bridge.

Bridge Temperatures

In order to provide data which would indicate times of maximum and minimum temperature differentials, temperature readings were taken every 30 minutes during 24 hour and longer periods at various times during 1979 between February and September. For the first several field tests, only

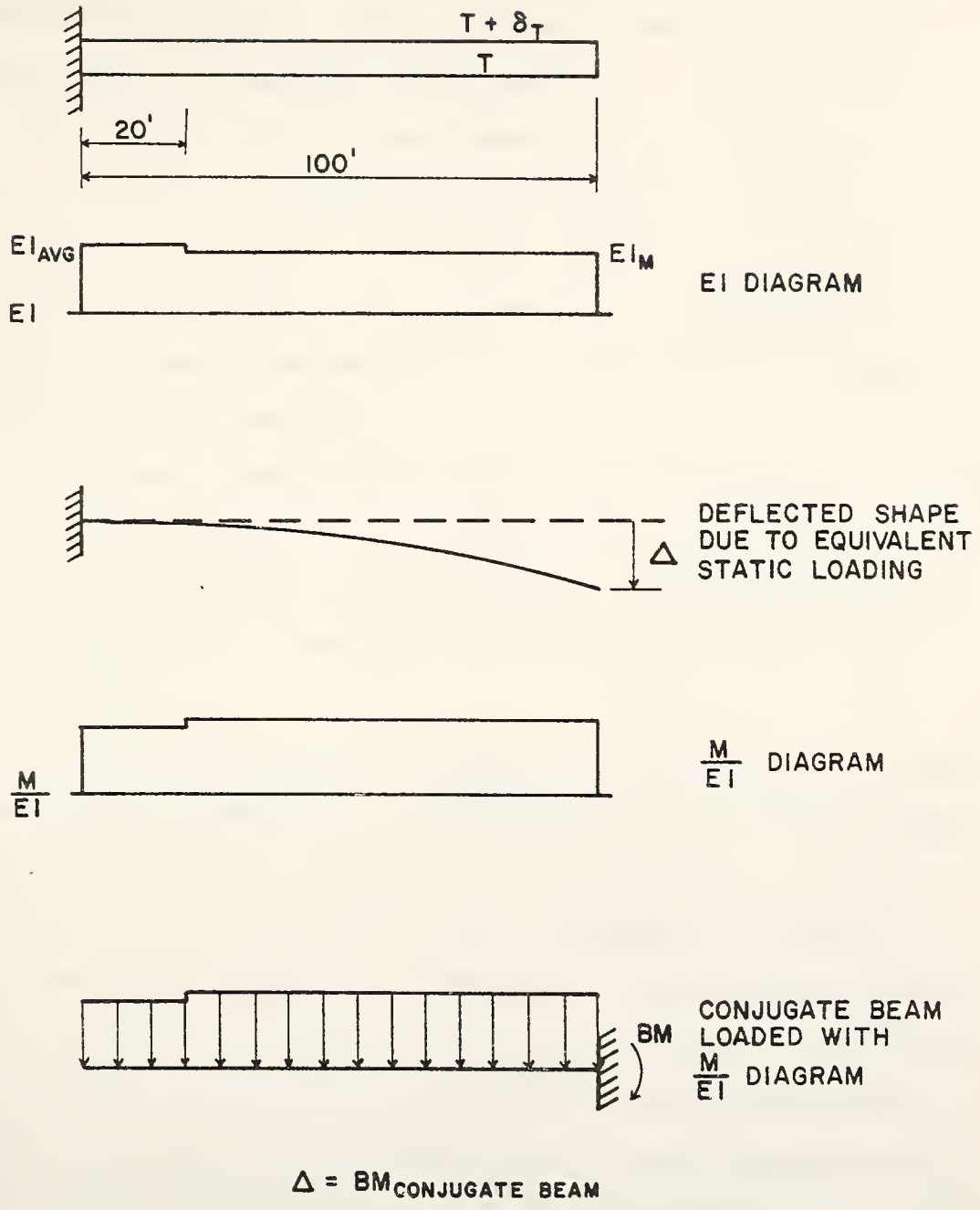

Figure 5.6 Linear-Elastic Deflection Theory

those thermistors located in the top and bottom slabs of the bridge were monitored (see Figure 5.7). These readings provided data concerning daily variations in temperature differentials.

In early July 1979, additional thermistors were installed in the webs of the north girder as illustrated in Figure 5.8. The purpose of installing this instrumentation was to make possible a more complete determination of the nature of the temperature distributions within the segments. The exact dimensions locating the thermistors in a typical segment are given in Appendix C.

A 40-channel automatic data acquisition system has been used to record the thermistor outputs (see Figures 5.9 and 5.10). An input voltage is supplied to the thermistor circuit by means of an external power supply. The thermistor output is recorded on a printer tape in the form of a voltage reading.

A computer program has been developed to facilitate reduction of the output voltages to temperatures. The program includes a plotting routine which is used to graph temperatures as a function of time. Test results from the days during which the most severe temperature differentials existed are shown in Figures 5.11 through 5.17. Temperature distributions through the depth of the segments have also been plotted when such data were available. Climatological data has been provided so that correlations can be made between bridge temperatures and ambient weather conditions. Additional test results are presented in Appendix F.

From these plots, several inferences can be made. In general, minimum temperature differentials occur between 7:00 AM and 9:00 AM and maximum differentials occur between 5:00 PM and 7:00 PM. It is seen that the temperature of the bottom slab fluctuates very little as compared to the

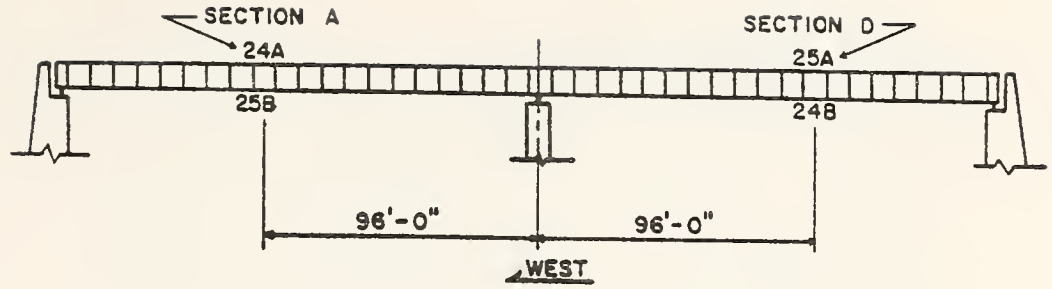

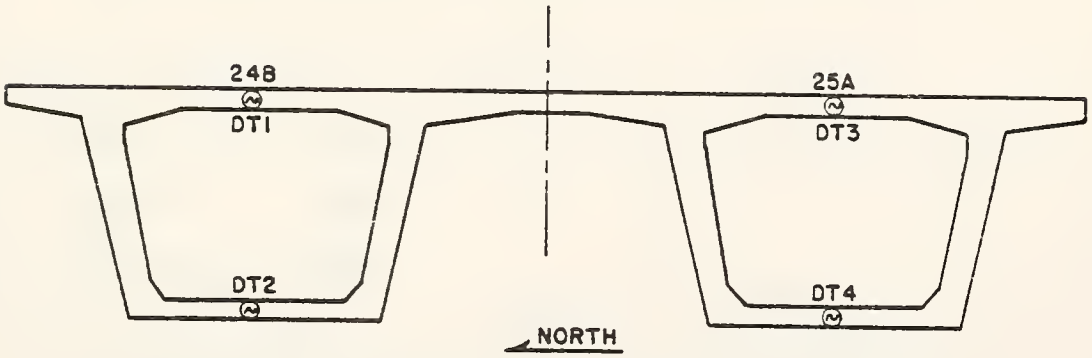

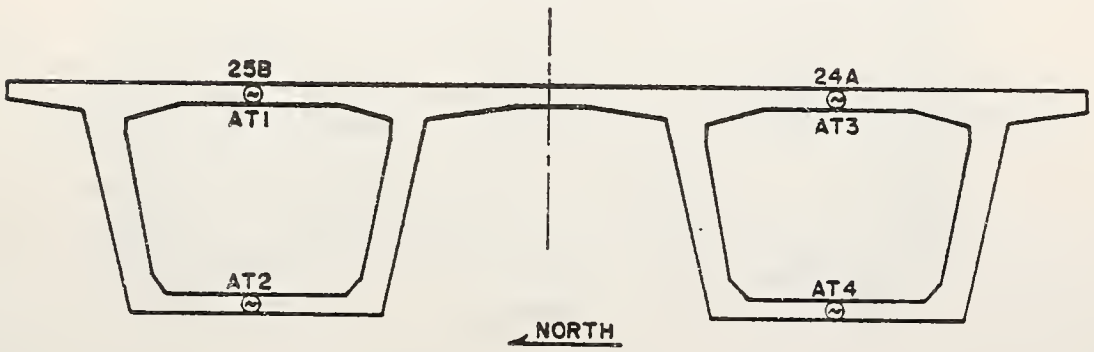

Figure 5.7 Original Temperature Instrumentation

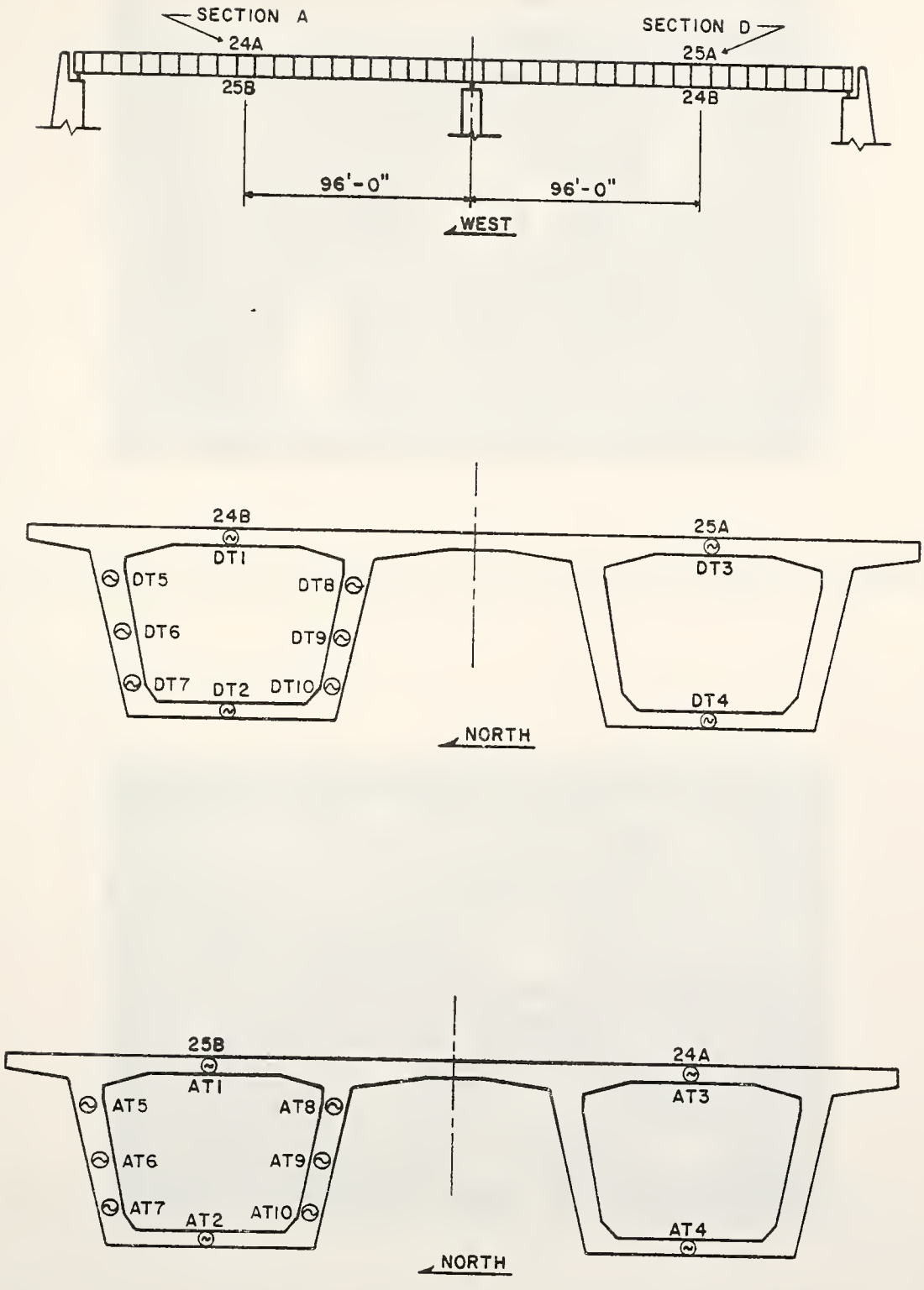

Figure 5.8 Additional Temperature Instrumentation in Webs

Figure 5.9 Data Acquisition System Monitoring Eight Original Thermistors

Figure 5.10 Monitoring 20 Channels Including Additional Thermistors

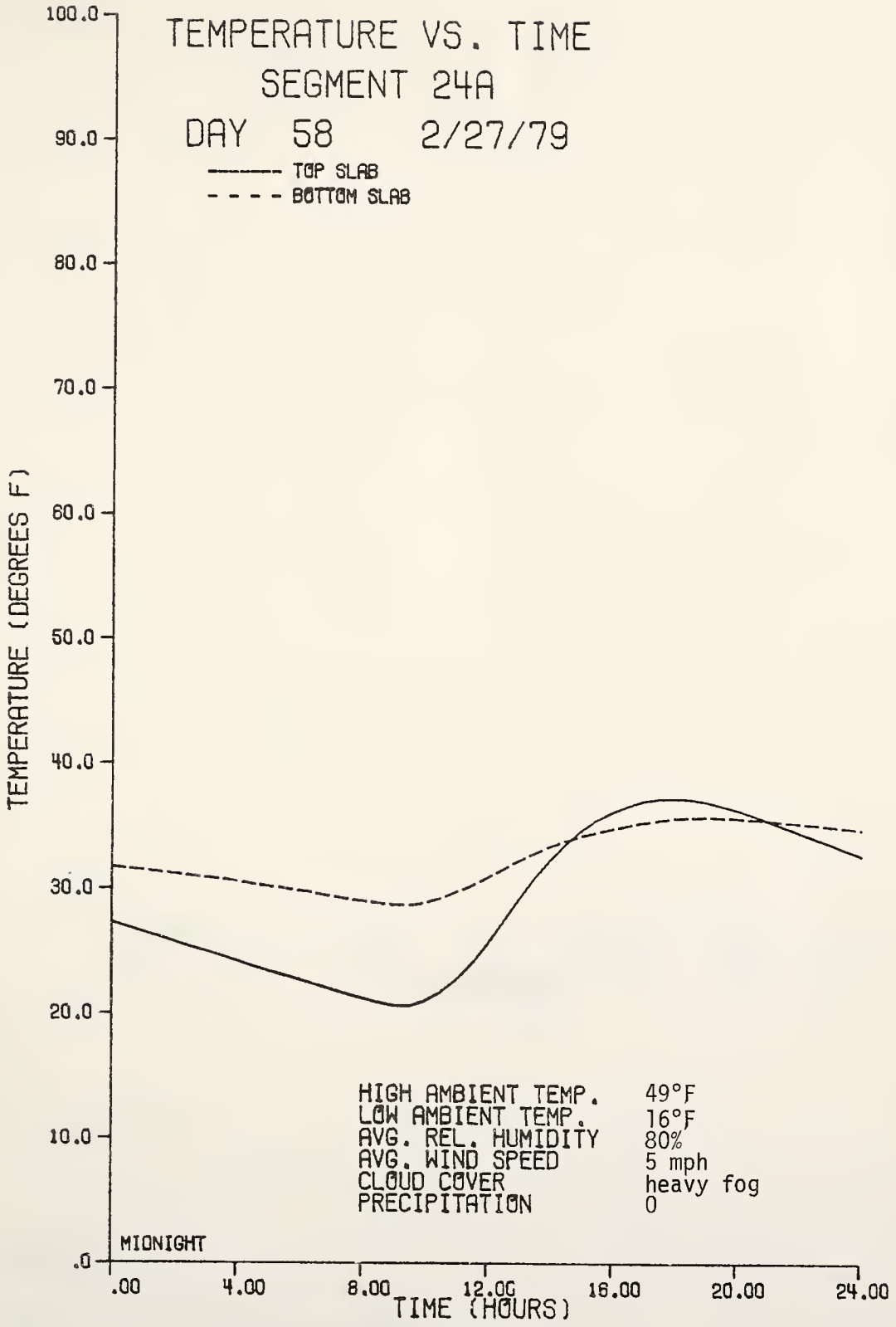

Figure 5.11 Bridge Temperatures

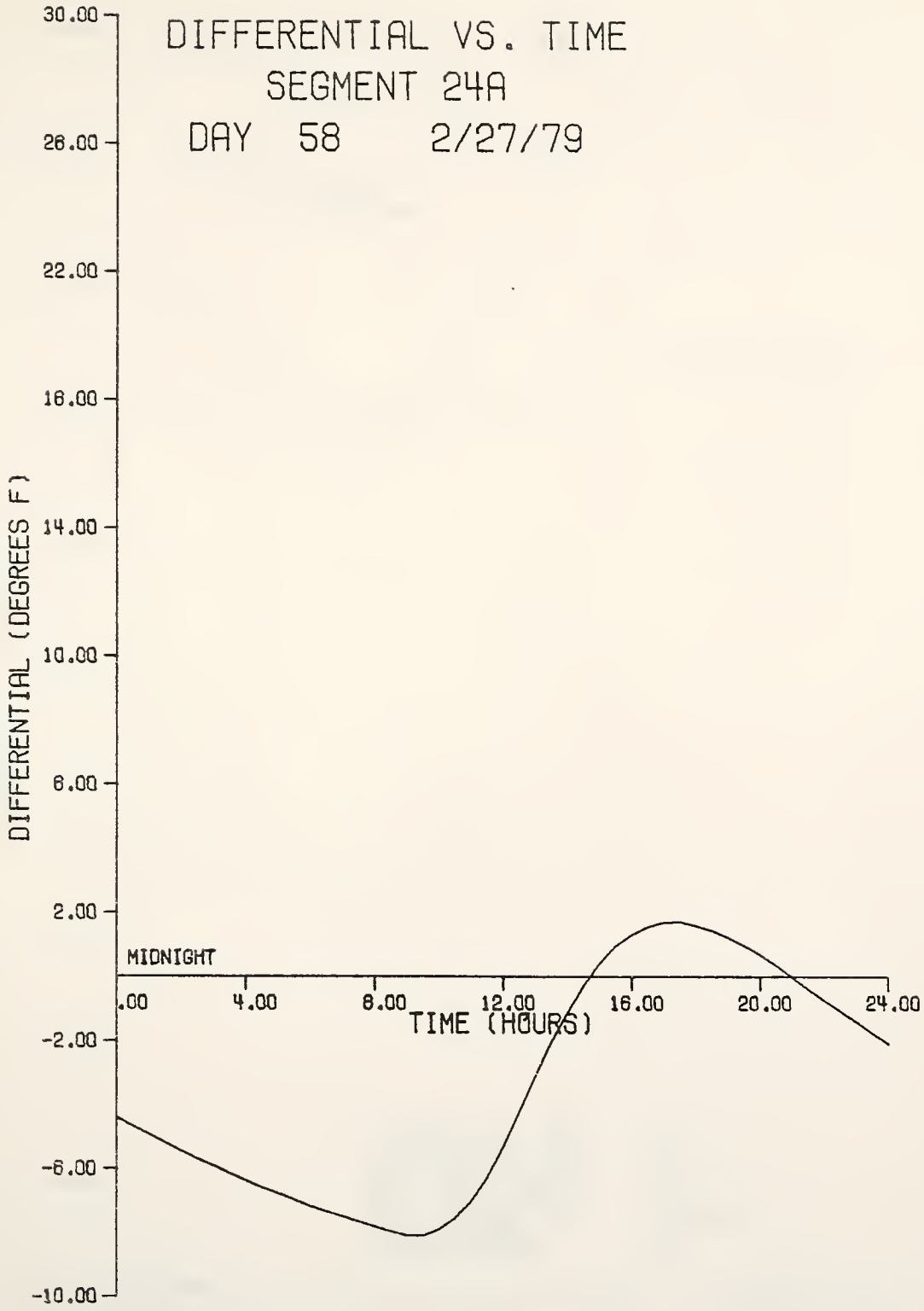

Figure 5.12 Bridge Temperatures

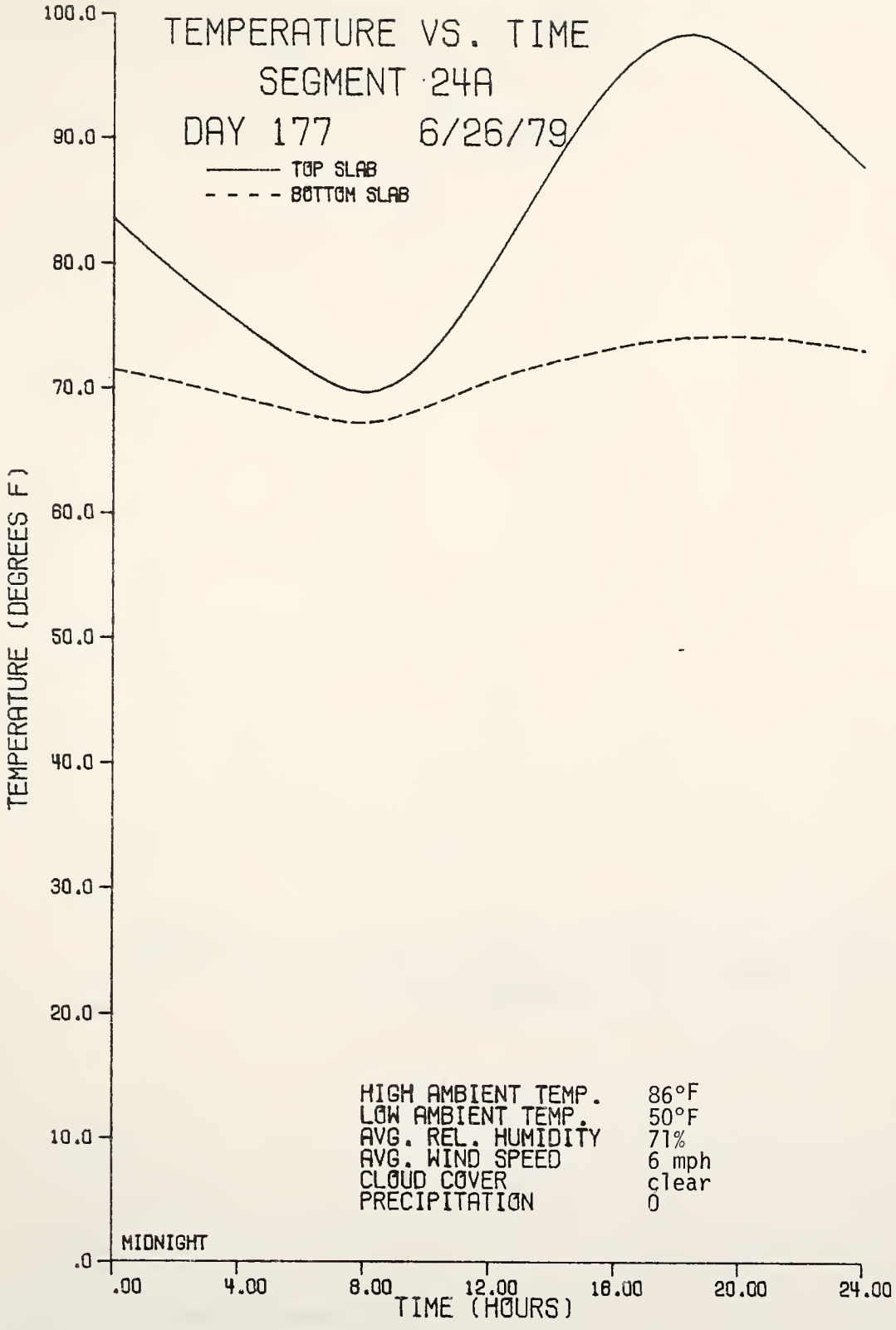

Figure 5.13 Bridge Temperatures

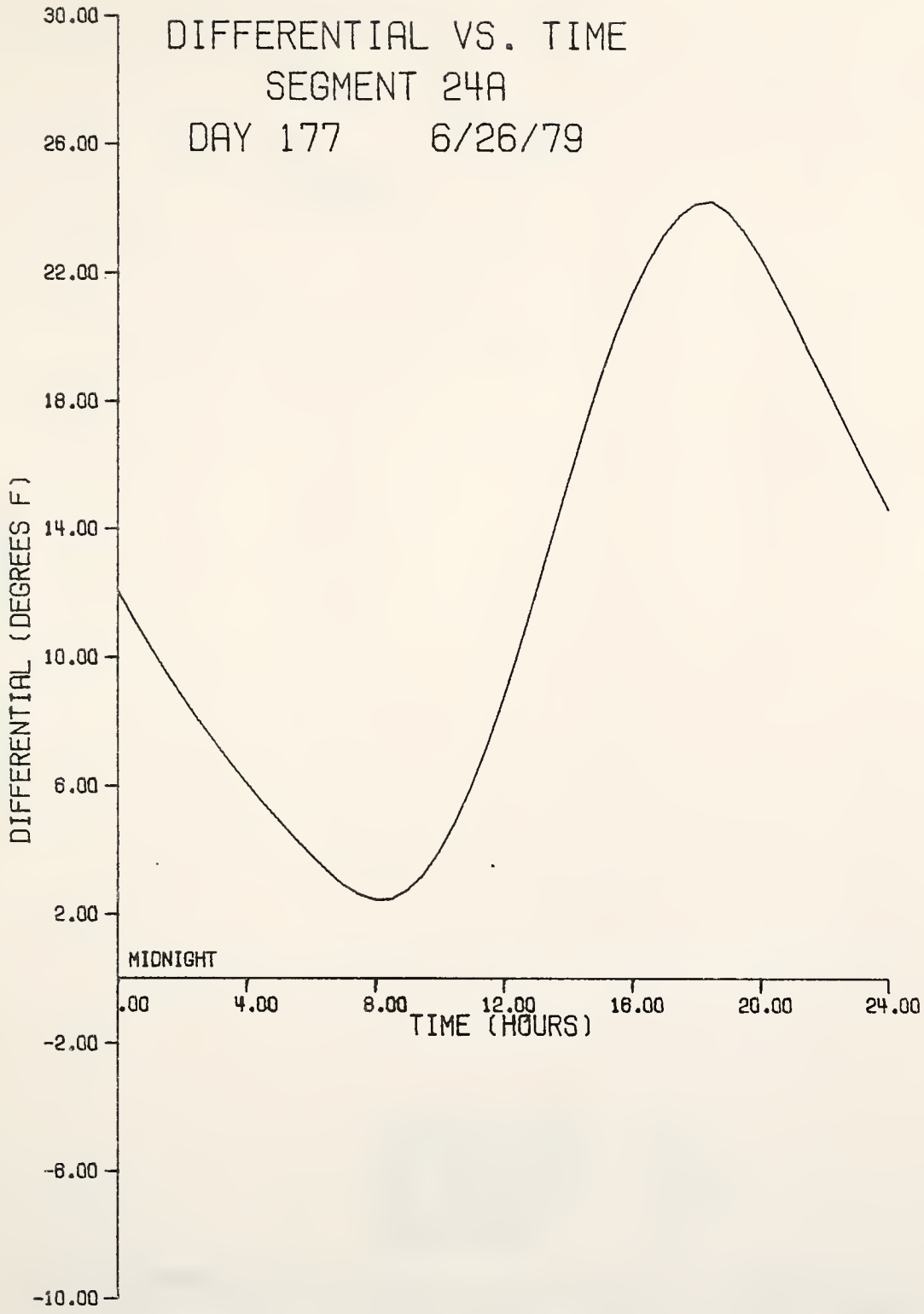

Figure 5.14 Bridge Temperatures

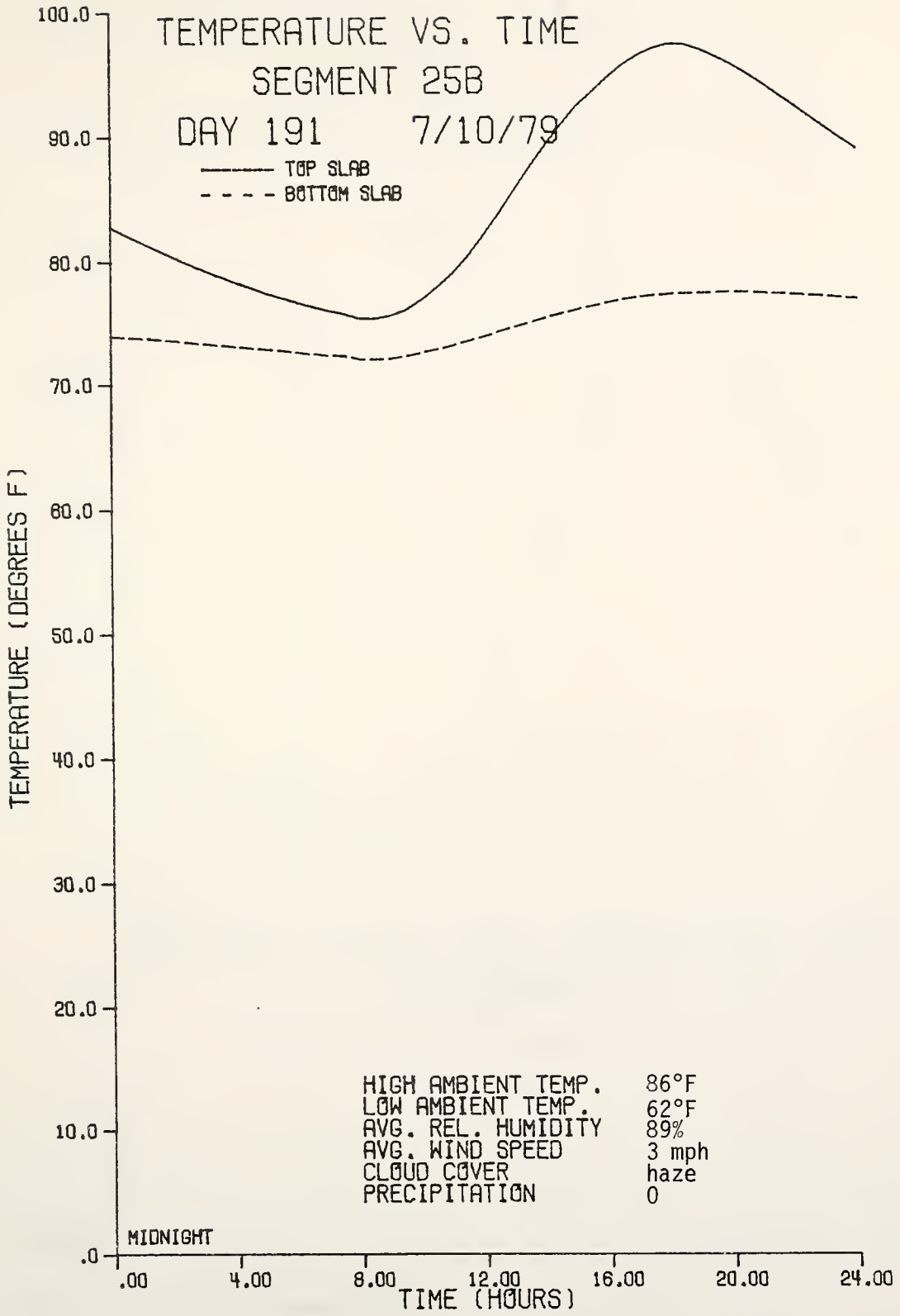

Figure 5.15 Bridge Temperatures

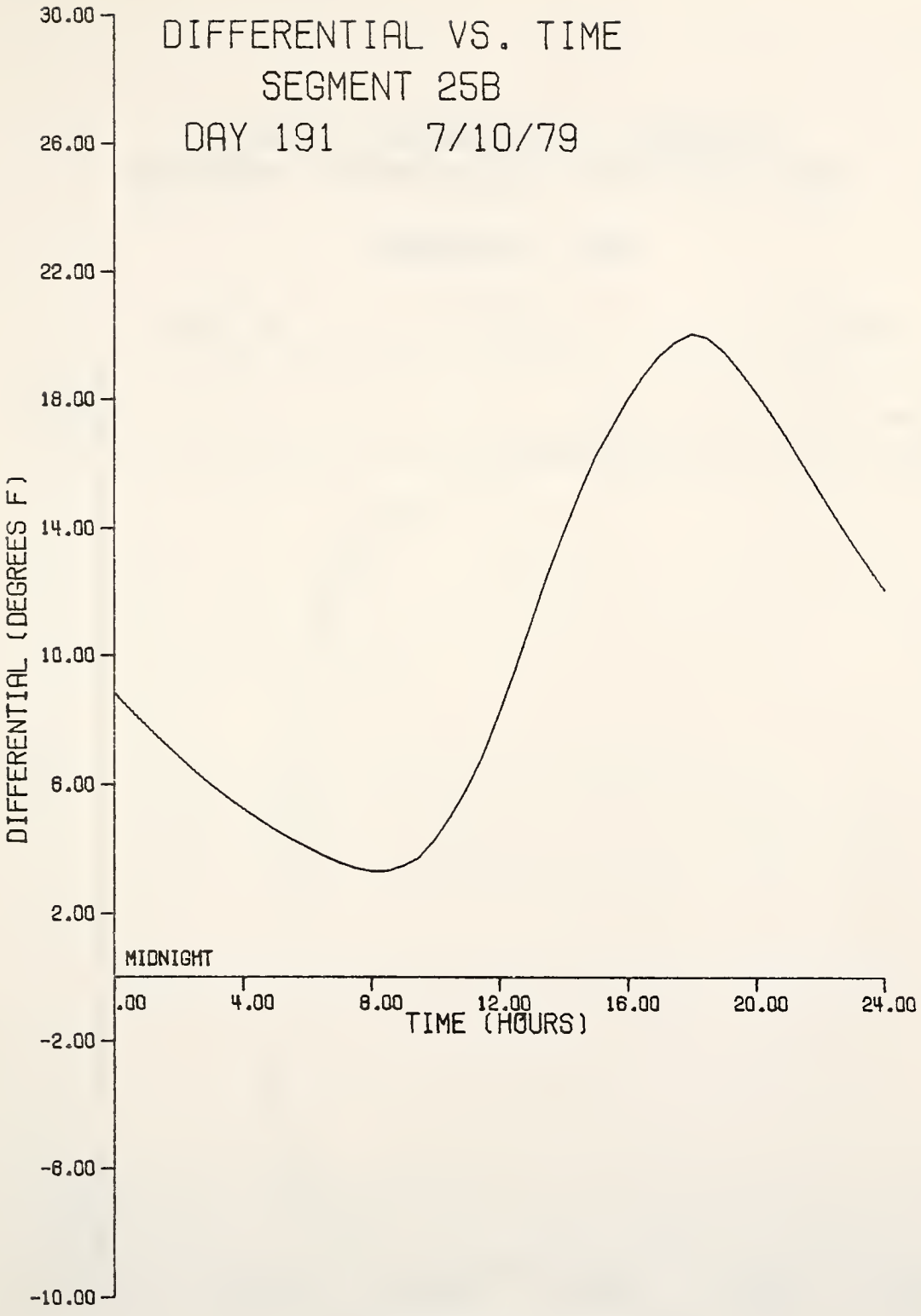

Figure 5.16 Bridge Temperatures

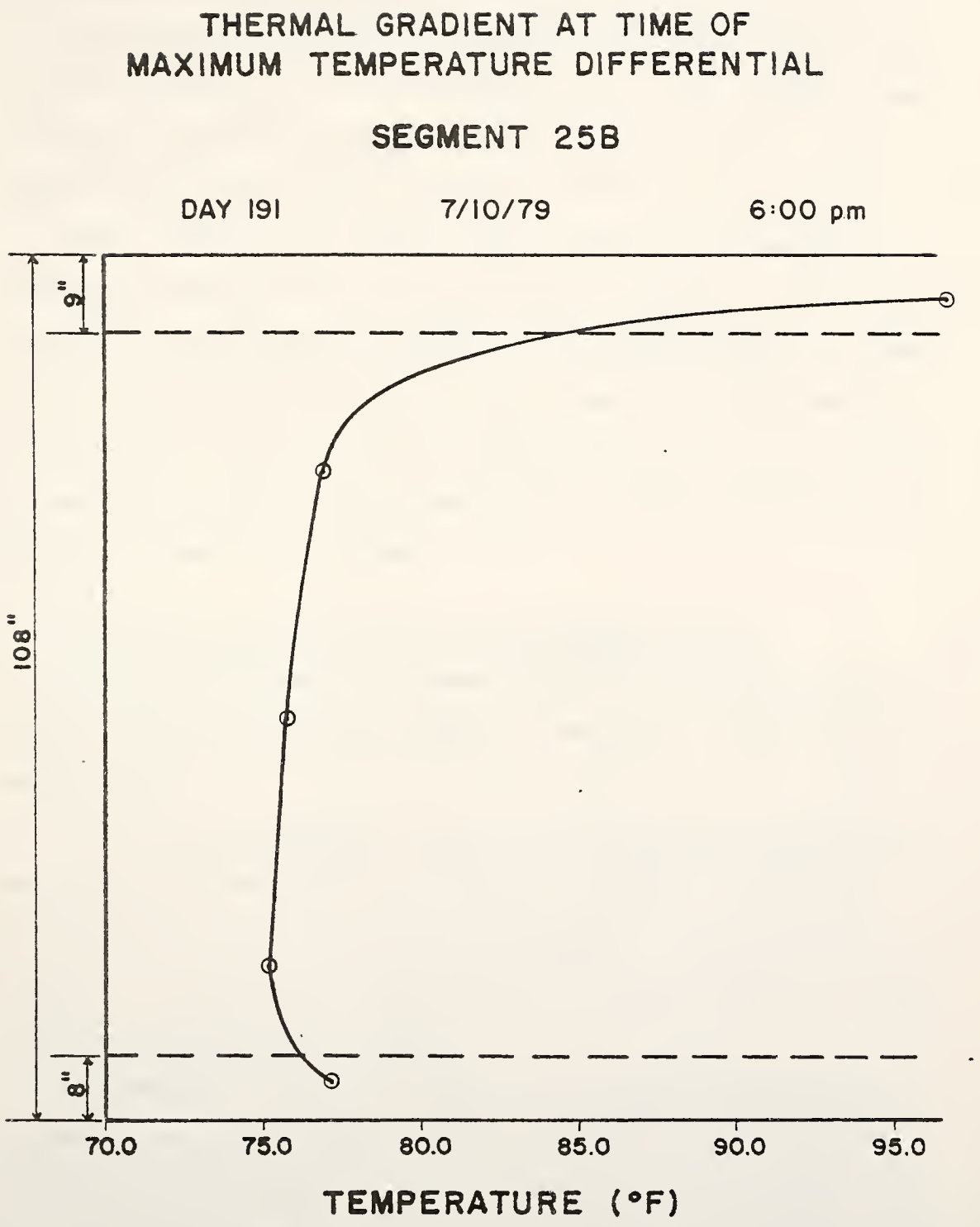

Figure 5.17 Bridge Temperatures

variation in temperature of the top slab. Negative temperature differentials often exist during periods of overcast skies and rain and in the early morning hours during the winter months. The largest negative differential recorded was -8.0 °F on February 27, 1979. During other times of the year, positive temperature differentials normally exist. The largest positive differential recorded was +24.3 °F on June 26, 1979.

Plots of the thermal gradients clearly show that the temperature distribution through the depth of the segment is nonlinear. It is seen that most of the temperature increase occurs in the top slab. The assumption that the temperature of the top slab increases while the remainder of the section maintains a constant temperature is often made when analyzing temperature effects in box girder bridges. The test results indicate that this assumption is justified.

Temperature Induced Strains in the Completed Structure

Temperature differentials between the top and bottom slabs of box girder bridges induce internal stresses if the bridge is statically indeterminate.

In a field test conducted in August 1979, strain levels and bridge temperatures were monitored over a period of 11 hours. Experimental data obtained during the test are presented herein. The results are compared to those obtained using an analytical procedure similar to that described previously in this chapter.

Deformations at the sites of the Whittemore strain gage implants at all three instrumented segments in the north girder of the bridge were monitored hourly throughout the duration of the study (see Figure 5.18). Each instrumented segment has three sets of implants in both the top and

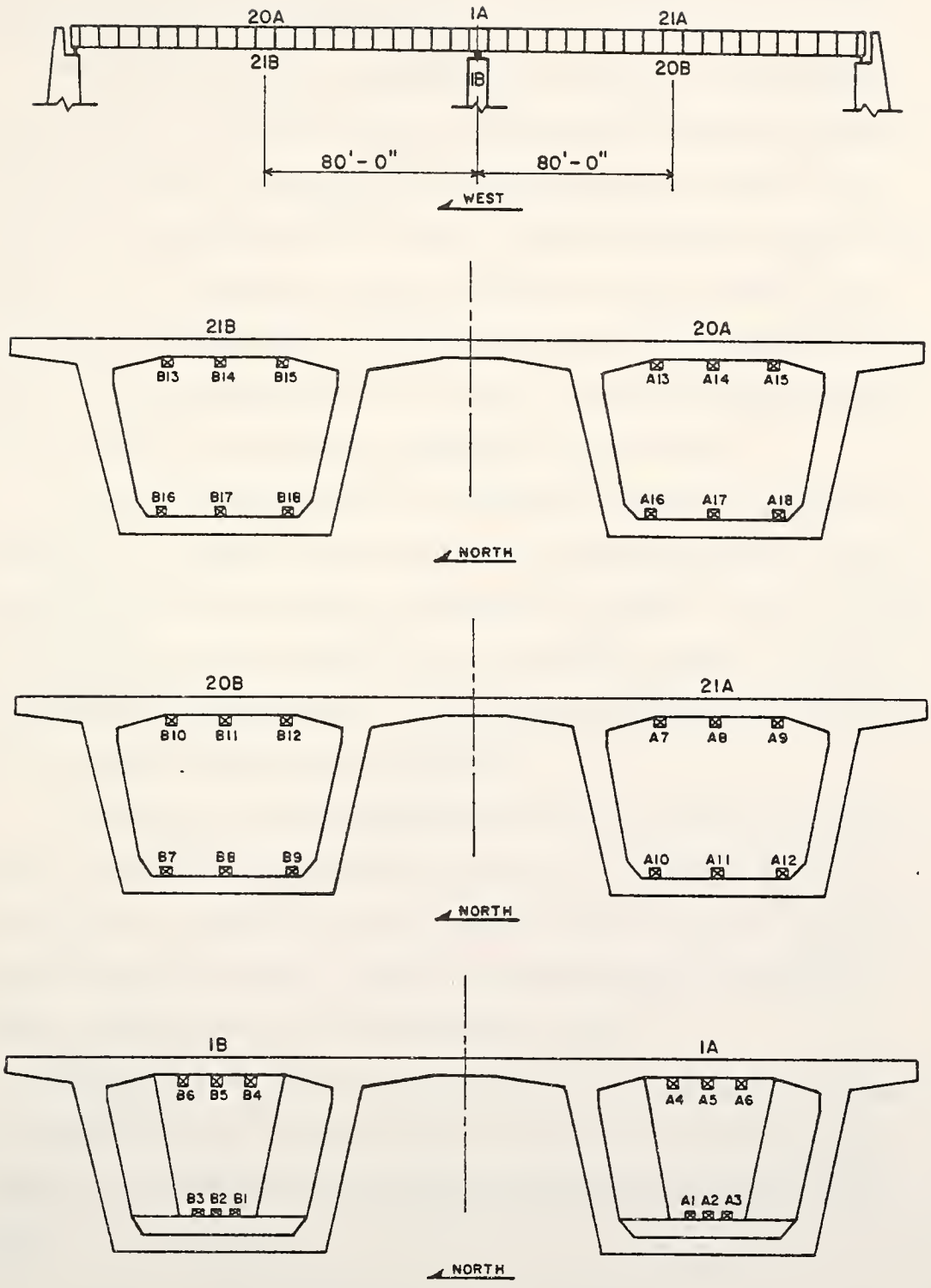

Figure 5.18 Whittemore Strain Gage Implants

bottom slabs. The strain in each slab was determined as the average value of the three readings at that location. Experimental results are presented in Figures 5.19 through 5.24.

The analytical model is presented in Figure 5.25. With the rotational restraint removed, a positive temperature differential produces a statically equivalent moment M and axial force P' (see Figure 5.5) resulting in the deflected shape shown. A redundant moment M' must then be applied so as to produce an equal and opposite change in slope at the pier section. M' can then be solved for in terms of M. When the axial force P' and the moments M and M' are known, strains produced by temperature differentials can easily be determined at any section.

The strain resulting from the longitudinal effects of temperature is equal to the product of the coefficient of thermal expansion of the concrete and the axial change in temperature. Changes in overall length of the structure are accomodated by the relatively flexible neoprene bearing pads at the abutments. It can be shown that the shearing resistance provided by these pads is negligible.

The variation in bridge temperatures which was measured during the testing procedure is illustrated by the plots of Figures 5.26 and 5.27. From these data, theoretical curves were determined using the analytical procedure described above. These curves are presented in Figures 5.19 through 5.24 together with the experimental results.

From the plots it appears that the behavior of the top slab agrees more closely with the predicted behavior than that of the bottom slab. In general, the observed strain levels exceed those predicted by the analysis.

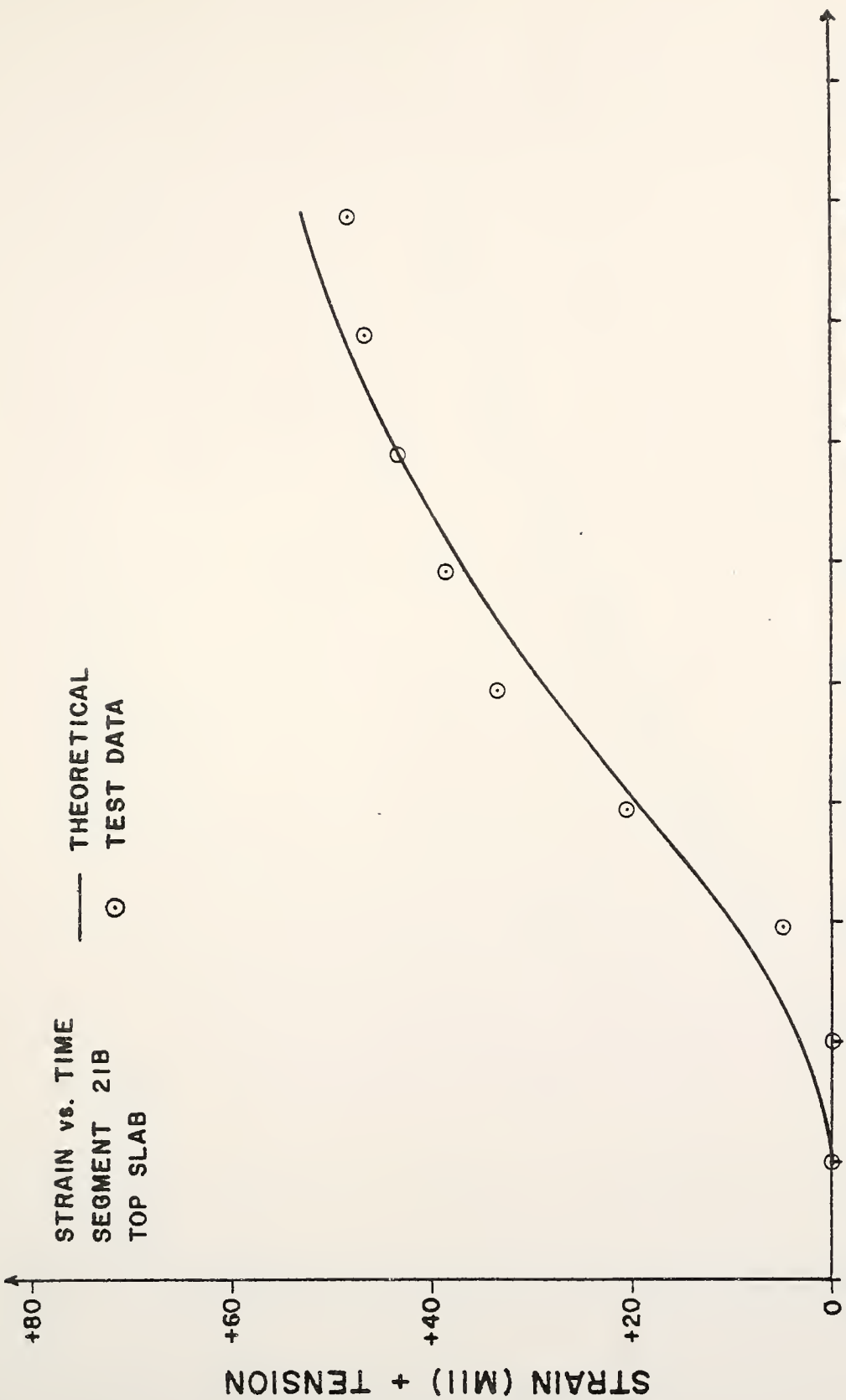

Figure 5.19 Temperature Induced Strain

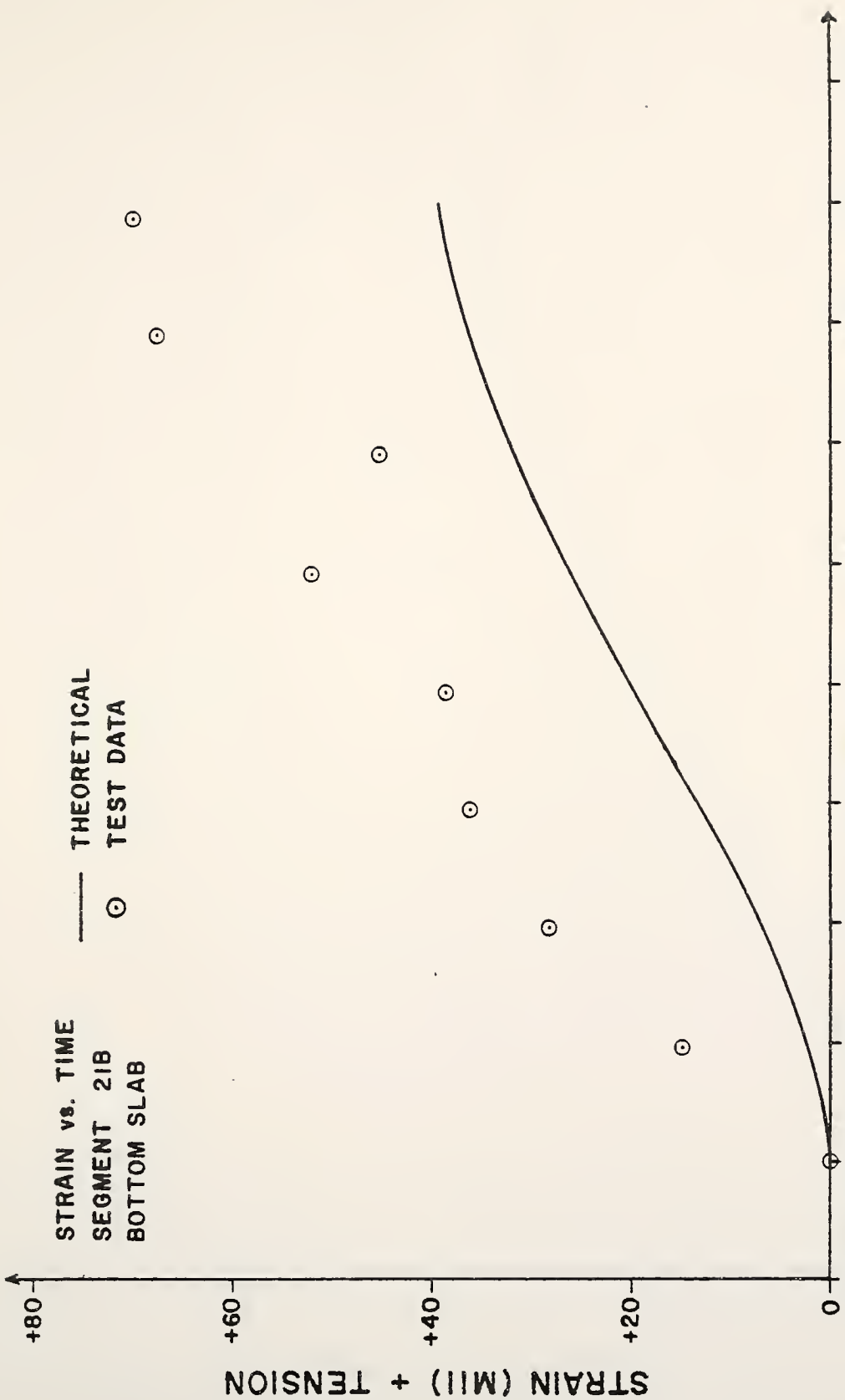

Figure 5.20 Temperature Induced Strain

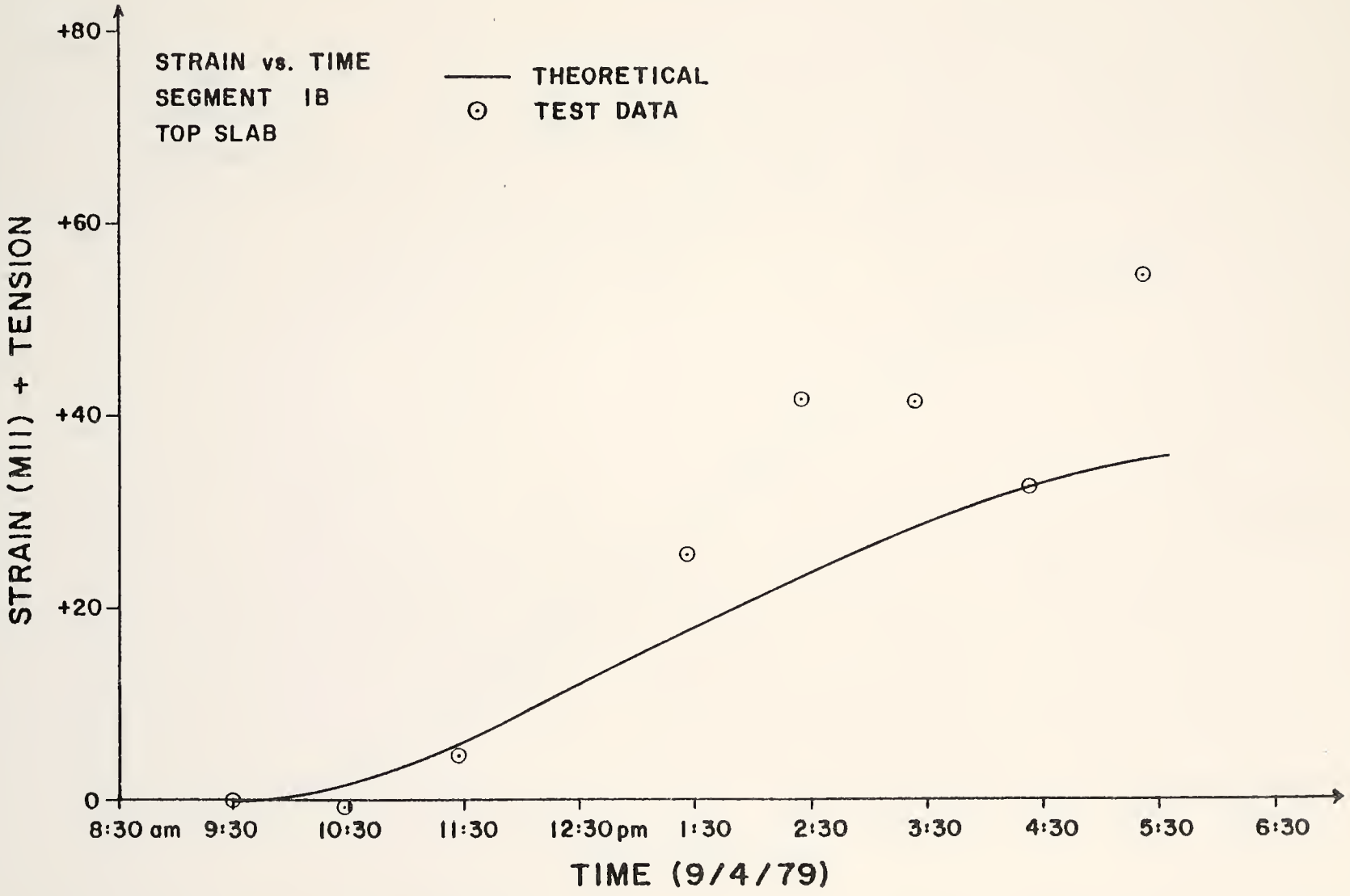

Figure 5.21 Temperature Induced Strain

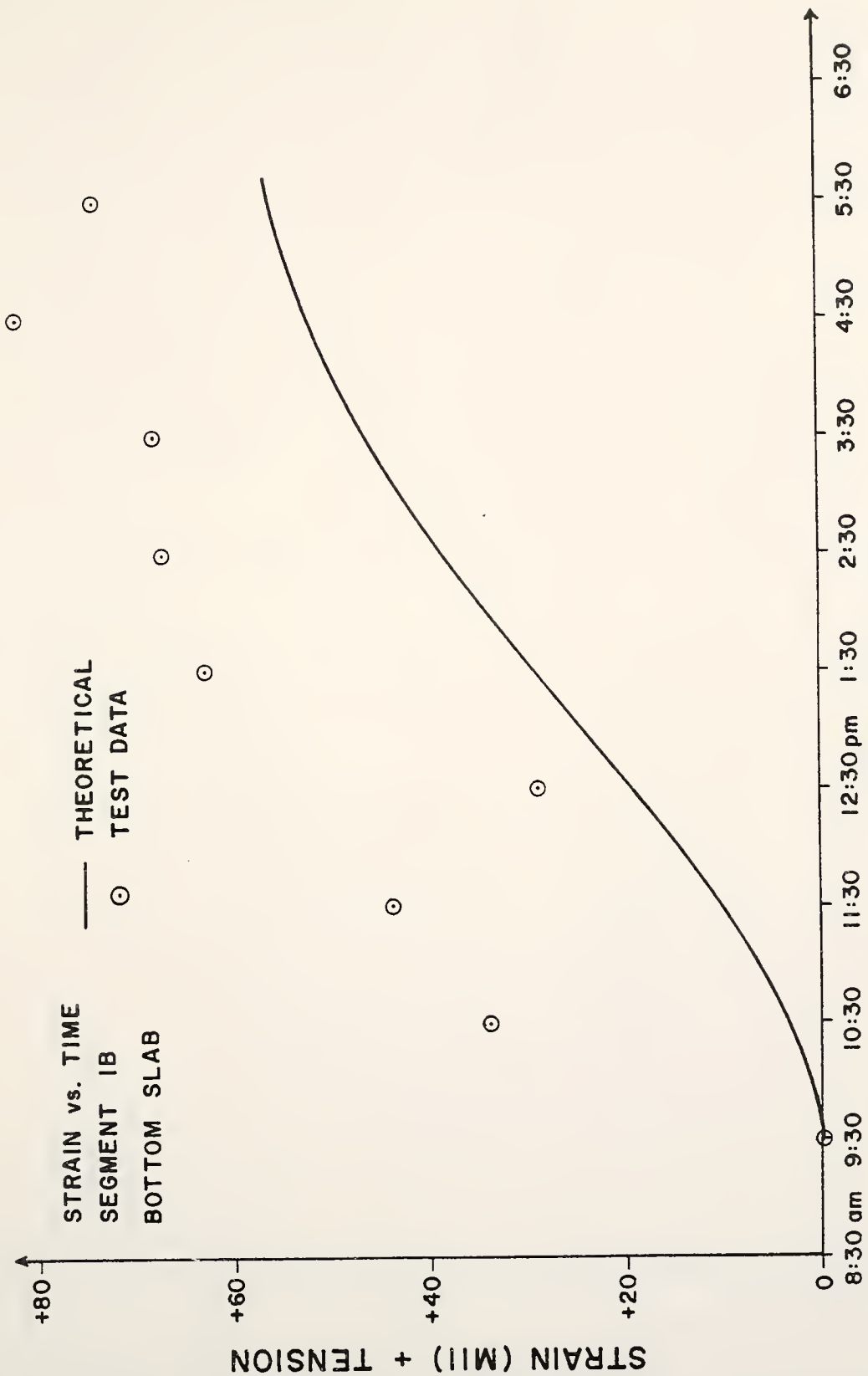

Figure 5.22 Temperature Induced Strain

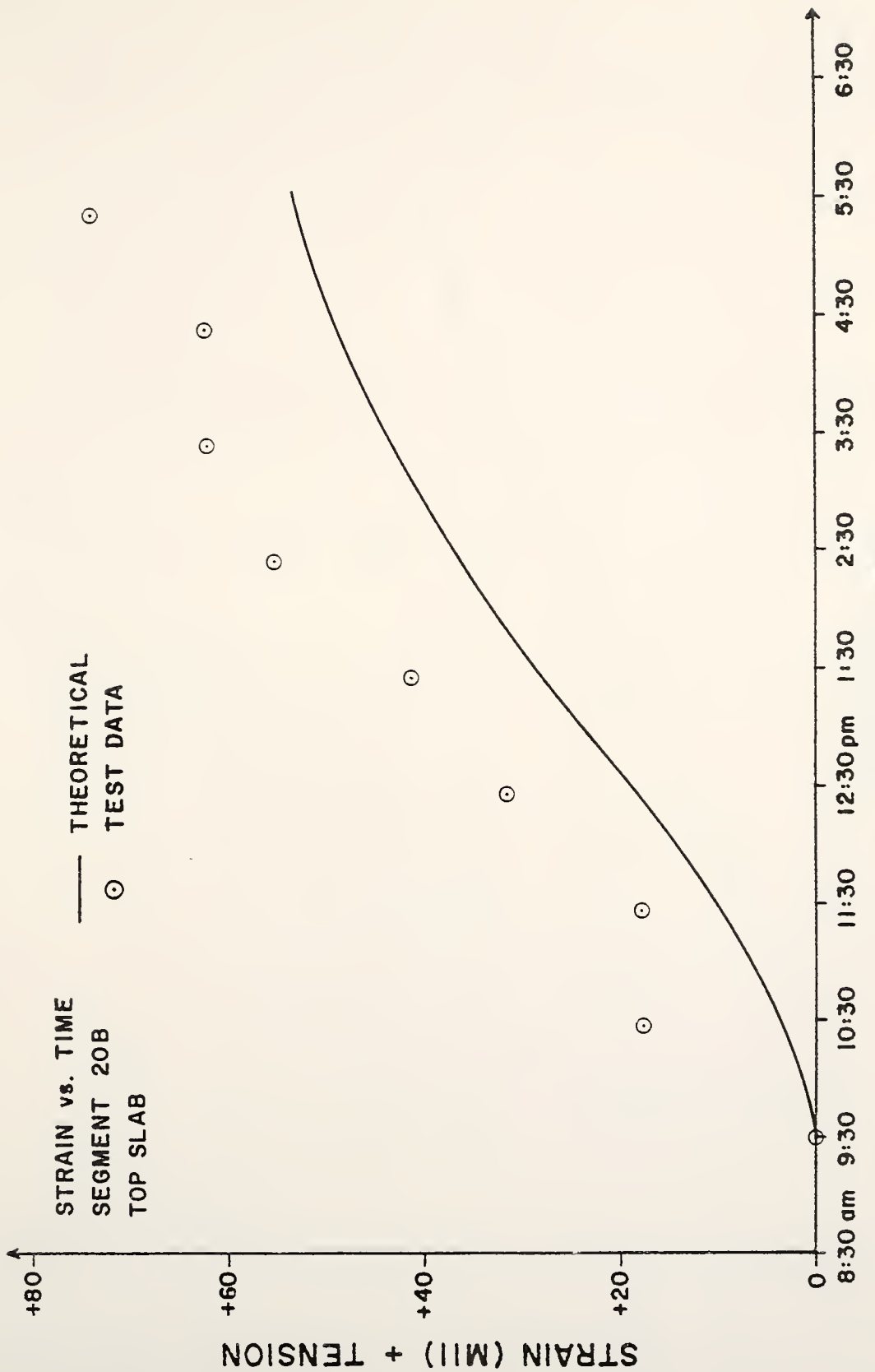

Figure 2.23 Temperature Induced Strain

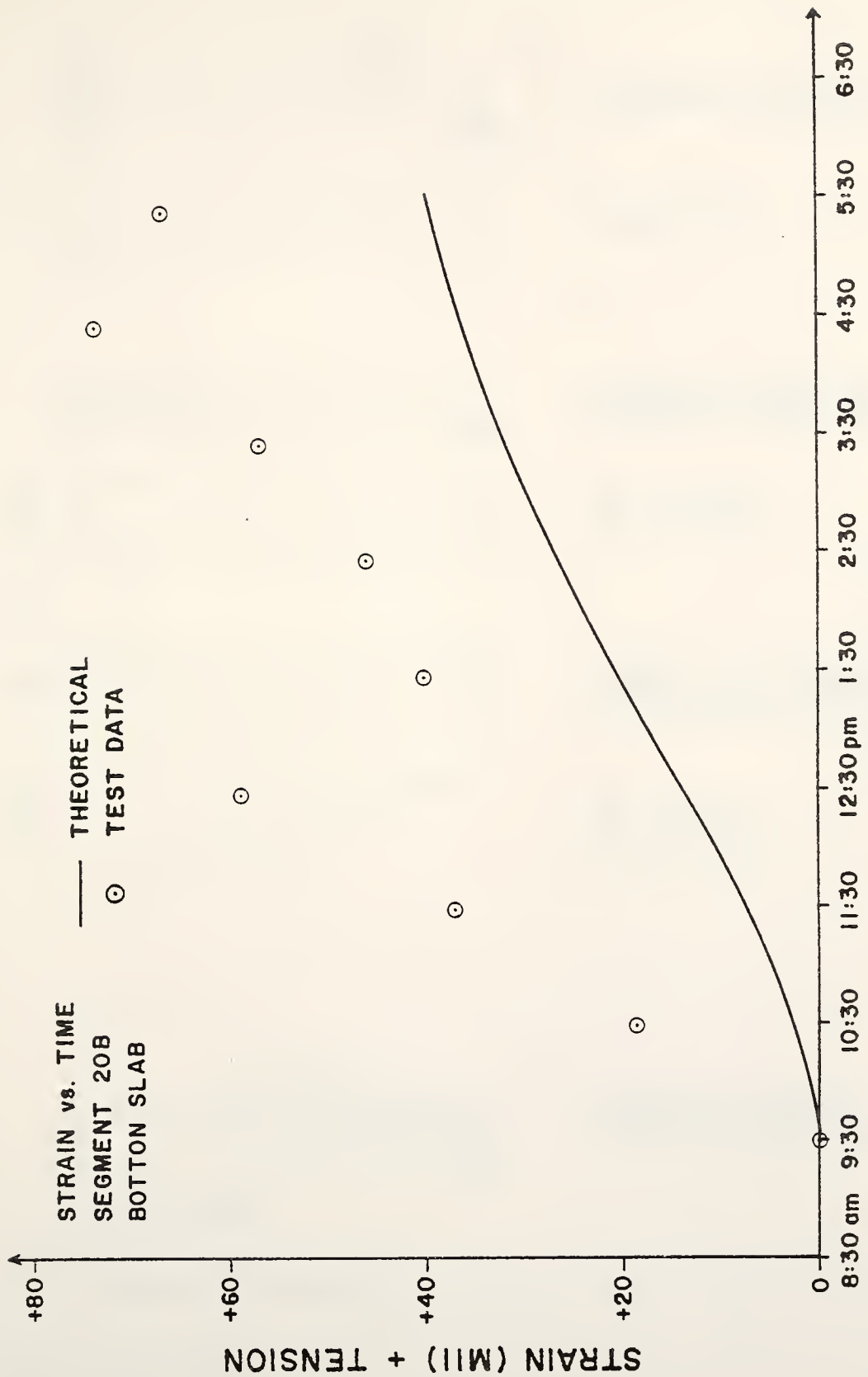

Figure 5.24 Temperature Induced Strain

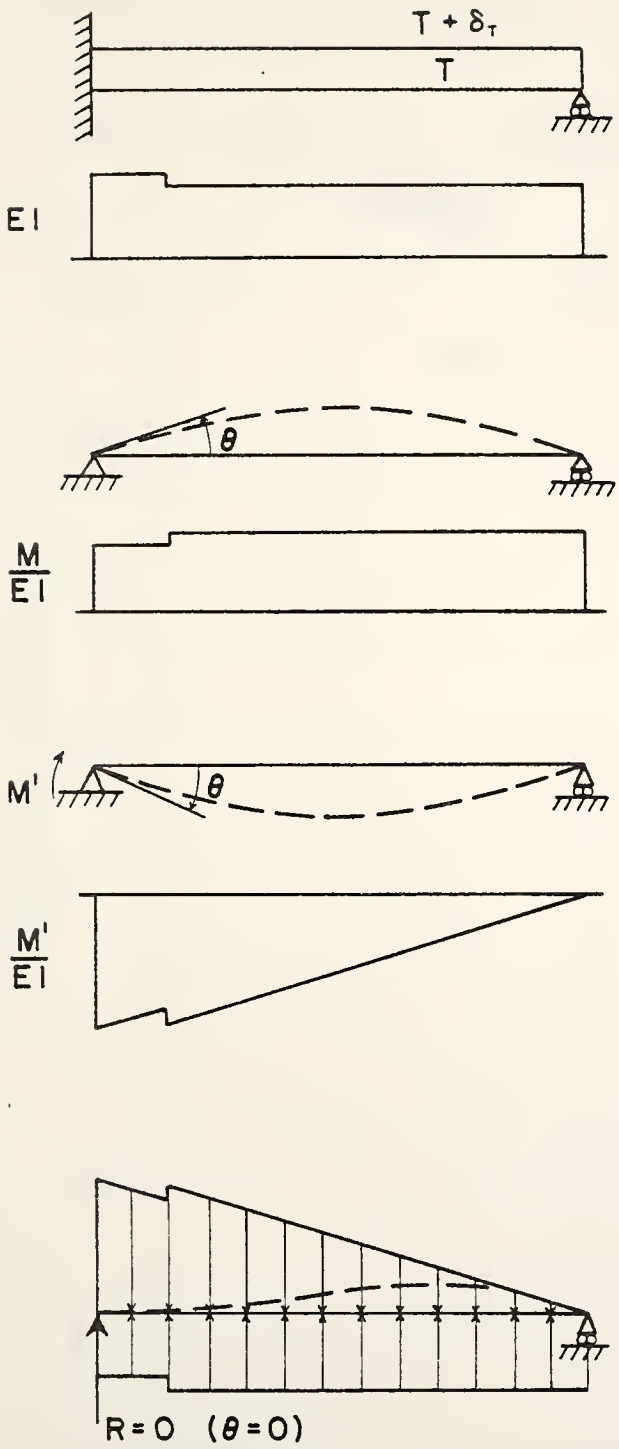

Figure 5.25 Analytical Model

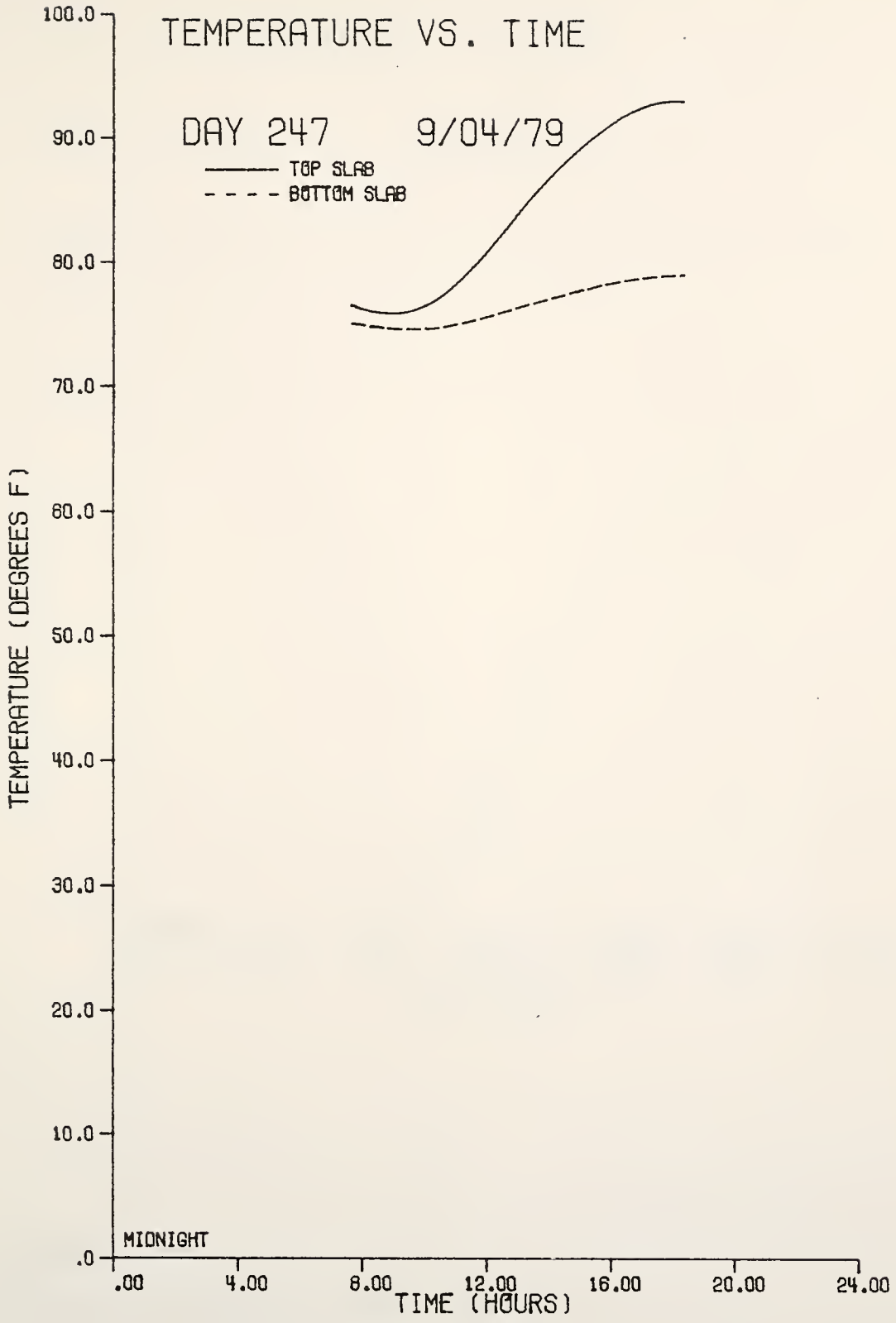

Figure 5.26 Variation In Bridge Temperatures

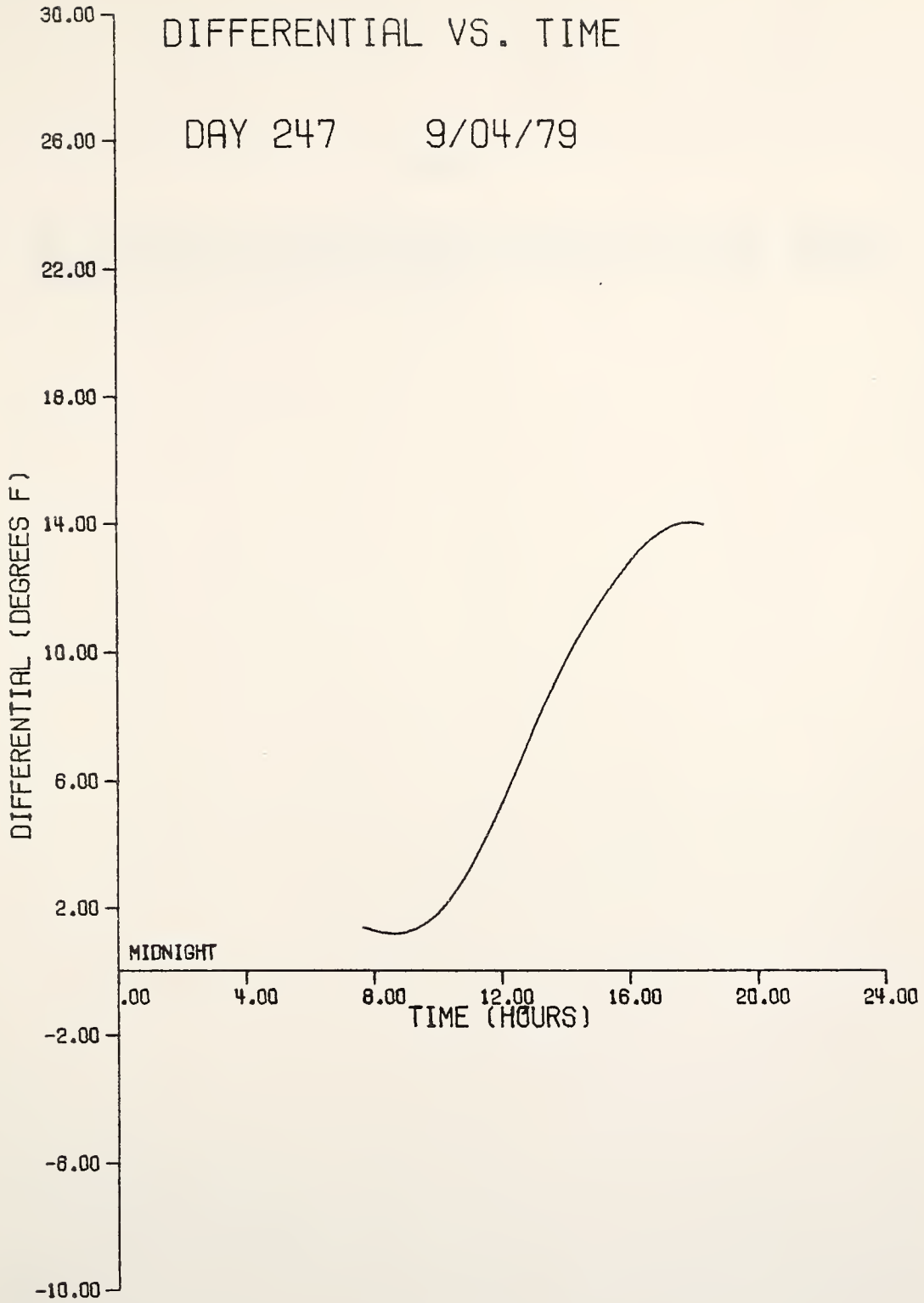

Figure 5.27 Variation In Bridge Temperatures

NOTES

1 Post-Tensioning Institute/Prestressed Concrete Institute, Precast Segmental Box Girder Bridge Manual, Glenview, IL/Chicago, IL, 1978

CHAPTER VI

LONG-TERM DEFORMATIONS

Introduction

Long-term deformations in concrete structures result from the combined effects of creep and shrinkage of the concrete and relaxation of the prestressing steel. Since most shrinkage takes place before erection in the case of precast bridges, it is generally assumed that this effect is minimal. As a result of creep deformations caused by sustained dead load and prestressing forces, segmental concrete box girder bridges which are erected in a different configuration than that which they assume during their service life undergo a redistribution of dead load moments[1]. Consequently internal stresses are different from the initial stresses immediately following construction. The Turkey Run bridge, which was erected by the cantilever method of segmental construction, is a two span continuous structure and is therefore susceptible to this phenomenon.

In an attempt to determine the significance of long-term deformations, strain levels and elevations have been monitored continuously at key locations on the Turkey Run bridge. From this information, it is hoped that inferences can be made regarding the redistribution of dead load moments and long-term deflections caused by creep and loss of prestress. Experimental data concerning long-term strain and midspan deflection measurements are presented in this chapter.

Long-Term Strain Measurement

Longitudinal strain measurements have been made periodically at the locations illustrated in Figure 6.1. Deformations between permanent implants are monitored with a Whittemore strain gage as shown in Figure 6.2 and 6.3. Strain levels are determined by dividing the relative movement of the implants by the ten inch gage length of the instrument.

Plots of strain versus time are presented in Figures 6.4 through 6.9. At each instrumented section, strain levels were determined as the average of the three readings at that section. Bridge temperatures, which were recorded when strain measurements were taken, were utilized in determining the temperature-induced strains. These effects were subtracted from the strain data using the technique described in Chapter V. Nevertheless, as can be seen from the plots, the reduced strain data still appears to be slightly influenced by seasonal effects[2].

The times corresponding to the dates when the individual segments were cast and erected and when the bridge was completed are shown on the time axis. Longitudinal stresses vary considerably during construction due to the increasing dead load as segments are cantilevered and due to post-tensioning forces. As a result, long-term creep strains are referenced from the levels existing at the end of construction.

As expected, the strains across the instrumented sections are more compressive near the locations of the post-tensioning tendons, i.e. near the top slab over the pier and near the bottom slab at the midspan sections. At the pier sections, it is seen that the strain in the top slab increases in the compressive sense at a slightly faster rate than that in the bottom slab. This indicates that post-tensioning forces are the dominant contributor to creep deformations at this location. Although the

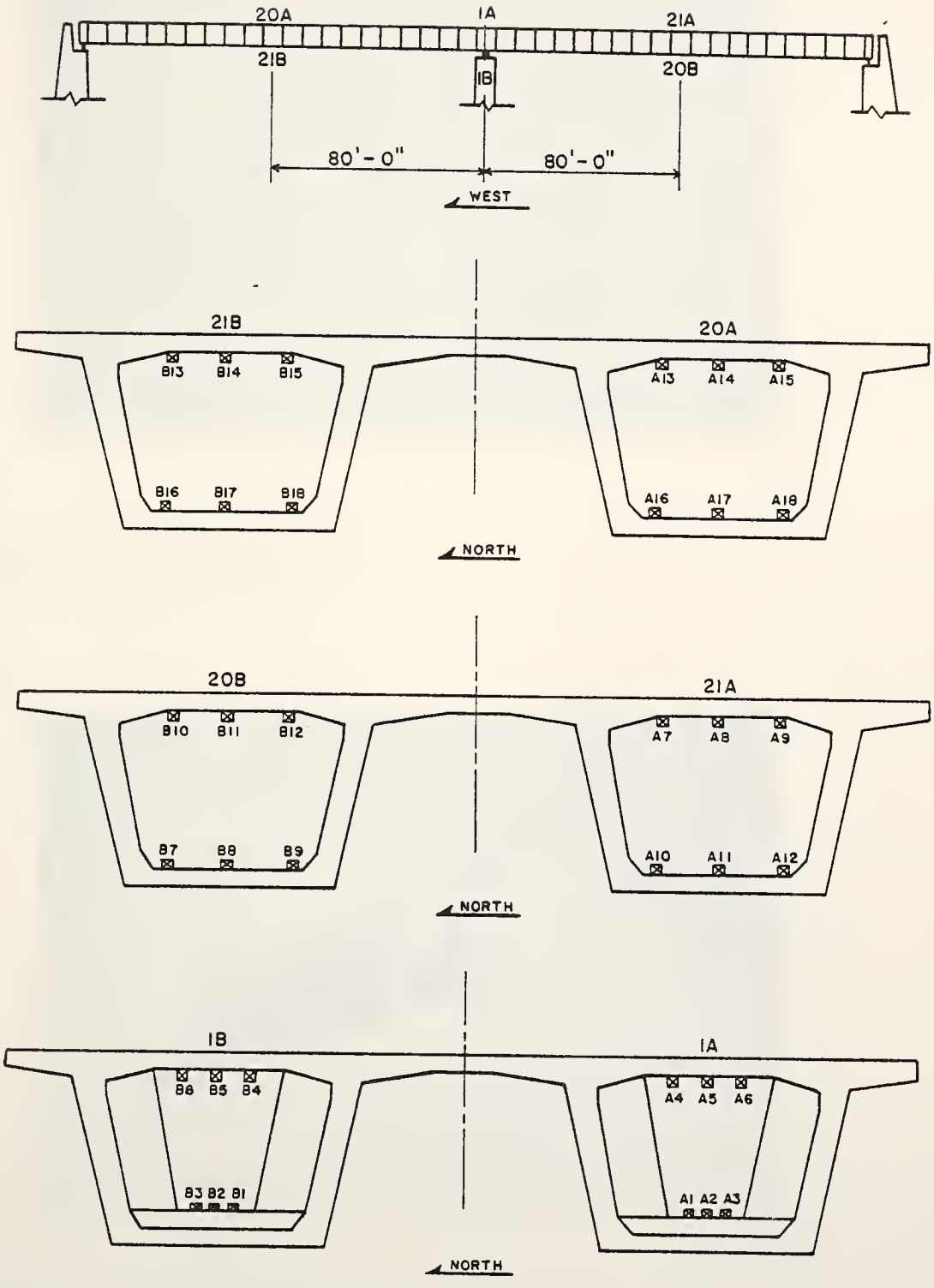

Figure 6.1 Whittemore Instrumentation

Figure 6.2 Whittemore Implants

Figure 6.3 Whittemore Gage

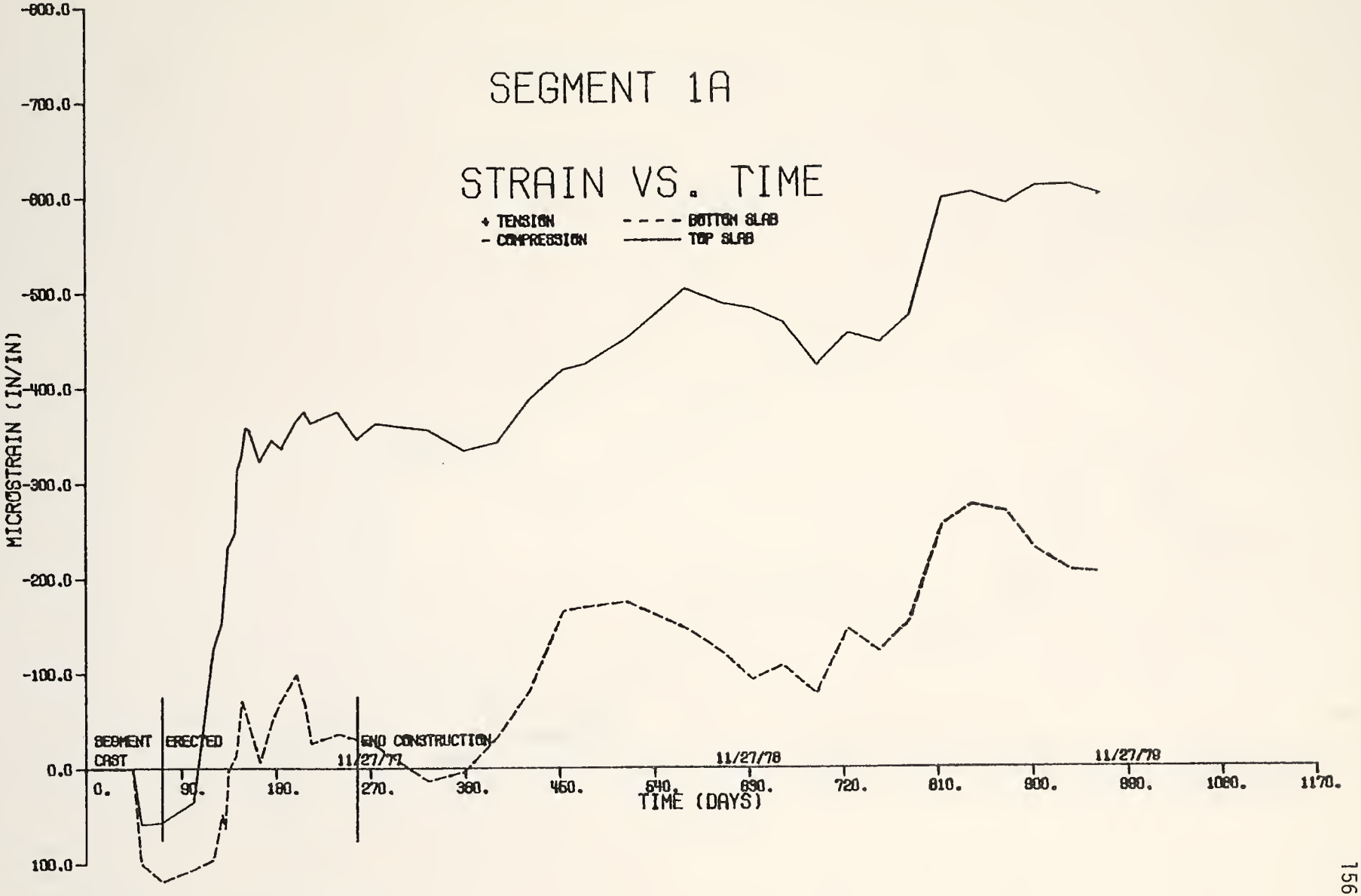

Figure 6.4 Long-Term Strain

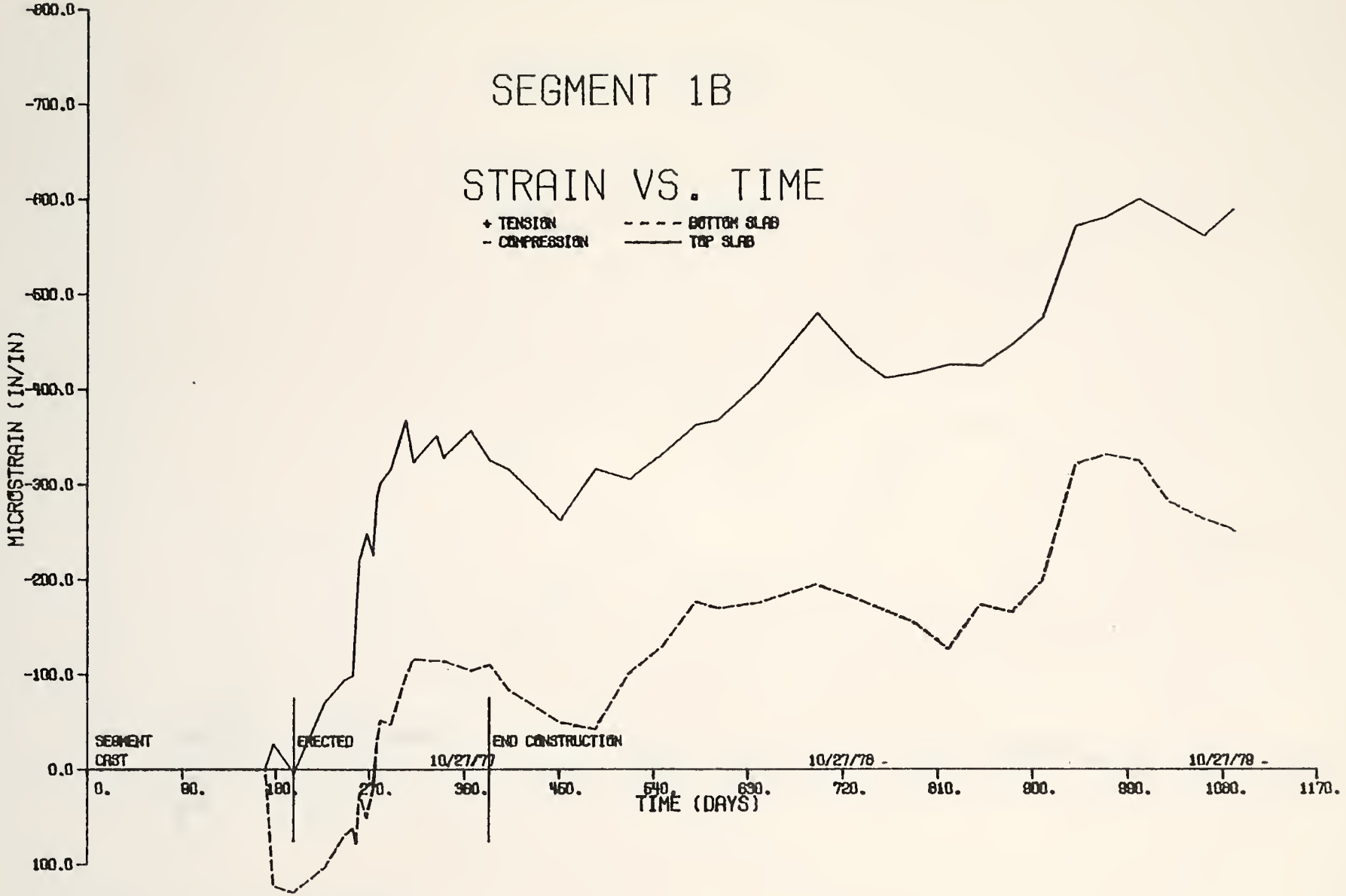

Figure 6.5 Long-Term Strain

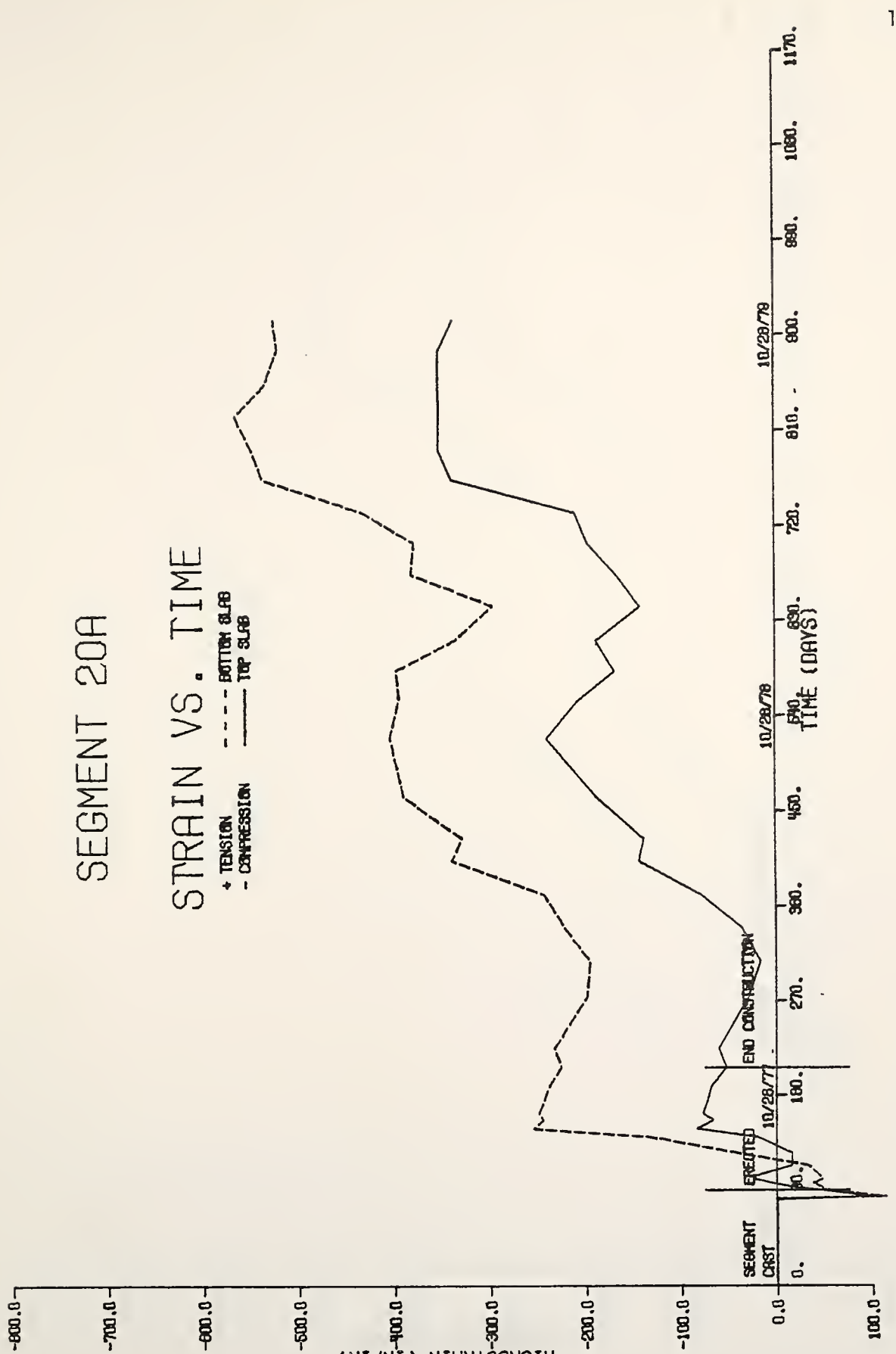

Figure 6.6 Long-Term Strain

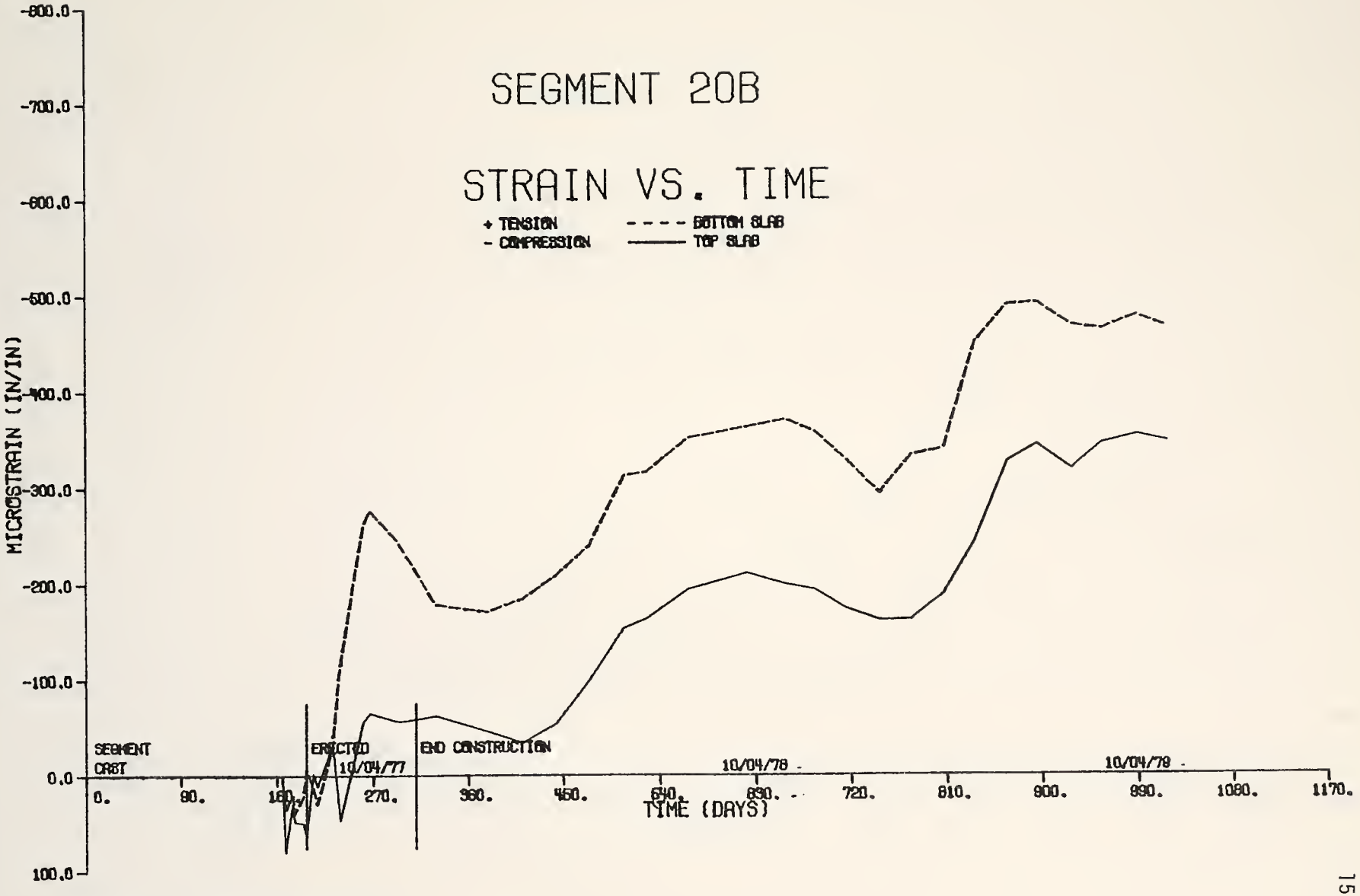

Figure 6.7 Long-Term Strain

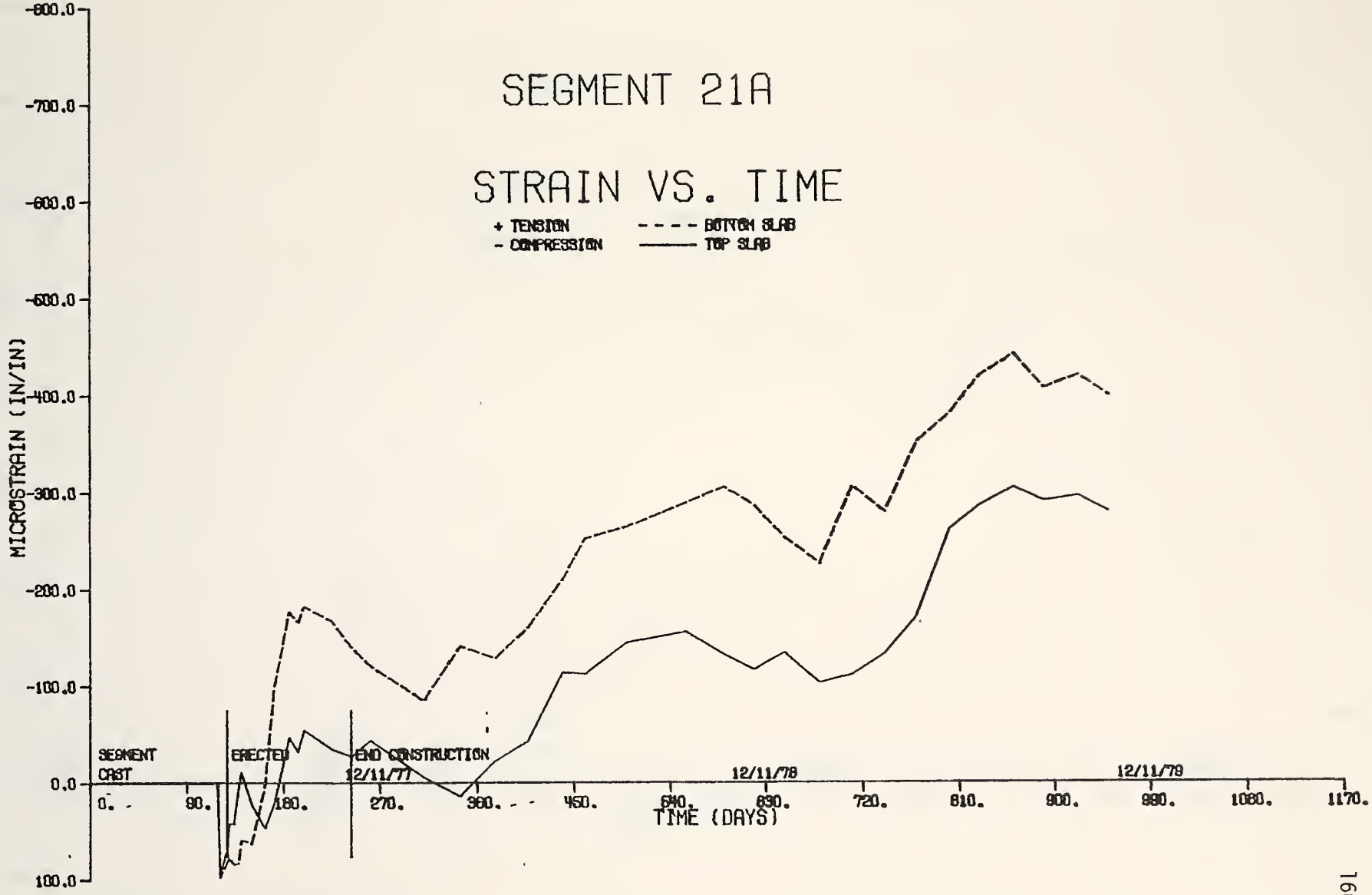

Figure 6.8 Long-Term Strain

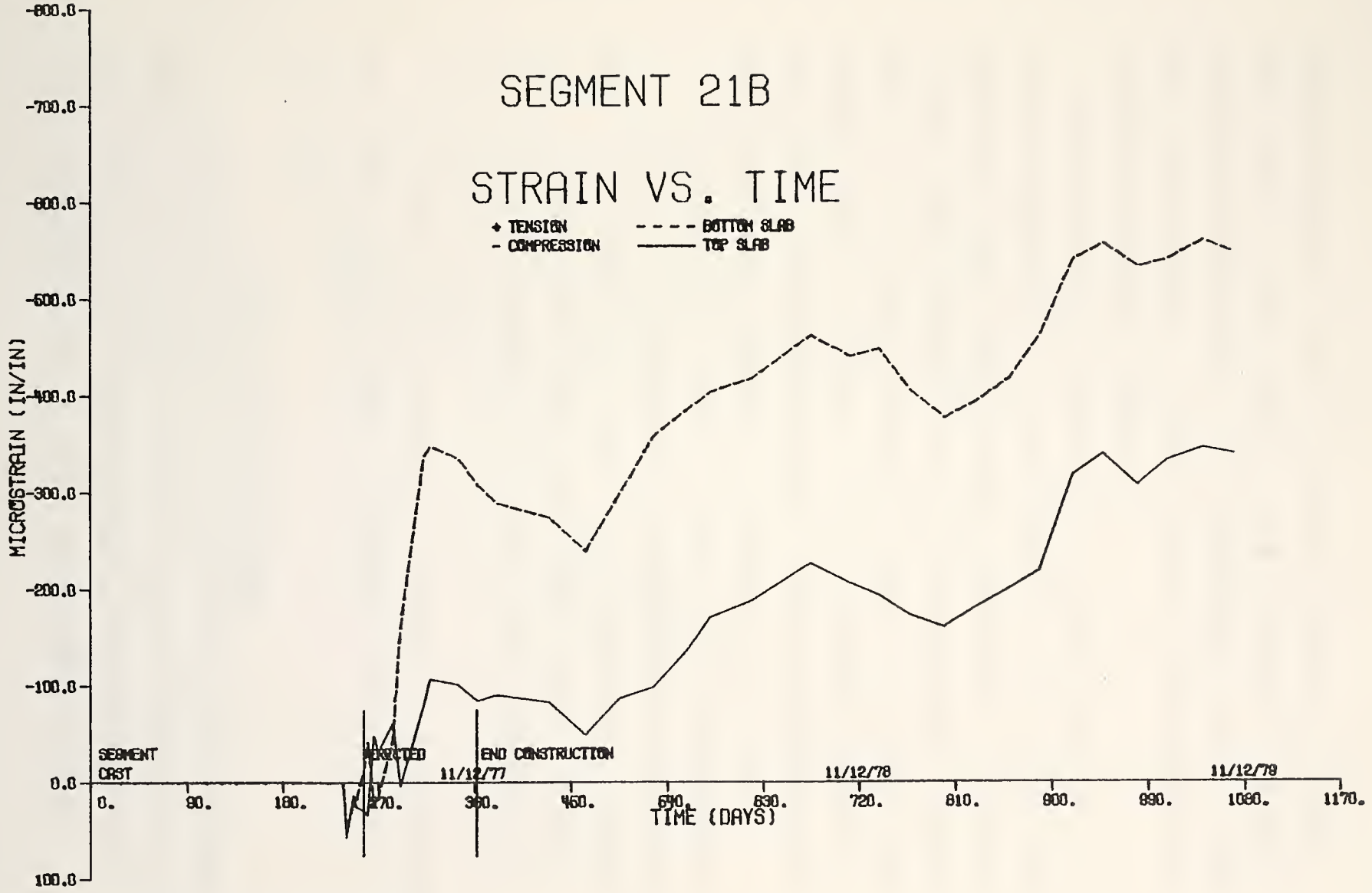

Figure 6.9 Long-Term Strain

compressive strains in both slabs continue to increase at the midspan sections, very little relative rotation occurs, indicating that sustained dead load and post-tensioning forces contribute equally to creep deformations at these sections. The numerical data from which these plots were developed are tabulated in Appendix G.

The strains which have been monitored in the two years since the bridge was constructed are produced by two effects. One is the creep of the concrete caused by prestressing forces and dead loads. The other contributing factor is the redistribution of dead load moments, which takes place as a result of the creep rotations, because of the statically indeterminate nature of the structure. The strains produced by these two effects are coupled and therefore only a qualitative understanding of the moment redistribution phenomenon can be developed at this time.

It is possible that a numerical procedure could be developed to predict the long-term strains caused by the prestressing forces and the dead loads. This information could then be used together with the available strain data to determine the net change in strain caused by the moment redistribution. Consideration will be given to this matter during the next phase of the project.

Approximate methods of determining the effects of creep-induced moment redistribution have been proposed. References are listed at the end of this chapter[3,4,5,6].

Midspan Deflection Measurement

Deflection measurements have been taken monthly at the instrumented sections shown in Figure 6.10. Elevations, which are referenced to a benchmark embedded in the west abutment wing wall, have been measured with a Zeiss Ni-2 automatic level. At each of the instrumented sections,

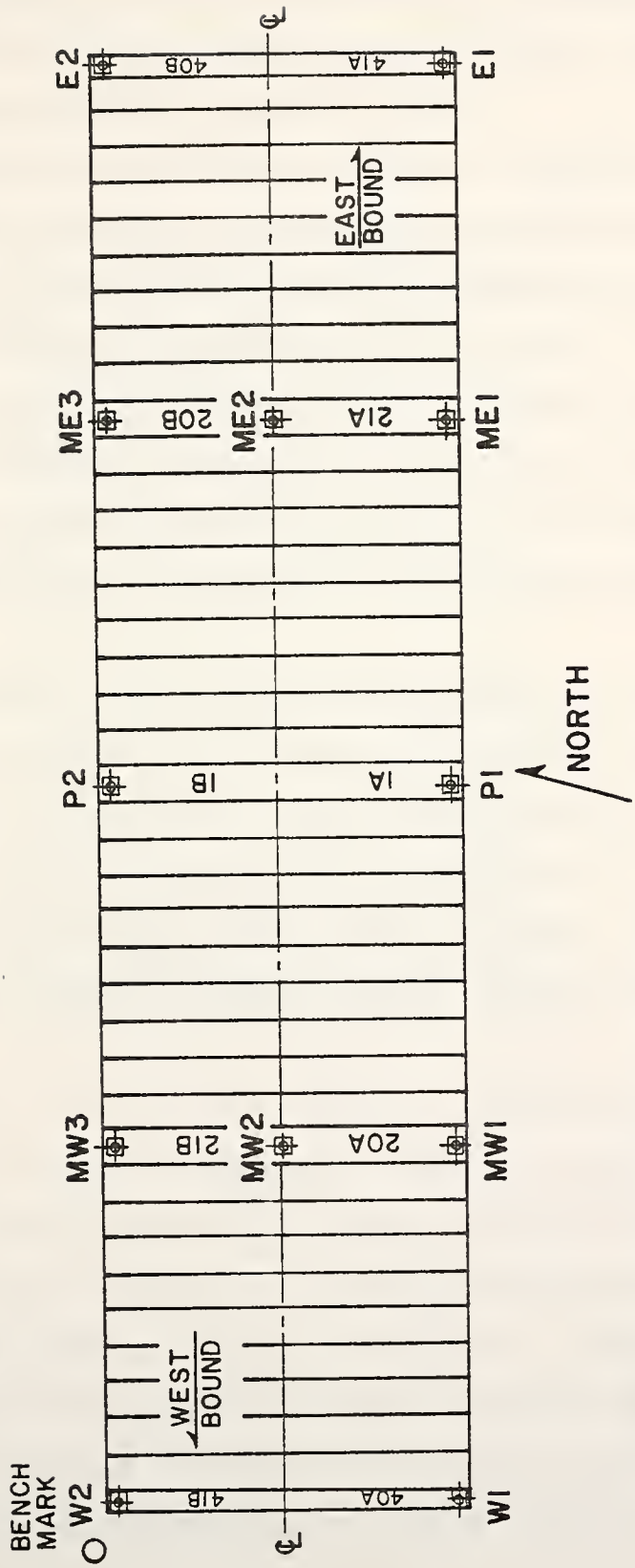

Figure 6.10 Deflection Instrumentation

permanent implants are used as base plates for a Philadelphia rod. The resolution of the elevation measurements is 0.005 ft. Figures 6.11 and 6.12 illustrate the data collection procedure.

Elevations are significantly affected by temperature fluctuations because of their influence on the expansion and contraction of the central piers. The midspan deflections are therefore determined with respect to the relative elevations at the abutment and pier sections. Further data reduction involves subtracting out deflections induced by temperature differentials between the top and bottom slabs of the box girder. This is done using conjugate beam analysis similar to that outlined in Chapter V. Bridge temperatures are recorded during the elevation measurement procedure.

Theoretical long-term deflection calculations for the Turkey Run bridge were performed by V. D. Bouvy and V. D. Niet, Consulting Civil Engineers in The Netherlands. Their results, which take into account creep and shrinkage of the concrete and relaxation and friction losses in the prestressing steel, predict that a net camber of 0.016 ft will develop over a period of 27 years from the time when service loads are applied.

A total of 20 sets of data have been recorded over a period of 697 days since the bridge was completed. According to Pauw[7], normally about 90 percent of the ultimate time-dependent deflections will be developed by the end of a year. However, no significant deflections have been detected after 23 months, i.e. less than 0.005 ft. Although the resolution of measurement attainable does not permit meaningful experimental determination of long-term deflections for this bridge, the deflections are very small as was anticipated by the initial design calculations.

Figure 6.11 Backsight on Benchmark

Figure 6.12 Foresight on Deflection Implant

In an independent study conducted during the summer of 1979, a positive 16°F temperature differential between the top and bottom slabs was seen to produce a midspan camber of approximately 0.008 ft. The fact that temperature induced deflections are of the same magnitude as the long-term deflections being measured causes difficulty in data reduction. Similar results were determined by Pauw in an investigation of a five-span, continuously reinforced concrete bridge in Jackson County, Missouri[8].

NOTES

1 Libby, James R., "Segmental Box Girder Bridge Superstructure Design", Journal of the American Concrete Institute, V. 73, No. 5, May, 1976, p. 283.

2 Richmond, B., "The Creep-Temperature Mechanism in Concrete Bridges", Bridge Temperatures, Supplementary Report 442, Transport and Road Research Laboratory, Crowthorne, Berkshire, 1978, pp. 81-84.

3 Muller, Jean, "Long-Span Precast Prestressed Concrete Bridges Built in Cantilever", First International Symposium on Concrete Bridge Design, SP-23, American Concrete Institute, Detroit, 1969, pp. 705-740.

4 Subcommittee 5, ACI Committee 435, "Deflections of Prestressed Concrete Members", Journal of the American Concrete Institute, V. 60, No. 12, December, 1963, pp. 1697-1728.

5 Thenoz, M., "Redistribution of Moments Due to Creep in Bridges Constructed in Cantilever", Contributions Techniques Francaises, 7th Congress of the Federation Internationale de la Precontrainte, New York, 1974, pp. 25-27.

6 Atallah, R., and Lau, M. Y., "Redistribution of Moments Due to Creep in Bridges Constructed in Cantilever", Contributions Techniques Francaises, 7th Congress of the Federation Internationale de la Precontrainte, New York, 1974, pp. 28-30.

7 Pauw, Adrian, "Time Dependent Deflections of a Box Girder Bridge", Designing for Effects of Creep, Shrinkage and Temperature, SP-27, American Concrete Institute, Detroit, 1971, p. 142.

8 Ibid., p. 142.

CHAPTER VII

SUMMARY

An instrumentation system has been installed on the segmental box girder bridge at Turkey Run to monitor certain aspects of its short-term and long-term behavior, both during construction and under service conditions. Electrical resistance strain gages have been placed on the transverse reinforcement and the interior surface of the concrete at selected sections for monitoring transverse bending tractions. Thermistors have been embedded in the concrete at several sections for measuring the daily and seasonal variations in bridge temperatures. Whittemore strain gage implants have been attached to the interior surface of the top and bottom slabs at the pier and midspan segments for monitoring long-term strains. Deflection implants have been secured to the surface of the bridge deck at the midspan sections for measuring long-term deflections.

Preliminary experimental measurements of the transverse flexural response of representative cross-sections due to pre-specified truck loadings have been made. The tractions determined from the strain measurements are somewhat less than those predicted by a finite element analysis of this structure under identical loading conditions. However, more comprehensive testing during the next phase of the project will be necessary before any conclusions can be reached.

Cantilever tip deflections were monitored during construction after placement of segments 24 and 25. The purpose of this part of the research

was to determine the nature of the relationship between tip deflections and existing temperature differentials in the structure. Although the resolution of the readings was quite large in comparison to the magnitude of the deflections being measured, causing some scatter in the observed values, the results generally agreed with the analytical prediction equation. The results obtained from this study were utilized by agents of the general contractor, J. L. Wilson Co., in making elevation corrections when establishing superstructure-abutment connections for the Turkey Run bridge.

From the temperature data collected thus far, several inferences can be made. In general, minimum temperature differentials occur between 7:00 AM and 9:00 AM and maximum differentials occur between 5:00 PM and 7:00 PM. The temperature of the bottom slab fluctuates very little as compared to the variation in temperature of the top slab. Negative temperature differentials (bottom slab warmer than the top slab) often exist during periods of overcast skies and rain and in the early morning hours during the winter months. During other times of the year, positive temperature differentials normally exist. The temperature distribution through the depth of the segment is non-linear; most of the temperature increase occurs in the top slab.

In an attempt to determine the significance of long-term deformations on the Turkey Run bridge, strains and deflections have been monitored periodically at key locations. Longitudinal strains in the top and bottom slabs at the pier and midspan segments have been measured with a Whittemore mechanical strain gage. From the data, it was found that the strains at all levels of the cross-section continue to increase in the compressive sense due to creep caused by post-tensioning and

dead load stresses. Relative rotations occur because the strains are not uniform through the depth of the segments; thus, a redistribution of moments takes place. Consideration will be given to the problem of developing a quantitative understanding of this phenomenon during the next phase of the project.

Deflection measurements have been made monthly at the midspan sections of the bridge. No significant deflections have been detected after 23 months, i.e. all deflections have been less than the measurement resolution, which is 0.005 ft. From these findings it was therefore concluded that the resolution of measurement attainable without expensive instrumentation does not permit meaningful experimental determination of long-term deflections for this bridge. Nevertheless, the long-term deflections are very small as was anticipated by the initial design calculations.

LIST OF REFERENCES

LIST OF REFERENCES

Atallah, R. and Lau, M. Y., "Redistribution of Moments Due to Creep in Bridges Constructed in Cantilever", Contributions Techniques Francaises, 7th Congress of the Federation Internationale de la Precontrainte, New York, 1974, pp. 28-30.

Batla, F. A., "Finite Element Analysis of Prestressed Concrete Box Girders", Ph.D. Dissertation, Purdue University, December, 1976.

Danon, J. R. and Gamble, W. L., "Time-Dependent Deformations and Losses in Concrete Bridges Built by the Cantilever Method", Department of Civil Engineering, University of Illinois, Urbana, IL/Illinois Department of Transportation, Springfiled, IL, Report No. UILU-ENG-77-2002, January, 1977.

Emerson, M., "Bridge Temperatures Estimated from the Shade Temperature", Transport and Road Research Laboratory Report LR 696, Crowthorne, Department of the Environment, 1976.

Emerson, M., "The Calculation of the Distribution of Temperature in Bridges", TRRL Report LR 561, Crowthorne, Department of the Environment, 1973.

Emerson, M., "Extreme Values of Bridge Temperatures for Design Purposes", TRRL Report LR 744, Crowthorne, Department of the Environment, 1976.

Emerson, M., "Temperatures in Bridges During the Hot Summer of 1976", TRRL Report LR 783, Crothorne, Department of the Environment, 1977.

Emerson, M., "Temperature Differences in Bridges: Basis of Design Requirements", TRRL Report LR 765, Crowthorne, Department of the Environment, 1977.

Haight, F. A., "An Experimental Segmental Bridge - A Research Continuation Proposal to the Pennsylvania Department of Transportation", The Pennsylvania Transportation Institute, PTI 1777, The Pennsylvania State University, May, 1977.

Holman, R. J., "Development of an Instrumentation Program for Studying Behavior of a Segmental Concrete Box Girder Bridge", Joint Highway Research Project 77-4, Purdue University, March 2, 1977.

Kashima, S. and Breen, J. E., "Construction and Load Tests of a Segmental Precast Box Girder Bridge Model", University of Texas at Austin, February, 1975.

Libby, James, R., "Segmental Box Girder Bridge Superstructure Design", Journal of the American Concrete Institute, V. 73, No. 5, May, 1976, pp. 279-290.

Muller, Jean, "Long-Span Precast Prestressed Concrete Bridges Built in Cantilever", First International Symposium on Concrete Bridge Design, SP-23, American Concrete Institute, Detroit, 1969, pp. 705-740.

Pauw, Adrian, "Static Modulus of Elasticity of Concrete as Affected by Density", Journal of the American Concrete Institute, V. 57, No. 6, December, 1960, pp. 679-688.

Pauw, Adrian, "Time-Dependent Deflections of a Box Girder Bridge", Designing for Effects of Creep, Shrinkage and Temperature in Concrete Structures, SP-27, American Concrete Institute, Detroit, 1971, pp. 141-158.

Portland Cement Association, Research and Development, Construction Technology Laboratories, "Time-Dependent Behavior of Segmental Cantilever Concrete Bridges", Skokie, IL, June, 1977.

Post-Tensioning Institute/Prestressed Concrete Institute, Precast Segmental Box Girder Bridge Manual, Glenview, IL/Chicago, IL, 1978.

Priestly, M. J. N., "Design of Concrete Bridges for Temperature Gradients", Journal of the American Concrete Institute, V. 75, No. 5, May, 1978, pp. 209-217.

Priestly, M. J. N., "Design Thermal Gradients for Concrete Bridges", New Zealand Engineering (Wellington), V. 31, No. 9, September, 1976, pp. 213-219.

Priestly, M. J. N., "Thermal Gradients in Bridges - Some Design Considerations", New Zealand Engineering (Wellington), V. 27, No. 7, July, 1972, pp. 228-233.

Reynolds, J. C. and Emanuel, J. H., "Thermal Stresses and Movements in Bridges", Proceedings of the American Society of Civil Engineers, V. 100, St. 1, January, 1974, pp. 63-78.

Richmond, B., "The Creep-Temperature Mechanism in Concrete Bridges", Bridge Temperatures, Supplementary Report 442, Transport and Road Research Laboratory, Crowthorne, 1978, pp. 81-84.

Subcommittee 5, ACI Committee 435, "Deflections of Prestressed Concrete Members", Journal of The American Concrete Institute, V. 60, No. 12, December, 1963, pp. 1697-1728.

Technical Bulletin of Association Francaise des Ponts et Charpentes, "Long-Term Experiments on a Prestressed Concrete Bridge: The Bridge of Champigny-Sur-Yonne", March, 1972, pp. 19-37.

Thenoz, M., "Redistribution of Moments Due to Creep in Bridges Constructed in Cantilever", Contributions Techniques Francaises, 7th Congress of the Federation Internationale de la Precontrainte, New York, 1974, pp. 25-27.

Transport and Road Research Laboratory, Department of the Environment/ Department of Transport, Bridge Temperatures, Supplementary Report 442, Crowthorne, 1978.

White, I. G., B. Sc., "Non-Linear Differential Temperatures Distributions in Concrete Bridge Structures: A Review of the Current Literature", Technical Report 525 of the Cement and Concrete Association, 1979.

APPENDICES

Special Note

This copy of the Report does not contain the following Appendices listed in the Table of Contents:

A copy of any or all of the listed Appendices may be obtained for the cost of duplication and postage by writing to:

Joint Highway Research Project
Civil Engineering Building
Purdue University
West Lafayette, Indiana 47906

and indicating the title and number (JHRP-79-25) of this Report and the Appendices desired.

COVER DESIGN BY ALDO GIORGINI